

# **An experimental investigation of the potential role of liquid hydrocarbons as ore fluids for sediment-hosted ore deposits**

by Jethro Sanz-Robinson

April 2020

A thesis submitted to McGill University in partial fulfillment of the requirements for the degree of Doctor of Philosophy

---

Department of Earth and Planetary Sciences  
McGill University  
Montreal, QC, Canada

© Jethro Sanz-Robinson, 2020



## Abstract

---

Crude oils and the solidified remains of hydrocarbon fluids are commonly found in sediment hosted ore deposits. Little is known, however, of the role that petroleum may play in the formation of these deposits. Here we use an experimental approach to determine whether crude oil may act as an ore fluid for these deposits by dissolving the ore metals from the underlying sediments and transporting them to the site of ore deposition. To this end, the steady-state concentrations of Ni, Zn and Pd in crude oil at 150, 200 and 250°C were determined. The experimental approach involved reacting wires of native metal with a series of crude oils for variable periods of time until metal concentrations were seen to plateau. Metal concentrations were determined by digesting the reacted oils and analyzing the resulting solutions using Inductively-Coupled Plasma Mass Spectrometry (ICPMS). The surface of the reacted metal wires was then analyzed using X-ray Photoelectron Spectroscopy (XPS) to identify the ligands in crude oil that bind to these metals.

The results of these experiments indicate that Pd, Ni and Zn are all highly soluble in crude oil from an ore deposit perspective, reaching concentrations of up to 1700 ppm Zn, 240 ppm Ni and 127 ppb Pd. From the results of the XPS experiments it is evident that Zn solubility is highest as carboxylate complexes in very acidic oils. During catagenesis, these oils may be expelled from their source rocks and injected into carbonate reservoir rocks, where they become altered through reactions with aqueous sulfate to form large volumes of hydrogen sulfide gas. This reaction is referred to as Thermochemical Sulfate Reduction (TSR) and occurs commonly in petroleum carbonate reservoirs and the carbonate-hosted ore zones of Mississippi Valley Type (MVT) deposits, a class of sediment hosted Zn-Pb deposits forming at temperatures between 100 and

140°C. An experiment was devised to emulate the geochemical environment present in the ore zones of MVT deposits by reacting Zn-rich crude oil, with hydrogen sulfide gas and a calcite-buffered brine. Sphalerite (ZnS), the principal Zn ore mineral in MVT deposits, was observed to crystallize from the oil at the oil-brine interface, demonstrating that MVT deposits can be created from petroleum. The composition of the crystals was confirmed using X-ray Diffraction (XRD).

The results of the XPS analyses of the reacted Pd and Ni wires show that these metals are most readily dissolved in crude oil as thiol complexes. Coincidentally, anomalous concentrations of thiols are commonly found in crude oils that have undergone TSR. Moreover, the results of this research indicate that Ni, Fe (and potentially Pd) play a role in catalyzing the reduction of sulfur compounds in crude oil to form thiols. Thus, it is likely that the dissolution of Ni, Fe and Pd in crude oil is not only enhanced by TSR but may also promote the reaction. Furthermore, sediment-hosted deposits containing large concentrations of these metals (e.g., the Kupferschiefer Deposit in Poland and the Talvivaara deposit in Finland) display signs of having interacted with crude oil, and the reduced sulfur in the ore minerals in these deposits appears to have been derived from TSR. It is therefore proposed that during arc-tectonic events, crude oils are generated and travel along faults in sedimentary basins, leaching metals along the way. Reactions between these crude oils and sulfate-bearing sequences are catalyzed by transition metals dissolved in the hydrocarbon liquid. As the reaction proceeds, crude oil is gradually consumed and sulfide ore minerals are precipitated to form a deposit.

## **i. Acknowledgements**

---

First and foremost, I'd like to acknowledge my supervisor Willy, for his guidance and support during my PhD. He showed me that geoscience can be fun and captivating, that it's not worth taking myself too seriously and perhaps most importantly, to always trust my gut. His fearless and adventurous spirit has inspired me to grab life by the horns both inside and outside of the lab and I'm a happier person for it. I cannot thank him enough.

I'd also like to thank those people who worked closely with me towards the completion of my project. Firstly, I'm grateful to Ichiko Sugiyama who showed me the ropes when I first arrived at the lab, helped me run experiments and boosted my morale with her eccentric and humorous style. I'm also very grateful to Prof. Scott Bohle for his friendly support and undying fascination for the natural world. His help was vital in developing the experimental techniques that made my project successful. Similarly, I'd like to express my gratitude to Anna Jung for teaching me how to use the Inductively-Coupled Plasma Mass Spectrometer. She stood by me patiently through innumerable analyses year after year. I'm also very thankful for the support of Kyle Henderson who worked alongside me on the same project. Our discussions during our shared fieldtrips, conferences and presentations have been enlightening and entertaining. I'm also indebted to Equinor who provided me with the oil samples and the funding that made this project possible.

I'm also hugely appreciative to The Department of Earth and Planetary Science at McGill University who provided me with a familial environment during my stay. The comradery, the laughs and the smiles that we have shared made everything worthwhile. I feel blessed to have

been part of such a great department.

Finally, I'd like to thank my family for always having my best interests at heart. Without their unwavering love and support, particularly in times of duress, none of this would have been possible. They will always be the centerpiece of my success.

## ii. Table of Contents

Abstract.....	3
i. Acknowledgements.....	5
ii. Table of Contents.....	7
iii. List of Figures.....	10
iv. List of Tables.....	12
v. Preface and Contributions of Authors.....	13
<hr/>	
1. Introduction.....	14
1.1 Overview.....	15
1.2 Evidence for metal transport by oil in natural systems.....	17
1.2.1 Pb-Zn Mississippi Valley type deposits.....	17
1.2.2 Au and U deposits.....	19
1.2.3 Mercury, Platinum Group Element and copper deposits.....	22
1.2.4 Ni-polyelement deposits.....	24
1.3 Ability of crude oils to dissolve ore metals as a function of oil composition.....	26
1.4 Depositional Mechanisms in sediment-hosted ore deposits.....	31
1.5 References.....	33
<hr/>	
2. The Solubility of Palladium (Pd) in Crude Oil at 150, 200 and 250°C and its Application to Ore Genesis.....	49
2.1 Introduction.....	52
2.2 Crude Oil Characterization.....	54
2.3 Methodology.....	55
2.3.1 Experimental Methods.....	55
2.3.2 Analytical Method.....	56
2.4 Experimental Parameters.....	58
2.4.1 Temperatures of the experiments.....	58
2.4.2 Duration of the experiments.....	58
2.5 Results.....	60
2.5.1 Results from the Palladium Solubility Experiments.....	60
2.5.2 Results of XPS Analyses.....	62
2.6 Discussion.....	64
2.6.1 Factors determining Pd concentration and speciation in crude oil.....	64

2.6.2	The environment of hydrocarbon-associated palladium ore formation .....	66
2.6.3	Evaluation of the potential of crude oils to act as ore fluids for palladium .....	69
2.7	Conclusions.....	71
2.8	Acknowledgements.....	72
2.9	References.....	72
<hr/>		
3.	Zinc solubility, speciation and deposition: A role for liquid hydrocarbons as ore fluids for Mississippi Valley Type Pb-Zn deposits. ....	90
3.1	Introduction.....	92
3.2	Materials and methods .....	94
3.2.1	Crude oil characterization .....	94
3.2.2	The solubility and speciation of zinc in liquid hydrocarbons .....	95
3.2.3	Precipitation of sphalerite from a synthetic zinc-rich oil .....	98
3.3	Results.....	99
3.3.1	Solubility and speciation of Zinc in crude oil.....	99
3.3.2	Precipitation of sphalerite from a Zn-rich oil.....	102
3.4	Discussion .....	104
3.4.1	Factors affecting the solubility and speciation of Zn in crude oil .....	104
3.4.2	The potential of liquid hydrocarbons to act as zinc ore fluids. ....	105
3.4.3	Precipitation of sphalerite from zinc-rich oils.....	107
3.5	Conclusion .....	109
3.6	Acknowledgements.....	110
3.7	References.....	110
<hr/>		
4.	The solubility of Nickel (Ni) in crude oil at 150, 200 and 250°C and its Application to Ore Genesis 126	
4.1	Introduction.....	129
4.2	Materials and Methods.....	131
4.2.1	Crude Oil Characterization .....	131
4.2.2	Solubility and speciation of Nickel in liquid hydrocarbons .....	132
4.3	Results.....	135
4.3.1	Nickel solubility.....	135
4.3.2	Results of X-ray Photoelectron Spectroscopy Analyses .....	137
4.4	Discussion .....	140

4.4.1	Nickel solubility and speciation in liquid hydrocarbons as a function of petroleum composition.....	140
4.4.2	Geochemical factors affecting oil composition and ore deposit formation.....	142
4.4.3	Evidence for the involvement of liquid hydrocarbons in the genesis of shale-hosted nickel deposits.	145
4.5	Conclusions.....	149
4.6	Acknowledgments.....	150
4.7	References.....	150
<hr/>		
5.	Conclusions.....	182
5.1	General Conclusions and Contributions to Knowledge.....	182
5.2	Recommendations for future studies.....	184
5.3	References.....	187

### iii. List of Figures

---

<b>Figure 1.1</b> Typical MVT deposit setting. Modified from Li et al., 2017. ....	18
<b>Figure 1.2</b> Pyrobitumen nodules from the Witwatersrand Carbon Leader lined by gold (Au) with small randomly distributed uraninite (Urn) grains. Nodules are bound by sericite (Ser) and quartz (Qtz). (Fuchs et al., 2016) .....	20
<b>Figure 1.3</b> Typical uraniferous nodule hosted in red-siltstone matrix (Curiale et al, 1983) .....	21
<b>Figure 1.4</b> View of a low-angle breccia from the Culver-Baer deposit containing intergrown cinnabar and petroleum. ....	22
<b>Figure 1.5</b> Cross-section of the Kupferschiefer deposit at the Lubin Mine location showing the vertical distribution of Cu and noble metals in the stratigraphy. The mineralized black shales directly overly a hematite-rich sandstone (Kucha and Przyłowicz, 1999). ....	24
<b>Figure 1.6</b> Stratigraphy at Zunyi Ni-Mo-PGE deposit. The thin Ni-Mo ore bed is comprised within black shales which closely overly a sequence of Precambrian dolostone. ....	25

---

<b>Figure 2.1</b> The experimental protocol employed for the investigation of Pd solubility and speciation in oils A, B, and C at 150, 200 and 250 °C. ....	57
<b>Figure 2.2</b> Concentration of Pd in oils A, B and C at 150, 200 and 250 °C as a function of the duration of the experiments. ....	59
<b>Figure 2.3</b> The maximum Pd solubility (ppb) in crude oils A, B and C versus the thiol content (ppm). ....	61
<b>Figure 2.4</b> An XPS spectrum illustrating the sulfur speciation of residual oil on a palladium wire after reaction with oil C at 150 °C. The thiol peak is resolved into an unbound thiol peak in yellow (~164eV) and a palladium-thiolate peak in green (~162eV). ....	63
<b>Figure 2.5</b> An XPS spectrum for palladium after reaction with crude oil C at 150 °C. The grey doublet correspond to the Pd (II) species whilst the green doublet corresponds to Pd(0). ....	64
<b>Sup. Fig. 2.1</b> Linear extrapolation showing the amount of Pd extracted from the Polish Kupferschiefer every year. ....	86

---

<b>Figure 3.1</b> Concentration of Zn in crude oils A, B and C at 150, 200 and 250 °C as a function of the duration of the experiments. The vertical lines are error bars indicating the experimental uncertainty. ....	98
<b>Figure 3.2</b> Zn solubility (ppm) in crude oils A, B and C versus the oil TAN (mgKOH/g). ....	101
<b>Figure 3.3</b> An XPS spectrum identifying the major elements bound to the Zn wire after reaction with Oil C at 200 °C. The relative abundances of these elements changed as the wire was progressively etched. ....	102
<b>Figure 3.4</b> Reaction vessel containing sphalerite that was precipitated from a 1000 ppm zinc-sulphonate oil. ....	103
<b>Figure 3.5</b> An XRD spectrum for sphalerite precipitated from a 1000 ppm zinc-sulphonate oil. ....	103

**Supplementary Figure 3.1** The experimental setup for the precipitation of sphalerite from a zinc-rich oil.....121

**Supplementary Figure 3.2** Oil TAN versus carboxylic acid content (modified from Meredith et al., 2000).....123

**Figure 4.1** The concentration of Ni (3 S.D.) in crude oils A, B and C at 150, 200 and 250 °C as a function of the duration of the experiments. The vertical lines are error bars indicating the experimental uncertainty..... 135

**Figure 4.2** A XPS spectrum identifying the major elements bound to the Ni wire after reaction with Oil C at 200°C. The relative abundances of these elements changed as the wire was progressively etched. Peak binding energies for the different elements are as follows: S 2p =163eV, C 1S= 285eV, O 1S = 532eV and Ni 2p = 853eV. The peaks between 650eV and 750eV that appear after etching are Ni Auger Lines, resulting from the relaxation of core Ni electrons (Wagner, 1972, Potočnik et. al., 2016)..... 138

**Figure 4.3** An XPS spectrum illustrating the sulfur speciation of residual oil on a nickel wire after reaction with Oil C at a) 200°C and b) ambient temperature. The sulfur 2p peak centered at a binding energy of 163eV corresponds to the thiol functional group whereas the sulfur 2p peak centered at 168eV corresponds to oxidized sulfur compounds. .... 138

**Figure 4.4** An XPS spectrum illustrating the sulfur speciation of residual oil on a nickel wire after reaction with Oil B at a) 200°C and b) ambient temperature. .... 139

**Figure 4.5** An XPS spectrum of the nickel wire after reaction with Oil C at 200°C. Progressive etching revealed the presence of trace amounts of iron. .... 140

**Sup. Fig. 4.1** X-ray photoelectron spectra of the residual oil left on the Ni wire after reaction with Oil A at a) 200° and b) ambient temperature.....169

**Sup Fig. 4.2-4.25** Sulphur(S2p), Iron (Fe2p), Carbon(C1s), Oxygen (O1s) XPS of the residual oil left on the Ni wire after reaction with Oils A, B and C at 150 and 200°C before and after etching.....169

## iv. List of Tables

---

<b>Table 1.1</b> Examples of compounds typically found in crude oil (Tissot and Welte, 1978; Hughley et al, 2004).....	27
<b>Table 2.1</b> The characteristics and compositions of the three crude oils, A, B and C, employed in our experimental study.....	54
<b>Table 2.2</b> A summary of the experimentally determined solubility of Pd in oils A, B and C at 150, 200 and 250 °C. The palladium concentration at 25 °C is the background concentration in the unreacted oils. ....	61
<b>Table 3.1</b> The characteristics and compositions of the three crude oils, A, B and C, employed.	95
<b>Table 3.2</b> The experimentally determined solubility of Zn in crude oils A, B and C at 150, ....	100
<b>Supplementary Table 3.1</b> The composition and properties of the Hibernia Crude oil used in the Conostan® Zn oil standard.....	120
<b>Table 4.1</b> The composition and properties of the three crude oils, A, B and C, employed in our experiments. ....	132
<b>Table 4.2</b> Results of experiments designed to determine the solubility of Ni in crude oils A, B and C at 150, 200 and 250 °C. The Ni concentration at 25°C is the background concentration in the unreacted oil.....	136

## **v. Preface and Contributions of Authors**

---

This thesis contains three manuscripts, which have all been published in the peer-reviewed journal, *Chemical Geology*. The manuscripts report results of experiments designed to determine the solubility and speciation of Pd, Zn and Ni, respectively, in crude oil, and relate the research findings to examples of sediment-hosted deposits that appear to have involved petroleum in their genesis. The petroleum samples and funding for this research were provided by Equinor. The products of all the solubility experiments were analyzed using the Inductively-Coupled Plasma Mass Spectrometer (ICP-MS) at McGill University, and the X-ray Photoelectron Spectroscopic (XPS) experiments used to investigate metal speciation in crude oil were conducted at the McGill Institute for Advanced Materials (MIAM).

The hypothesis that metals can dissolve in ore-forming concentrations in liquid hydrocarbons was proposed by Williams-Jones and tested by Sanz-Robinson, and the first manuscript (Chapter 2), which deals with palladium, was written by Sanz-Robinson and edited by Williams-Jones. The solubility experiments undertaken to ascertain the steady-state concentration of Pd in oil were carried out by Sanz-Robinson with assistance from Sugiyama, based on a method developed by Sanz-Robinson. The metal speciation experiments were carried out by Sanz-Robinson.

The experimental research of Chapter 3 and Chapter 4 was conducted by Jethro Sanz-Robinson in collaboration with A.E. Williams-Jones. Experiments devised to precipitate sphalerite crystals from metalliferous crude oil were conceived and conducted by Sanz-Robinson, the latter with assistance from Sugiyama. X-ray diffraction (XRD) analyses conducted by Sanz-Robinson confirmed the composition of the precipitated crystals. The manuscripts constituting these chapters were written by Sanz-Robinson and edited by Williams-Jones.

**1.**

## **Introduction**

## 1.1 Overview

Sediment-hosted ore deposits account for a significant proportion of the World's zinc (Zn) and copper (Cu) production (Hitzman, et al., 2005; Leach et al., 2005) and are commonly enriched in transition metals such as nickel (Ni), platinum group elements (PGE), lead (Pb), gold (Au), molybdenum (Mo), mercury (Hg), uranium (U) and vanadium (V) (Gu. et al., 2012). These deposits are often discovered in close spatial proximity to petroleum both on the regional and microscopic scale. On a regional scale, sediment-hosted deposits such as the Zn deposits of the Canning Basin in northern Australia, the Kupferschiefer deposit in Poland, the Zunyi Ni-Mo-PGE deposit in southern China and the Hg deposits of California all occur near petroleum systems, the source rocks of which are pre-to-syn-genetic in age with respect to the ore mineralization (Peabody and Einaudi, 1992; Gautier, 2003; EIA 2011; EIA, 2015). Most of these deposits display signs of having interacted with petroleum on a much smaller scale, in some cases with liquid hydrocarbon inclusions occurring within the ore minerals (Kelly and Nishioka, 1985; Etminan and Hoffman, 1989; Peabody and Einaudi, 1992).

Most researchers consider that the ore metals in the above deposits were transported as aqueous complexes in hydrothermal fluids to the site of ore formation and deposited as sulfide minerals in response to changes in physicochemical conditions (e.g., Coveney and Nansheng, 1991; Loukola-Ruskeeniemi and Heino, 1996; Williams-Jones et al., 2009). The presence of petroleum inclusions in these ore minerals, however, may indicate that the ore fluid was petroleum rather than a hydrothermal fluid. Support for this idea is provided by the observation that crude oils (natural liquid hydrocarbons) can be significantly enriched in ore metals, containing as much as 1580 ppm V, 105 ppm Ni, 160 ppm Zn, 11.7 ppm Cu, 2.1 ppm Pb, 10.1 ppm Mo and 3 ppb Au

(Jones, 1975). Furthermore, experiments have shown that saturated hydrocarbons, such as octane that are an important component of crude oil, can dissolve large amounts of Hg (up to 821ppm at 200°C), which is consistent with the common occurrence of petroleum in epithermal Hg deposits (Meidaner et al., 2005). It also has been shown that Au and U can dissolve in crude oil at temperatures between 200 and 300°C in concentrations (~50ppb Au and 300ppb U) comparable to those thought to be necessary for ore formation (Migdisov et al., 2017). In addition, Au has been shown to partition strongly into thiol-rich oils over saline brines under ore-forming temperatures, indicating that oils rather than brines may serve as ore fluids in sediment-hosted Au deposits (Crede et al., 2019). Finally, it is noteworthy that some organic carbon-rich shale-hosted deposits contain percentage level concentrations of Ni (Coveney and Nansheng, 1991; Orberger et al., 2003 Jowitt and Keays, 2011), a metal that is relatively insoluble in aqueous fluids, even at elevated temperatures (Liu, 2012), and is therefore unlikely to be concentrated by hydrothermal processes.

Despite abundant evidence indicating a direct spatio-temporal relationship between the injection of crude oil and the mineralization in many sediment-hosted ore deposits (e.g., metal-enriched bitumen veins within or proximal to the ores; Emsbo and Koenig, 2007; Henderson et al., 2019), the accepted wisdom is that the ore metals in these deposits are either precipitated during sedimentation or during diagenesis or at a much later time, in all cases by hydrothermal fluids (Coveney and Nansheng, 1991; Loukola-Ruskeeniemi and Heino, 1996; Jowitt and Keays, 2011). Petroleum systems and sediment-hosted deposits may be more closely related than previously thought and studying the link between them will lead to a broader understanding of

the processes that simultaneously control ore mineralization, petroleum composition, basin evolution and the cycling of trace metals in the geosphere.

## **1.2 Evidence for metal transport by liquid hydrocarbons in natural systems.**

### **1.2.1 Pb-Zn Mississippi Valley type (MVT) deposits**

Sediment-hosted deposits contain the world's largest Pb and Zn resources and a significant number of these deposits, particularly those belonging to the MVT deposit class, display a close association with bitumen and petroleum (Anderson and Macqueen, 1982; Leach et al., 2005).

Mississippi Valley Type deposits are a class of carbonate hosted Zn-Pb deposits that typically form on the flanks of sedimentary basins, orogenic forelands or foreland thrust belts inboard of clastic rock-dominated passive margin sequences (Leach et al., 2010). The temperatures at which MVT deposits commonly form (100-150 °C) (Anderson and Macqueen, 1982; Parnell, 1988) overlap to a large extent with the temperatures corresponding to petroleum maturation and expulsion (80 - 160 °C; Peters et al., 2004) and the major element compositions, salinities, D/H and  $^{18}\text{O}/^{16}\text{O}$  ratios, and temperatures of MVT ore-forming brines closely resemble those of oil-field brines (Sverjensky, 1986).

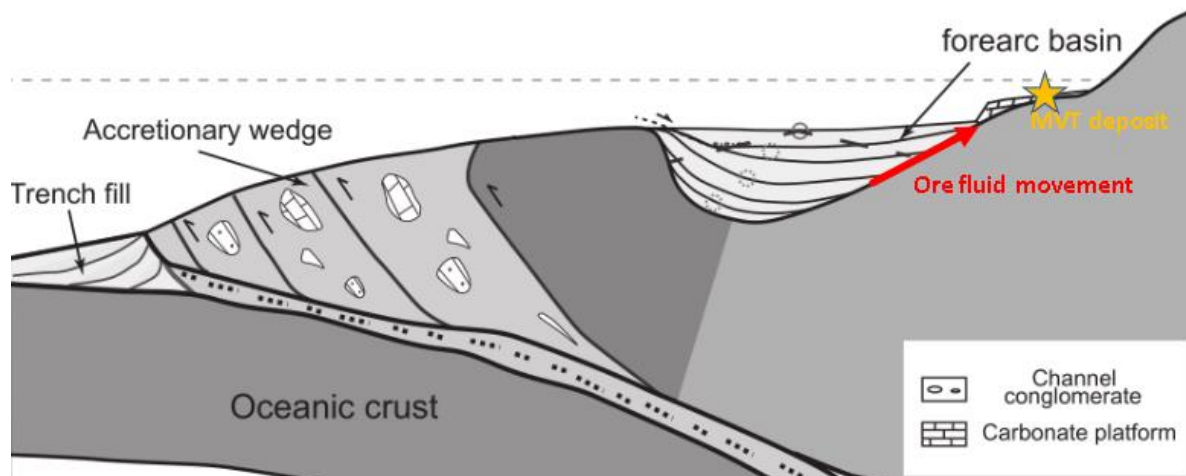


**Figure 1.1** Typical MVT deposit setting. Modified from Li et al., 2017.

The ore metals of MVT deposits are generally thought to be transported to the site of ore deposition as chloride complexes in basinal brines (Kesler et al., 1995; Leach et al., 2010). Recent evidence, however, from a study of the world-class Laisvall Zn-Pb MVT deposit in Sweden highlights the potential importance of crude oil as an ore fluid for this class of deposits (Saintilan et al., 2019). Based on the Pb isotopic ratios of bitumen intergrown with the ores, galena and sphalerite from the Laisvall deposit, organic matter in the underlying Alum shale and the granitic basement, Saintilan et al. (2016, 2019) were able to show that the ores and intergrown bitumen lie on a mixing line limited at one end by the organic matter of the Alum shale and at the other end by the granitic basement. This allowed them to conclude that ~ 50% of the Pb came from the organic matter of the Alum shale and that it had been transported by petroleum from this source, the residues of which are preserved as bitumen in the deposit. This example provides compelling evidence that petroleum is potentially an effective fluid for the transport and re-concentration of Pb in MVT ore-forming systems.

In addition to Laisvall, the ore zones of several other MVT deposits have also been infiltrated by petroleum. These include the Gays River deposit in Nova Scotia, the San Vincente deposit in Peru and the MVT deposits of the Canning Basin in Australia (Gize and Barnes, 1987; Etminan and Hoffman, 1989; Spangenberg, 1999). In the case of the Canning basin, several MVT deposits have been found to contain sphalerite (ZnS) ore that host a large number of liquid hydrocarbon inclusions (Etminan and Hoffman, 1989). These hydrocarbons are compositionally different from and more mature than other hydrocarbons sourced from the same formation, indicating that they likely entered the carbonate host rocks from an external source contemporaneously with MVT Zn-Pb mineralization (Wallace et al., 2002). These examples provide evidence that petroleum may also be responsible for the transport of the Zn concentrated in MVT deposits.

### **1.2.2 Au and U deposits**

Several sediment hosted Au and U deposits also display a close association with petroleum. For example, the Carlin-Type Au deposits of the Alligator Ridge in Nevada contain abundant oil-bearing inclusions that can be found in calcite and realgar ( $As_4S_4$ ) veins that encircle the ore. Free oil also infills vugs and fractures in the limestones proximal to the ore zone (Hulen and Collister 1999). Similarly, veins of pyrobitumen in the El Rodeo deposit in Nevada can contain up to 100 ppm Au and may be the relic of solidified hydrocarbon ore fluids (Emsbo and Koenig, 2007; Williams-Jones et al., 2009).

Another mining district where gold is intimately associated with hydrocarbons is the Witwatersrand (South Africa), where 40% of the gold is in reefs with carbon seams, many of

which contain in excess of 1000 ppm Au (Williams-Jones et al., 2009). The carbon seams also host much of the U ore at the Witwatersrand deposit which occurs as nanoparticles of uraninite ( $\text{UO}_2$ ) that are uniform in size (5-7nm) and aggregate to form clusters 10s of microns in diameter. It has been proposed that these clusters represent the residues of hydrocarbon liquids that transported U in solution or as nanoparticles in suspension (Fuchs et al., 2015). Independent evidence of such liquids is provided by the presence of hydrocarbons preserved as fluid inclusions in overgrowths on detrital quartz grains from the deposit (England et al., 2002; Fuchs et al, 2016). The carbon seams at the Witwatersrand deposit are now generally considered to represent residues from the migration of liquid hydrocarbons (Williams-Jones et al., 2009).

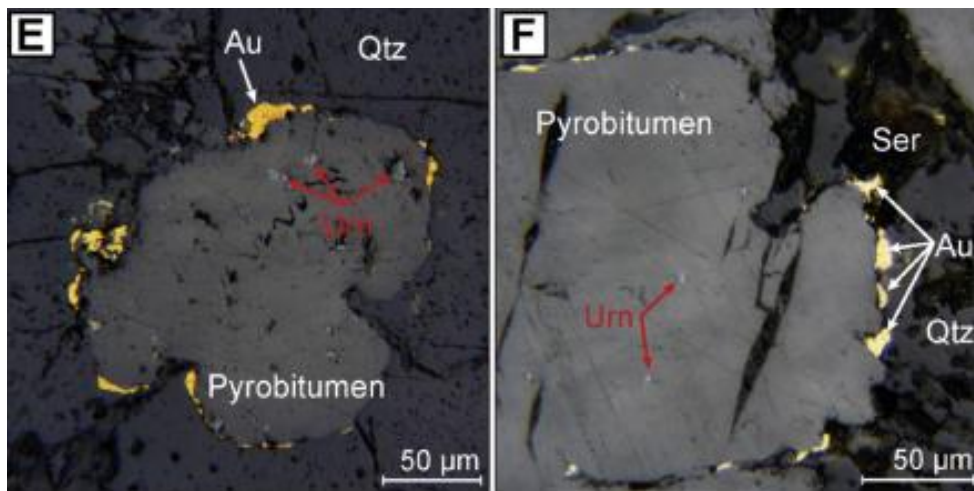


**Figure 1.2** Pyrobitumen nodules from the Witwatersrand Carbon Leader lined by gold (Au) with small randomly distributed uraninite (Urn) grains. The nodules are bound by sericite (Ser) and quartz (Qtz). (Fuchs et al., 2016)

Sandstone-hosted deposits are also known to contain large quantities of bitumen and U and are particularly abundant in Utah and Colorado (Parnell, 1988). The hydrocarbons from these deposits are probably petroleum derivatives, as there are rapid lateral transitions within the same formation between uraniferous hydrocarbons, solid non-uraniferous hydrocarbons and petroleum

(Parnell and Eakin, 1987). There are also many cases of U mineralization in red beds that are concentrated in and around accretionary nodules of replacive organic matter. Although the ore grades are not high enough to constitute ore deposits, many such nodules are still significantly enriched in U, Cu, V and other metals in multiple locations around the world (e.g., Harrison, 1970; 1975; Curiale et al. 1983). Based on carbon isotope measurements performed on Permian red beds in Oklahoma, Curiale et al. (1983) proposed that the bitumen in these replacive uraniferous nodules was derived from petroleum which most likely leaked into the red beds from deep reservoirs. Nonetheless, much research needs to be conducted to determine whether the metalliferous bitumen in these deposits represents the solidified remains of migrated metal-rich hydrocarbon fluids or in-situ generated bitumen, participated only in the deposition of ore metals but not in their transport. Although it has been long thought that the role of petroleum or bitumen in these deposits is that of a reductant promoting the precipitation of ore metals from the hydrothermal fluid, the notion that petroleum may serve as an ore fluid in the formation of these deposits remains relatively unexplored (Parnell 1988, Migdisov et al., 2017).

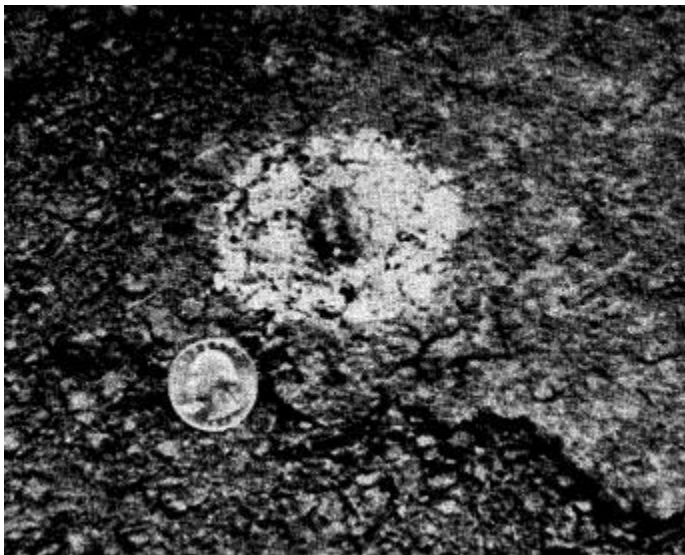


**Figure 1.3** Typical uraniferous nodule hosted in red-siltstone matrix (Curiale et al, 1983)

### 1.2.3 Mercury, Platinum Group Element and copper deposits

The occurrence of oil or bitumen is commonplace in Hg ore deposits from around the world (Parnell, 1988). For example, small amounts of petroleum occur in numerous cinnabar (HgS) deposits that extend for up to 600 km along the Coast Range of California. In some cases, such as at the Culver-Baer deposit in California, petroleum is intergrown with cinnabar. High concentrations of Hg are also present in petroleum of the Cymric oil field of the San Joaquin Valley adjacent to the cinnabar deposits, implying a genetic relation between the two (Peabody and Einaudi, 1992).

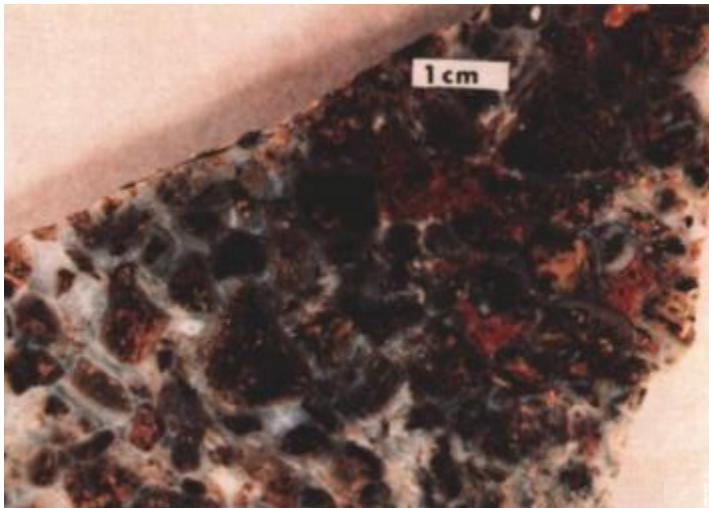


**Figure 1.4** View of a breccia from the Culver-Baer deposit containing intergrown cinnabar and bitumen.

Liquid hydrocarbons may have also been involved in the formation of the epithermal deposit exploited briefly at the Boss Mine, Nevada, in the early part of the 20th century, where percentage level concentrations of Pd and Hg (1.85 wt. % Pd, 0.89wt% Au+Pt and 5.83wt% Hg) were present in bitumen contained within siliceous ore shoots that fractured a horizontal stratum of dolomite. The precious metals occur as nanoparticles of the alloy Potarite ((Pd, Au, Pt) Hg)

that are dispersed within the bitumen matrix. It is thought that the bitumen represents relicts of liquid hydrocarbons that impregnated the fossiliferous calcareous country rocks (Jedwab et al., 1999). The fact that mineralization is contained within the bitumen may indicate that the ore metals were transported in a liquid hydrocarbon medium.

In addition to the deposit exploited at the Boss Mine, very high PGE concentrations (up to 5000 ppm Pd and 1770 ppm Pt) have been reported for bitumen in the Kupferschiefer deposit in Poland (Kucha and Przyłowicz, 1999). The bitumen associated with the ore in the Kupferschiefer deposit contains abundant polyaromatic sulfur hydrocarbons (PASH), a class of compounds commonly found in crude oil, suggesting that petroleum may have infiltrated the system from the underlying strata (Püttmann and Goßel, 1990).

In addition to hosting considerable PGE resources, the Kupferschiefer is a world-class copper deposit (Kucha and Przyłowicz, 1999). A significant number of sediment-hosted copper deposits worldwide, including the Kupferschiefer, occur close to the interface between red beds and oil shale sequences (Eugster, 1985). In some cases, such as the White Pine deposit in Michigan, liquid oil is trapped as primary fluid inclusions in calcite crystals in late Cu-Fe sulfide-bearing veins that crosscut the cupriferous black shales, indicating that petroleum likely exerted an important control on the copper mineralization (Kelly and Nishioka, 1985).

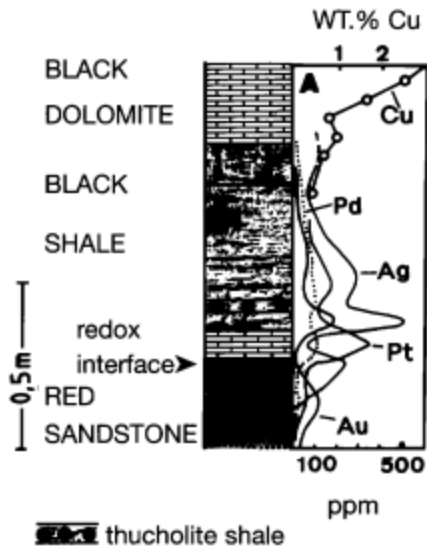


**Figure 1.5** Cross-section of the Kupferschiefer deposit at the Lubin Mine location showing the vertical distribution of Cu and noble metals in the stratigraphy. The mineralized black shales directly overlie a hematite-rich sandstone (Kucha and Przyłowicz, 1999).

#### 1.2.4. Ni-polymetal deposits

Nickel is one of the metals that is most commonly associated with petroleum in which it is known to reach concentrations  $> 100\text{ppm}$  (Jones, 1975). There are several Ni deposits that are hosted in black shales with good petroleum producing potential, these include the hyper enriched black shales (HEBS) of the Selwyn Basin in Yukon Canada, the Zunyi deposit in Southern China and the Talvivaara deposit in Finland. The Ni-Mo sulfide beds hosted in the black shales of the Selwyn and the Zunyi deposit closely resemble each other. In both deposits, the sulfide bed is usually only ~5-15 cm thick but contains several weight percent Ni and Mo (Coveney and Nansheng, 1991). Blebs of migrabitumen occur exclusively in the ore zone of the Zunyi deposit, indicating that brecciation by a petroleum fluid may have occurred during catagenesis (Křibek et al, 2007). Likewise, bitumen dykes found below the enriched sulfide bed at Nick Prospect in the

Yukon HEBS may indicate that hydrocarbon-rich ore fluids were being debouched into the ore zone (Hulbert et al, 1992).

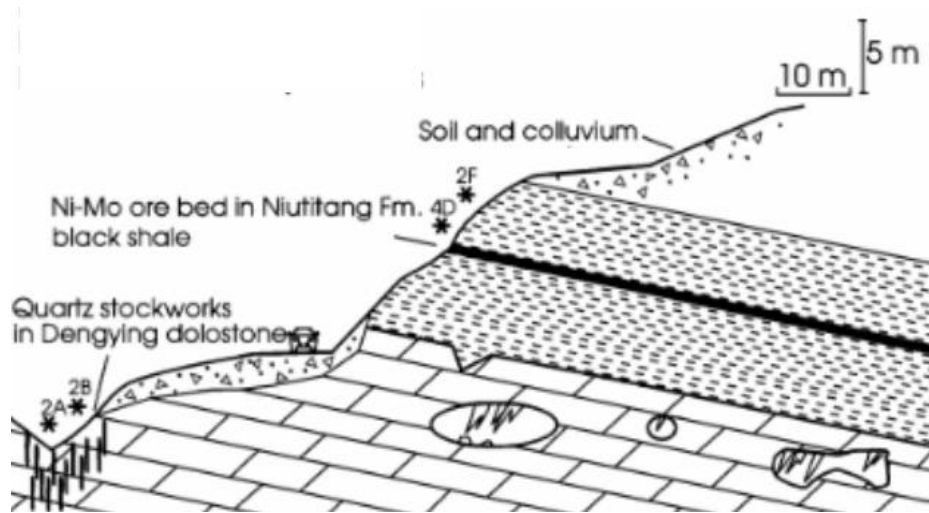


**Figure 1.6** Stratigraphy at the Zunyi Ni-Mo-PGE deposit. The thin Ni-Mo ore bed occurs within black shales which overlie a sequence of Precambrian dolostone.

Based on the abundance of framboidal pyrite in the ore zones of the South China and Yukon HEBS, it has been argued that the ores were produced through the metabolic action of microbes at the sediment water interface, which concentrated Ni from the overlying seawater column (Gadd et al., 2018, and 2019). However, framboidal pyrites can also form abiotically (Scott et al., 2009) and furthermore the millerite (NiS) ore in these deposits ‘mantles’ the pyritic framboids indicating that it was introduced epigenetically into the ore system (Gadd et. al., 2019). Given the low solubility of Ni in hydrothermal fluids it is much more likely that the Ni was introduced into the system in a hydrocarbon fluid. In addition, the concentration of Ni in seawater is very low (Kato et al., 1990) making it unlikely that sufficient Ni could concentrate from microbial processes alone to form a deposit with the percentage level Ni contents observed in the South China and Yukon HEBS.

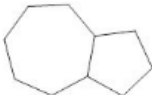
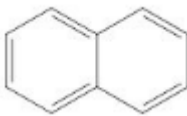
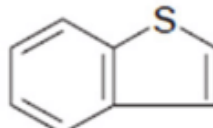
The black shale (black schist) hosted sulfide ore of the Talvivaara deposit is of much lower relative grade than the Zunyi deposit and Nick prospect (averaging 0.26 wt% Ni, 0.14 wt% Cu, and 0.53 wt% Zn), but is up to 330m thick and contains 300 million metric tons of ore (Loukola-Ruskeeniemi, K. and Heino, T., 1996). Uraninite crystals in the Talvivaara deposit are rimmed by bitumen that has been interpreted as evidence for the migration of hydrocarbons through the ore zone (Lecomte et al, 2014). The Talvivaara black schists were deposited 2.0-1.9Ga coincident with the Shunga event, a time marked by a worldwide accumulation of organic matter and the formation giant oilfields in Russian Fennoscandia (Melezhik et al, 2009).

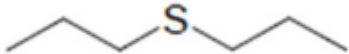
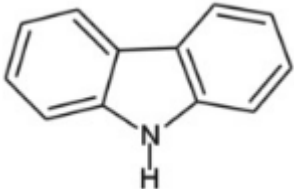
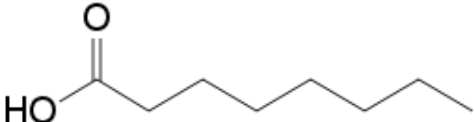
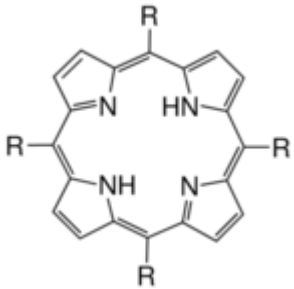
### **1.3 Compositional controls on the dissolution of metals by crude oils.**

Crude oils are composed largely of saturated and aromatic hydrocarbons with minor amounts of thiophenoaromatics, sulfides, neutral nitrogen, and polar compounds. The polar compounds (also referred to as NSO compounds) contain one or more heteroatoms of nitrogen(N), sulfur(S) or oxygen(O) and, although they typically compose less than 10 wt% of petroleum, they are commonly found to be complexed with metals. (Hughley et al., 2004). Bacterial biodegradation is regarded as an effective means for increasing the NSO and metal content of oils in reservoirs cooler than approximately 80°C. Petroleum soluble compounds of Zn, Cu, Ni, Ti, Ca, and Mg adsorb selectively at petroleum-water interfaces and are thought to be derived from bacterial metalloproteins that become incorporated into oil during biodegradation and early diagenesis (Dodd et al., 1952). It has long been observed that fresh, oxygenated waters in contact with reservoir oil can cause extensive aerobic biodegradation. More recently, it has been recognized

that anaerobic sulfate reducing and fermenting bacteria can also degrade petroleum (Wenger et al., 2002) and in doing so may incorporate polar ligands into oil that promote the dissolution of ore metals (Vairavamurthy and Mopper, 1987; Meredith et al, 2003) as occurs in modern-day sapropelic sediments. Likewise, reactions occurring at the oil-water interface between mineral oxidants like hematite ( $\text{Fe}_2\text{O}_3$ ) and sulfate-bearing minerals such gypsum ( $\text{CaSO}_4$ ) have been shown to contribute to an increase in the carboxylic acid and thiol content of crude oils, both of which are potentially effective ligands for the complexation of ore metals (Ho et al., 1974, Surdam et al, 1993, Giordano, 1994).

**Table 1.1** Examples of compounds typically found in crude oil (Tissot and Welte, 1978; Hughley et al, 2004).

Type of compound	
Saturated hydrocarbons	<div style="display: flex; justify-content: space-around; align-items: center;"> <div style="text-align: center;">  <p>Paraffins</p> </div> <div style="text-align: center;">  <p>Napthenes</p> </div> </div>
Aromatic Hydrocarbons	<div style="text-align: center;">  </div>
Thiophenoaromatics	<div style="text-align: center;">  </div>

Sulfides		
Neutral Nitrogen Compounds		
Polar Compounds	Carboxylic acids	
	Porphyrins	
	Thiols	

Metals are present in crude oils at concentrations from a few parts-per-billion in conventional light stocks to hundreds of parts-per-million in heavy crudes; the most abundant elements being Ni, V and Fe. Other metals commonly found in oils, such as Pb, Ba, Sn, Ag, Co, Cu, Mo, Ti and Zn, are mostly present in the 1–50 ppm range (Caumette et al., 2009). The ability of crude oils to dissolve and transport metals is dependent on the availability of specific metal-binding ligands. For example, NSO compounds are known for their ability to form metal organic complexes in crude oil and are most abundant in relatively immature, biodegraded oils (Hughley et al., 2004). Such oils tend to be viscous and rich in asphaltenes, a fraction of petroleum composed of large heterocyclic molecules, which result from the early breakdown of kerogen (Orr, 1986). One of the principal classes of metal species commonly associated with the asphaltene fraction of petroleum is metalloporphyrins (Caumette et al., 2009). Porphyrins are macrocyclic aromatic compounds composed of four pyrrole rings connected by methine bridges that bind mainly to Ni, V, Fe or Cu in crude oil via N-metal bonds (Caumette, 2009; Ptaszek, 2013). Petroleum porphyrins are derived from porphyrins and porphyrin-related molecules that are ubiquitous in living organisms, such as hemes (iron-containing porphyrins), chlorophylls or bacteriochlorophylls (Mg-containing porphyrins). During oil maturation most of the metals originally present in the porphyrins are replaced predominantly by Ni (II) or V(IV) oxide (Caumette et al., 2009).

Aside from porphyrins, which have been extensively studied, little is known about the other kinds of metal organic complexes that form in petroleum. These complexes are potentially more abundant than the metalloporphyrins and may account for up to 50–80% of the metal being complexed in oil (Caumette et al., 2009). It has been suggested that organic O and S ligands such

as carboxylic acids and thiols may promote the dissolution of metals in ore fluids from sediment-hosted deposits (Giordano, 1994). These ligands are present in petroleum, frequently in high concentrations. For example, crude oils from the Muglad basin in Sudan have been reported to contain up to 8620 ppm carboxylic acids (Chapter 4, Supplementary Materials) and the Rodney Crude in Canada up to 3179 ppm thiols (Chapter 2, Supplementary Materials). Although Zn, Ca, Mg and Ti- carboxylate complexes are known to occur in petroleum (Caumette et al., 2009), to our knowledge, the occurrence of metal thiolate complexes in petroleum has not yet been reported. Nonetheless, thiols are recognized for their ability to bind to sulfide minerals with relative ease, even at room temperature (Bradshaw et al., 1995; Goh et al, 2008; McFadzean et al., 2013) and thiol complexes of metals such as Hg, Cu, Ni and Au in humic acids are known to have exceptionally high stability constants (Vlassopoulos et al., 1990). Thus, crude oils that are enriched in thiols may be effective at scavenging pre-existing metal sulfides from the sediments. According to the HSAB (Hard and Soft Acid and Base) theory, thiols are a ‘soft’ ligand, that is to say that they are polarizable because of their high mass to charge ratio (Pearson, 1963) and are therefore expected to form stable bonds with ‘soft’ polarizable metals such the PGEs and Au.

Biodegradation is generally known to increase the sulfur and carboxylic acid content of oils (Meredith et al, 2000) and biodegradation of organic matter by sulfate reducing bacteria, is responsible for the production of thiols in marine sediments (Vairavamurthy and Mopper, 1987), which may eventually serve as source rocks for a thiol-enriched oil. Petroleum acidity can also be increased during catagenesis through reactions with water and mineral oxidants such as hematite (Surdam et al, 1993). These sorts of reactions may have occurred in mineral deposits like White Pine or the Kupferschiefer, where mineralized oil shales directly overlie a sequence of

red beds. During maturation, these shales could be expected to generate a high acidity petroleum ore fluid at the interface with the red beds which would in theory be effective for scavenging certain ore metals such as Zn (Caumette et al., 2009). In contrast, anomalously thiol-rich oils form as the result of Thermochemical Sulfate Reduction (TSR), an abiotic reaction between aqueous sulfate and petroleum that takes place in deep carbonate reservoirs (Ho et al, 1974; Cai et al, 2003; Wei et al, 2011; Nguyen et al 2013) at onset temperatures between 100-140°C (Machel, 2001). These thiol-rich oils could potentially serve as effective ore fluids for the transport of ‘soft’ metals like the PGEs and Au, and even a “borderline” metal like Ni.

#### **1.4 Depositional Mechanisms in sediment-hosted ore deposits**

A reaction that is known to occur in both petroleum reservoirs and ore-forming systems is Thermochemical Sulfate Reduction (TSR). During TSR, organic matter (kerogen, petroleum or gas) reacts with aqueous sulfate to produce carbon dioxide and H<sub>2</sub>S gas. The H<sub>2</sub>S gas so produced is known to further react with hydrocarbons, resulting in crude oils and condensates that are highly enriched in thiols (Ho et al, 1974; Cai et al, 2003; Wei et al, 2011; Nguyen et al 2013). Oils commonly undergo TSR in deep anhydrite-rich, carbonate reservoirs with onset temperatures between 100 and 140°C (Machel, 2001). In the case of the Puguang gas fields in China, TSR is thought to have occurred at a depth of 7000 m before uplift led to the present-day reservoir depth of 5000–5500m (Hao et al., 2008). Thermochemical Sulfate Reduction also commonly occurs in the carbonate-hosted ore zones of MVT deposits, where the production of H<sub>2</sub>S gas causes sphalerite (ZnS) and galena (PbS) to precipitate from the ore fluid (Machel, 2001). Most researchers consider that the ore fluids for MVT deposits are basinal brines. Based on the results of the research described in this thesis, it is proposed, instead, that the Pb and Zn in

these deposits were transported as polar complexes in petroleum and furthermore that these metals may be deposited from a petroleum in the presence of H<sub>2</sub>S gas as galena and sphalerite, respectively. This latter hypothesis is investigated in Chapter 4.

Thermochemical sulfate reduction may also be relevant to the formation of other sediment-hosted deposits. Evidence for this is provided by the reduced sulfur products of TSR experiments carried out between sulfate and organic compounds (glycine and alanine) at temperatures of 150-200°C, which show similar mass-anomalous fractionation ( $\Delta^{33}\text{S} = > 0 \pm 0.2 \text{ ‰}$ ) to the sulfide ore and organic sulfur extracted from the shale-hosted polymetallic Talvivaara deposit. Thus, it is thought that the TSR reaction was the main source of reduced sulfur for the Talvivaara sulfide ore (Young et al, 2013). Thermochemical sulfate reduction has also been proposed as a source of reduced sulfur for the sulfide ore at the Kupferschiefer deposit in Poland (Bechtel and Püttmann, 1991; Sun, 1998; Oszczepalski, 1999; Sun, and Püttmann, 2000).

It is possible that the reduced sulfur in these sediment-hosted deposits could also have been produced at low temperature (< 80 °C) by the action of sulfate-reducing bacteria at the sediment-water interface, resulting in the precipitation of ore metals directly from seawater (Jowitt and Keays, 2011). The relative importance of TSR and microbial sulfate reduction in the formation of the sulfide ores, however, is a subject of ongoing discussion (Machel 2001; Watanabe, 2009).

The link between petroleum systems and sediment-hosted deposits is potentially important but poorly understood and warrants further investigation. Thus, the central goal of this project is to better understand the processes that promote the dissolution of ore metals in liquid hydrocarbons

and likewise elucidate how metals can be precipitated from oil under changing physicochemical conditions to create a highly concentrated ore deposit.

## 1.5 References

Anderson, G.M. and Macqueen, R.W., 1982. Ore deposit models-6. Mississippi Valley-type lead-zinc deposits. *Geoscience Canada*, **9(2)**.

Bechtel, A. and Püttmann, W., 1991. The origin of the Kupferschiefer-type mineralization in the Richelsdorf Hills, Germany, as deduced from stable isotope and organic geochemical studies. *Chemical Geology*, *91*(1), pp.1-18.

Bradshaw, D.J., Cruywagen, J.J. and O'connor, C.T., 1995. Thermochemical measurements of the surface reactions of sodium cyclohexyl-dithiocarbamate, potassium n-butyl xanthate and a thiol mixture with pyrite. *Minerals Engineering*, *8*(10), pp.1175-1184.

Cai, C., Worden, R.H., Bottrell, S.H., Wang, L. and Yang, C., 2003. Thermochemical sulphate reduction and the generation of hydrogen sulphide and thiols (mercaptans) in Triassic carbonate reservoirs from the Sichuan Basin, China. *Chemical Geology*, *202*(1-2), pp.39-57.

Cammack, R., 1992. Iron—Sulfur Clusters in Enzymes: Themes and Variations. In *Advances in inorganic chemistry*(Vol. 38, pp. 281-322). Academic Press.

Caumette, G., Lienemann, C.P., Merdrignac, I., Bouyssi re, B. and Lobinski, R., 2009. Element speciation analysis of petroleum and related materials. *Journal of Analytical Atomic Spectrometry*, 24(3), pp.263-276.

Crede, L.S., Evans, K.A., Rempel, K.U., Grice, K. and Sugiyama, I., 2019. Gold partitioning between 1-dodecanethiol and brine at elevated temperatures: Implications of Au transport in hydrocarbons for oil-brine ore systems. *Chemical Geology*, 504, pp.28-37.

Coveney, R.M. and Nansheng, C., 1991. Ni-Mo-PGE-Au-rich ores in Chinese black shales and speculations on possible analogues in the United States. *Mineralium Deposita*, 26(2), pp.83-88.

Curiale, J.A., Bloch, S., Rafalska-Bloch, J. and Harrison, W.E., 1983. Petroleum-related origin for uraniferous organic-rich nodules of southwestern Oklahoma. *AAPG Bulletin*, 67(4), pp.588-608.

Disnar, J.R. and Sureau, J.F., 1990. Organic matter in ore genesis: Progress and perspectives. *Organic Geochemistry*, 16(1-3), pp.577-599.

Dodd, C.G., Moore, J.W. and Denekas, M.O., 1952. Metalliferous Substances Adsorbed at Crude Petroleum—Water Interfaces. *Industrial & Engineering Chemistry*, 44(11), pp.2585-2590.

EIA, 2011. World Shale Gas Resources: an Initial Assessment of 14 Regions Outside the United States. U.S. Department of Energy, Washington. DC.

EIA (2015). Technically recoverable Oil and Shale Gas Resources: Australia. Washington D.C.

Emsbo, P. and Koenig, A.E., 2007, August. Transport of Au in petroleum: evidence from the northern Carlin trend, Nevada. In *Proceedings of the 9th Biennial SGA Meeting, Dublin*. Millpress (pp. 695-698).

England, G.L., Rasmussen, B., Krapez, B. and Groves, D.I., 2002. Archaean oil migration in the Witwatersrand Basin of South Africa. *Journal of the Geological Society*, 159(2), pp.189-201.

Eugster, H.P., 1985. Oil shales, evaporites and ore deposits. *Geochimica et Cosmochimica Acta*, 49(3), pp.619-635.

Fuchs, S., Schumann, D., Williams-Jones, A.E. and Vali, H., 2015. The growth and concentration of uranium and titanium minerals in hydrocarbons of the Carbon Leader Reef, Witwatersrand Supergroup, South Africa. *Chemical Geology*, 393, pp.55-66.

Fuchs, S., Williams-Jones, A.E., Jackson, S.E. and Przybylowicz, W.J., 2016. Metal distribution in pyrobitumen of the Carbon Leader Reef, Witwatersrand Supergroup, South Africa: Evidence for liquid hydrocarbon ore fluids. *Chemical Geology*, 426, pp.45-59.

Gadd, M. G., and Peter, J. M., 2018, Field observations, mineralogy and geochemistry of Middle Devonian Ni-Zn-Mo-PGE hyper-enriched black shale deposits, Yukon, in Rogers, N., ed.,

*Targeted Geoscience Initiative: 2017 report of activities, volume 1; Geological Survey of Canada, Open File 8358, p. 193-206.*

Gadd, M. G., Peter, J. M., Jackson, S. E., Yang, Z., and Petts, D., 2019, Platinum, Pd, Mo, Au and Re deportment in hyper-enriched black shale Ni-Zn-Mo-PGE mineralization, Peel River, Yukon, Canada: *Ore Geology Reviews*, v. 107, p. 600-614.

Gautier, D.L., 2003. *Carboniferous-Rotliegend total petroleum system description and assessment results summary* (p. 29). USGS Bulletin, 2211.

Gize, A.P. and Barnes, H.L., 1987. The organic geochemistry of two Mississippi Valley-type lead-zinc deposits. *Economic Geology*, **82(2)**, pp.457-470.

Giordano, T.H., 1994. Metal transport in ore fluids by organic ligand complexation. In *Organic acids in geological processes*(pp. 319-354). Springer, Berlin, Heidelberg.

Goldstein, T. and Aizenshtat, Z., 1994. Thermochemical sulfate reduction a review. *Journal of Thermal Analysis and Calorimetry*, **42(1)**, pp.241-290.

Goh, S.W., Buckley, A.N., Gong, B., Woods, R., Lamb, R.N., Fan, L.J. and Yang, Y.W., 2008. Thiolate layers on metal sulfides characterised by XPS, ToF-SIMS and NEXAFS spectroscopy. *Minerals Engineering*, **21(12-14)**, pp.1026-1037.

Gu, X.X., Zhang, Y.M., Li, B.H., Dong, S.Y., Xue, C.J. and Fu, S.H., 2012. Hydrocarbon-and ore-bearing basinal fluids: a possible link between gold mineralization and hydrocarbon accumulation in the Youjiang basin, South China. *Mineralium Deposita*, 47(6), pp.663-682.

Hao, F., Guo, T., Zhu, Y., Cai, X., Zou, H. and Li, P., 2008. Evidence for multiple stages of oil cracking and thermochemical sulfate reduction in the Puguang gas field, Sichuan Basin, China. *AAPG bulletin*, 92(5), pp.611-637.

Harrison, R.K., 1970. Hydrocarbon-bearing nodules from Heysham, Lancashire. *Geological Journal*, 7(1), pp.101-110.

Harrison, R.K., 1975. Concretionary concentrations of the rarer elements in Permo-Triassic red beds of south-west England. *Bulletin of the Geological Survey of Great Britain*, 52, pp.1-26.

Henderson, K.M., Williams-Jones, A.E. and Clark, J.R., 2019. Metal transport by liquid hydrocarbons: Evidence from metalliferous shale and pyrobitumen, Yukon. In Targeted Geoscience Initiative: 2018 Report of Activities (pp. 179-187).

Hitzman, M., Kirkham, R., Broughton, D., Thorson, J. and Selley, D., 2005. The sediment-hosted stratiform copper ore system. *Economic geology*, 100.

Ho, T.Y., Rogers, M.A., Drushel, H.V. and Koons, C.B., 1974. Evolution of sulfur compounds in crude oils. *AAPG Bulletin*, 58(11), pp.2338-2348.

Hughey, C.A., Rodgers, R.P., Marshall, A.G., Walters, C.C., Qian, K. and Mankiewicz, P., 2004. Acidic and neutral polar NSO compounds in Smackover oils of different thermal maturity revealed by electrospray high field Fourier transform ion cyclotron resonance mass spectrometry. *Organic geochemistry*, 35(7), pp.863-880.

Hulbert, L.J., Gregoire, D.C., Paktunc, D. and Carne, R.C., 1992. Sedimentary nickel, zinc, and platinum-group-element mineralization in Devonian black shales at the Nick property, Yukon, Canada: a new deposit type. *Exploration and Mining Geology*, 1(1), pp.39-62.

Hulen, J.B. and Collister, J.W., 1999. The oil-bearing, carlin-type gold deposits of Yankee Basin, Alligator Ridge District, Nevada. *Economic Geology*, 94(7), pp.1029-1049.

Jedwab, J., Badaut, D. and Beaunier, P., 1999. Discovery of a palladium-platinum-gold-mercury bitumen in the Boss Mine, Clark County, Nevada. *Economic Geology*, 94(7), pp.1163-1172.

Jones, P., 1975. Trace Elements and Other Elements in Crude Oil—a Literature Review. *Report of British Petroleum Research Centre, Sunbury*.

Jowitt, S.M. and Keays, R.R., 2011. Shale-hosted Ni–(Cu–PGE) mineralisation: a global overview. *Applied Earth Science*, 120(4), pp.187-197.

Kato, T., Nakamura, S. and Morita, M., 1990. Determination of nickel, copper, zinc, silver, cadmium and lead in seawater by isotope dilution inductively coupled plasma mass spectrometry. *Analytical Sciences*, 6(4), pp.623-626.

Kelly, W.C. and Nishioka, G.K., 1985. Precambrian oil inclusions in late veins and the role of hydrocarbons in copper mineralization at White Pine, Michigan. *Geology*, 13(5), pp.334-337.

Kesler, S.E., Jones, H.D., Furman, F.C., Sassen, R., Anderson, W.H. and Kyle, J.R., 1994. Role of crude oil in the genesis of Mississippi Valley-type deposits: Evidence from the Cincinnati arch. *Geology*, 22(7), pp.609-612.

Kesler, S.E., Appold, M.S., Martini, A.M., Walter, L.M., Huston, T.J. and Richard Kyle, J., 1995. Na-Cl-Br systematics of mineralizing brines in Mississippi Valley-type deposits. *Geology*, 23(7), pp.641-644.

Kotarba, M.J., Peryt, T.M., Kosakowski, P. and Więclaw, D., 2006. Organic geochemistry, depositional history and hydrocarbon generation modelling of the Upper Permian Kupferschiefer and Zechstein Limestone strata in south-west Poland. *Marine and Petroleum Geology*, 23(3), pp.371-386.

Kříbek, B., Sýkorová, I., Pašava, J. and Machovič, V., 2007. Organic geochemistry and petrology of barren and Mo-Ni-PGE mineralized marine black shales of the Lower Cambrian Niutitang Formation (South China). *International Journal of Coal Geology*, 72(3-4), pp.240-256.

Kucha, H. and Przyłowicz, W., 1999. Noble metals in organic matter and clay-organic matrices, Kupferschiefer, Poland. *Economic Geology*, 94(7), pp.1137-1162.

Leach, D.L., Sangster, D.F., Kelley, K.D., Ross, R.L., Garven, G. and Allen, C.R., 2005. Sediment-hosted Pb-Zn deposits: a global perspective. *Economic Geology*, 100, pp.561-608.

Leach, D.L., Taylor, R.D., Fey, D.L., Diehl, S.F. and Saltus, R.W., 2010. *A deposit model for Mississippi Valley-Type lead-zinc ores: Chapter A in Mineral deposit models for resource assessment* (No. 2010-5070-A). US Geological Survey.

Lecomte, A., Cathelineau, M., Deloule, E., Brouand, M., Peiffert, C., Loukola-Ruskeeniemi, K., Pohjolainen, E. and Lahtinen, H., 2014. Uraniferous bitumen nodules in the Talvivaara Ni–Zn–Cu–Co deposit (Finland): influence of metamorphism on uranium mineralization in black shales. *Mineralium Deposita*, 49(4), pp.513-533.

Li, G., Kohn, B., Sandiford, M. and Xu, Z., 2017. India-Asia convergence: Insights from burial and exhumation of the Xigaze fore-arc basin, south Tibet. *Journal of Geophysical Research: Solid Earth*, 122(5), pp.3430-3449.

Lingang, X., Lehmann, B., Jingwen, M., Wenjun, Q. and Andao, D., 2011. Re-Os age of polymetallic Ni-Mo-PGE-Au mineralization in Early Cambrian black shales of South China—a reassessment. *Economic Geology*, 106(3), pp.511-522.

Liu, W., Migdisov, A. and Williams-Jones, A., 2012. The stability of aqueous nickel (II) chloride complexes in hydrothermal solutions: Results of UV–Visible spectroscopic experiments. *Geochimica et Cosmochimica Acta*, 94, pp.276-290.

Loukola-Ruskeeniemi, K. and Heino, T., 1996. Geochemistry and genesis of the black shale-hosted Ni-Cu-Zn deposit at Talvivaara, Finland. *Economic Geology*, 91(1), pp.80-110.

Machel, H.G., 2001. Bacterial and thermochemical sulfate reduction in diagenetic settings—old and new insights. *Sedimentary Geology*, 140(1-2), pp.143-175.

Melezhik, V.A., Fallick, A.E., Filippov, M.M., Lepland, A., Rychanchik, D.V., Deines, Y.E., Medvedev, P.V., Romashkin, A.E. and Strauss, H., 2009. Petroleum surface oil seeps from a Palaeoproterozoic petrified giant oilfield. *Terra Nova*, 21(2), pp.119-126.

Meredith, W., Kelland, S.J. and Jones, D.M., 2000. Influence of biodegradation on crude oil acidity and carboxylic acid composition. *Organic Geochemistry*, 31(11), pp.1059-1073.

McFadzean, B., Mhlanga, S.S. and O'Connor, C.T., 2013. The effect of thiol collector mixtures on the flotation of pyrite and galena. *Minerals Engineering*, 50, pp.121-129.

Miedaner, M.M., Migdisov, A.A. and Williams-Jones, A.E., 2005. Solubility of metallic mercury in octane, dodecane and toluene at temperatures between 100 C and 200 C. *Geochimica et cosmochimica acta*, 69(23), pp.5511-5516.

Migdisov, A.A., Guo, X., Williams-Jones, A.E., Sun, C.J., Vasyukova, O., Sugiyama, I., Fuchs, S., Pearce, K., Roback, R. and Xu, H., 2017. Hydrocarbons as ore fluids. *Geochemical Perspectives Letters*, 5.

Nguyen, V.P., Burklé-Vitzthum, V., Marquaire, P.M. and Michels, R., 2013. Thermal reactions between alkanes and H<sub>2</sub>S or thiols at high pressure. *Journal of analytical and applied pyrolysis*, 103, pp.307-319.

Orberger, B., Pasava, J., Gallien, J.P., Daudin, L. and Pinti, D.L., 2003. Biogenic and abiogenic hydrothermal sulfides: controls of rare metal distribution in black shales (Yukon Territories, Canada). *Journal of Geochemical Exploration*, 78, pp.559-563.

Orberger, B., Vymazalova, A., Wagner, C., Fialin, M., Gallien, J.P., Wirth, R., Pasava, J. and Montagnac, G., 2007. Biogenic origin of intergrown Mo-sulphide-and carbonaceous matter in Lower Cambrian black shales (Zunyi Formation, southern China). *Chemical geology*, 238(3-4), pp.213-231.

Orr, W.L., 1986. Kerogen/asphaltene/sulfur relationships in sulfur-rich Monterey oils. *Organic geochemistry*, 10(1-3), pp.499

Oszczepalski, S., 1999. Origin of the Kupferschiefer polymetallic mineralization in Poland. *Mineralium Deposita*, 34(5-6), pp.599-613.

Parnell, J. and Eakin, P., 1987. The replacement of sandstones by uraniferous hydrocarbons: significance for petroleum migration. *Mineralogical Magazine*, 51(362), pp.505-515.

Parnell, J., 1988. Metal enrichments in solid bitumens: a review. *Mineralium Deposita*, 23(3), pp.191-199.

Peabody, C.E. and Einaudi, M.T., 1992. Origin of petroleum and mercury in the Culver-Baer cinnabar deposit, Mayacmas district, California. *Economic Geology*, 87(4), pp.1078-1103.

Pearson, G., 1963, Hard and Soft Acids and Bases: *Journal of the American Chemical Society*, v.85, p. 3533–3539.

Peters, K.E., Walters, C.C., and Moldowan, J.M., 2004, *The Biomarker Guide: Volume 1, Biomarker and Isotopes in the Environment and Human History*: Cambridge University Press.

Ptaszek, M., 2013. Rational design of fluorophores for in vivo applications. In *Progress in molecular biology and translational science* (Vol. 113, pp. 59-108). Academic Press.

Püttmann, W. and Goßel, W., 1990. The Permian Kupferschiefer of southwest Poland: a geochemical trap for migrating, metal-bearing solutions. *Applied Geochemistry*, 5(1-2), pp.227-235.

Radtke, A.S. and Scheiner, B.J., 1970. Studies of hydrothermal gold deposition-(pt.) 1, carlin gold deposit, Nevada, the role of carbonaceous materials in gold deposition. *Economic Geology*, 65(2), pp.87-102.

Saintilan, N.J., Spangenberg, J.E., Samankassou, E., Kouzmanov, K., Chiaradia, M., Stephens, M.B. and Fontboté, L., 2016. A refined genetic model for the Laisvall and Vassbo Mississippi Valley-type sandstone-hosted deposits, Sweden: constraints from paragenetic studies, organic geochemistry, and S, C, N, and Sr isotope data. *Mineralium Deposita*, 51(5), pp.639-664

Saintilan, N.J., Spangenberg, J.E., Chiaradia, M., Chelle-Michou, C., Stephens, M.B. and Fontboté, L., 2019. Petroleum as source and carrier of metals in epigenetic sediment-hosted mineralization. *Scientific reports*, 9(1), p.8283.

Scott, R.J., Meffre, S., Woodhead, J., Gilbert, S.E., Berry, R.F. and Emsbo, P., 2009. Development of framboidal pyrite during diagenesis, low-grade regional metamorphism, and hydrothermal alteration. *Economic Geology*, 104(8), pp.1143-1168.

Spangenberg, J.E., Fontbote, L. and Macko, S.A., 1999. An evaluation of the inorganic and organic geochemistry of the San Vicente mississippi valley-type zinc-lead district, central Peru;

implications for ore fluid composition, mixing processes, and sulfate reduction. *Economic Geology*, **94(7)**, pp.1067-1092.

Spirakis, C.S., 1996. The roles of organic matter in the formation of uranium deposits in sedimentary rocks. *Ore Geology Reviews*, **11(1-3)**, pp.53-69

Sun, Y.Z., 1998. Influences of secondary oxidation and sulfide formation on several maturity parameters in Kupferschiefer. *Organic Geochemistry*, **29(5-7)**, pp.1419-1429.

Sun, Y.Z. and Püttmann, W., 2000. The role of organic matter during copper enrichment in Kupferschiefer from the Sangerhausen basin, Germany. *Organic Geochemistry*, **31(11)**, pp.1143-1161.

Surdam, R.C., Jiao, Z.S. and MacGowan, D.B., 1993. Redox reactions involving hydrocarbons and mineral oxidants: A mechanism for significant porosity enhancement in sandstones. *AAPG Bulletin*, **77(9)**, pp.1509-1518.

Sverjensky, D.A., 1986. Genesis of Mississippi Valley-type lead-zinc desposits. *Annual Review of Earth and Planetary Sciences*, **14(1)**, pp.177-199.

Tissot, B.P. and Welte, D.H., 1978, Petroleum formation and occurrence: Springer-Verlag, Berlin Germany

Vairavamurthy, A. and Mopper, K., 1987. Geochemical formation of organosulphur compounds (thiols) by addition of H<sub>2</sub>S to sedimentary organic matter. *Nature*, 329(6140), p.623.

Vlassopoulos, D., Wood, S.A. and Mucci, A., 1990. Gold speciation in natural waters: II. The importance of organic complexing—Experiments with some simple model ligands. *Geochimica et Cosmochimica Acta*, 54(6), pp.1575-1586.

Wallace, M.W., Middleton, H.A., Johns, B. and Marshallsea, S., 2002, October. Hydrocarbons and Mississippi Valley-type sulfides in the Devonian reef complexes of the eastern Lennard Shelf, Canning Basin, Western Australia. In *The sedimentary basins of Western Australia 3. Proceedings of the West Australian basins Symposium: Perth, Petroleum Exploration Society of Australia* (pp. 795-815).

Watanabe, Y., Farquhar, J. and Ohmoto, H., 2009. Anomalous fractionations of sulfur isotopes during thermochemical sulfate reduction. *Science*, 324(5925), pp.370-373.

Wei, Z., Mankiewicz, P., Walters, C., Qian, K., Phan, N.T., Madincea, M.E. and Nguyen, P.T., 2011. Natural occurrence of higher thiadiamondoids and diamondoidthiols in a deep petroleum reservoir in the Mobile Bay gas field. *Organic geochemistry*, 42(2), pp.121-133.

Williams-Jones, A.E., Bowell, R.J. and Migdisov, A.A., 2009. Gold in solution. *Elements*, 5(5), pp.281-287.

Williams-Jones, A.E. and Migdisov, A.A., 2014. Experimental constraints on the transport and deposition of metals in ore-forming hydrothermal systems. *Society of Economic Geologists*, 18, pp.77-96.

Young, S.A., Loukola-Ruskeeniemi, K. and Pratt, L.M., 2013. Reactions of hydrothermal solutions with organic matter in Paleoproterozoic black shales at Talvivaara, Finland: Evidence from multiple sulfur isotopes. *Earth and Planetary Science Letters*, 367, pp.1-14.

## Preface to Chapter 2

---

Chapter 2 entitled “**The Solubility of Palladium (Pd) in Crude Oil at 150, 200 and 250 °C and its Application to Ore Genesis**” provides an overview of factors controlling the solubility and speciation of Palladium (Pd) in crude oil at temperatures between 150 and 250°C. The methodology used to measure the solubility of Pd in crude oil involved reacting Pd(0) wire with a selection of crude oils at saturated vapor-pressure in silica glass reactors, digesting the oils in acids and analyzing the resulting aqueous solution using Inductively-Coupled Plasma Mass Spectrometry (ICP-MS). As a complement to these experiments, X-ray Photoelectron Spectroscopy (XPS) was used to scan the surface chemistry of the Pd wire that had reacted with the crude oils in order to identify the compounds in crude oil that have an affinity for Pd. The experimental findings are related to observations of sediment-hosted deposits which have high concentrations of Pd and bitumen.

## **2. The Solubility of Palladium (Pd) in Crude Oil at 150, 200 and 250°C and its Application to Ore Genesis**

---

**J. Sanz-Robinson<sup>a</sup>, I. Sugiyama<sup>b</sup> and A.E. Williams-Jones<sup>a</sup>**

<sup>a</sup> Department of Earth and Planetary Sciences, McGill University, 3450 University Street,  
Montreal, QC, H3A 0E8, Canada

<sup>b</sup> Department of Earth and Planetary Sciences, Weizmann Institute of Science, Hertzl st. 234  
Rehovot, 76100, Israel

---

Published in *Chemical Geology*, 2020

DOI: <https://doi.org/10.1016/j.chemgeo.2019.119320>

## Abstract

Although most economic palladium deposits occur in mafic igneous rocks and are the products of magmatic processes, there are a number of polymetallic deposits hosted by organic-rich (bituminous) black shales in which the palladium reaches exploitable concentrations. Considering that palladium is rarely concentrated by hydrothermal processes, and as organic-rich black shales are the source beds for the production of hydrocarbons and bitumen commonly records the path taken by these hydrocarbons, it is reasonable to entertain the possibility that liquid hydrocarbons may act as an ore fluid for palladium. In order to test the potential of liquid hydrocarbons to act as ore fluids, Pd(0) metal wires were reacted with three crude oils, A, B and C (A being the lightest and C being the heaviest crude oil), at temperatures of 150, 200 and 250 °C. After reaction at 150 °C, the Pd concentrations in crude oils A, B and C were  $60 \pm 20$  ppb,  $19 \pm 4$  ppb, and  $128 \pm 29$  ppb, respectively. The corresponding concentrations at 200 °C, were  $18 \pm 6$  ppb,  $17 \pm 6$  ppb, and  $50 \pm 15$  ppb, respectively, and at 250 °C, were  $16 \pm 2$  ppb,  $11 \pm 1$  ppb and  $26 \pm 2$  ppb, respectively ( $n = 3$ ). The measured solubility of Pd was highest in the heaviest crude oil, C. All three oils reached their maximum Pd concentration at 150 °C, with Pd concentration decreasing progressively as temperature increased to 250 °C. To gain insights into the mechanism controlling the dissolution of Pd in crude oil, we analyzed the reacted Pd wires using X-ray Photoelectron Spectroscopy (XPS). The XPS spectrum displays a well-defined thiol (R-SH) peak at a binding energy of 163eV, which indicates that Pd has an affinity for reduced organosulfur compounds. Moreover, Pd concentrations were observed to increase with the total thiol content of the oil, thereby corroborating the results of the XPS analyses. Our results clearly show that Pd solubility in crude oil is promoted by the presence of thiols. As thiol-rich hydrocarbons usually develop in deep, high temperature (100 to 140 °C) carbonate sequences containing abundant sulfate

mineralization, it is thought that the thiols are the products of thermochemical sulfate reduction (TSR) (Machel, 2001). We therefore propose that liquid hydrocarbons, which have interacted with sulfate at relatively high temperature, may serve as effective ore fluids for palladium.

## 2.1 Introduction

Platinum group elements (PGE) are intimately associated with hydrocarbons in a number of ore deposits. One such deposit is the Polish Kupferschiefer, in which palladium (Pd) and platinum (Pt) concentrations in the clay-organic matrix of the black shales reach 1,900 and 600 ppm, respectively (Kucha and Przybylowicz, 1999). In the Kupferschiefer, platinum group elements are particularly enriched in a variety of pyrobitumen known as a thucholite, which is composed primarily of thorium, uranium, carbon and hydrogen (Th, U, C, H; Barthauer et al., 1953). Palladium and platinum concentrations in the Kupferschiefer thucholite can be as high as 5,000 and 1,770 ppm, respectively (Vaughan et al., 1989; Kucha and Przybylowicz, 1999). Lower, but nevertheless significant concentrations of Pd and Pt, have been reported for black-shale-hosted deposits in the Zunyi district, Guizhou province, China, namely 0.4 and 0.3 ppm, respectively (e.g., Coveney, 1991; Coveney et al., 1992; Lott et al., 1999). In a similar black shale-hosted deposit in the Yukon, Canada, the Nick Prospect, Pd and Pt concentrations reach 0.9 and 0.7 ppm, respectively (Jowitt and Keays, 2011). Both the Zunyi deposits and the Nick prospect also contain percentage levels of Ni, a metal that is sparingly soluble in hydrothermal fluids (Liu et al., 2012) but is highly soluble in petroleum (Jones, 1975). It is therefore attractive to consider the possibility that instead of being transported in hydrothermal fluids, as has been generally assumed, the PGE (and Ni) in these deposits were concentrated by liquid hydrocarbons. Support for this idea, in the case of the Kupferschiefer deposit, comes from the fact that the ores formed at temperatures of 80 – 140 °C (Oszczepalski, 1999), which coincide with those of the oil window, and accumulations of polyaromatic sulfur hydrocarbons in the sulfide ore of the Polish Kupferschiefer (Püttmann and Goßel, 1990) suggest the influx of sulfur-rich crude oil into the ore zone from deeper Carboniferous sequences.

Arguably, the best evidence for the association of PGEs with hydrocarbons is provided by the Boss deposit in Nevada, U.S.A, which is hosted by bituminous dolomitic limestones (Knopf, 1915); the bitumen is interpreted to have formed from liquid hydrocarbons that are thought to have impregnated the limestones (Jedwab et al., 1999). Most of the PGE is concentrated in bitumen within fine-grained siliceous “ore shoots” that cut the limestone and contain an average of 660 ppm Pd, 150 ppm Pt and 1315 ppm Au. Transmitted Electron Microscopic (TEM) imaging showed that the PGEs are dispersed in the bitumen as nanoparticles of potarite, an alloy of Hg  $\{(Pd_{81}, Au_{13}, Pt_{01}) Hg\}$ , although they are also present in appreciable concentrations in bitumen that is apparently devoid of nanoparticles (Jedwab et al., 1999).

Despite the potential involvement of liquid hydrocarbons in the formation of the aforementioned PGE deposits, there have been no experimental studies of the solubility of these metals in this medium. Indeed, the only experimental study that bears on the topic is that of Plyusnina et al. (2000), who evaluated the capacity of organic matter to adsorb Pt from aqueous solutions. This study showed that at 200 and 400 °C, 0.02 and 1.95 g Pt was adsorbed per kg of organic matter (20 and 1950 ppm), respectively.

In this study, we report the results of experiments designed to determine the solubility of Pd in crude oils (Pd(0) wire) at temperatures of 150, 200 and 250 °C and saturated vapour pressure. Based on hard-soft-acid-base (HSAB) theory (Pearson, 1963), Pd is a soft acid and is expected to react with soft bases, such as reduced sulfur compounds. The oils were therefore selected to provide a range of compositions, particularly with respect to sulfur content. The results are

encouraging and show that liquid hydrocarbons can dissolve Pd in concentrations sufficient for them to constitute ore fluids.

## 2.2 Crude Oil Characterization

Three crude oils, A, B, and C were supplied by Statoil for this study. The crude oils were selected so as to provide a range of properties and compositions, i.e., API gravity, total acid number (TAN), the proportions of paraffins, naphthenes, aromatics and asphaltenes, and the contents of sulfur (S) and nitrogen (N). These are reported in Table 2.1.

**Table 2.1** The characteristics and compositions of the three crude oils, A, B and C, employed in our experimental study.

<b>Parameters</b>	<b>Oil A</b>	<b>Oil B</b>	<b>Oil C</b>
<b>API Gravity</b>	26.6	25	19
<b>Specific Gravity</b>	0.895	0.904	0.94
<b>Sulfur (wt.%)</b>	0.84	0.52	0.82
<b>Thiols/sulfides (ppm)</b>	44	0	52
<b>Thiophenes/Disulfides (ppm)</b>	1401	37	1052
<b>Benzothiophenes (ppm)</b>	3892	1884	3164
<b>Dibenzothiophenes (ppm)</b>	2575	2737	2024
<b>Benzonaphthothiophenes (ppm)</b>	490	549	109
<b>Nitrogen (wt.%)</b>	---	0.2	0.44
<b>TAN (mgKOH/g)</b>	0.2	2.9	2.3
<b>Paraffins (wt.%)</b>	---	37	19
<b>Naphthenes (wt.%)</b>	---	49	65
<b>Aromatics (wt.%)</b>	---	13	15
<b>Asphaltenes (wt.%)</b>	1.6	0.3	1.4

Crude oil is a complex mixture of organic and inorganic constituents, i.e., paraffins, naphthenes, aromatics and asphaltenes, together with inorganic constituents such as S, N, trace elements and silicate minerals (Manning and Gize, 1993). The proportions of the different organic constituents

determine the API gravity, an inverse measure of the density of oil relative to that of water (Speight, 2001). Crude oils are most simply distinguished by their API gravity. In this study, A is the lightest (highest API number) and C the heaviest (lowest API number) crude oil that was considered (Table 2.1). A parameter that is important in controlling metal uptake by crude oil is the S content, as the thiol group (-SH) is known to be involved in the formation of metal organic complexes (Lewan, 1984; Giordano, 1994; Speight, 2001). The crude oil with the lowest S content is crude Oil B (0.52 wt.%) and that with the highest S content is crude Oil A (0.84 wt.%); crude Oil C has a S content very similar to that of crude Oil A (Table 2.1). The TAN (mgKOH/g) value, a measure of acidity, is also important to quantify because high acidity can lead to the demetallation of metal organic compounds via ion-exchange reactions (Falk, 1964; Buchler, 1978; Manning and Gize, 1993; Giordano, 1994). The TAN values for oils A, B and C are 0.2, 2.9 and 2.3 mg KOH/g respectively. Finally, the nitrogen content is important to know because it is a measure of the porphyrin content, although other nitrogen compounds may also be present, including amine, pyridine, quinolone, pyrrole and carbazole (Tissot and Welte, 1978). The crude oil with the lowest N content is crude Oil B (0.2 wt.%), and that with the highest N content crude is crude Oil C (0.44 wt.%; Table 2.1).

## **2.3 Methodology**

### **2.3.1 Experimental Methods**

The experiments were performed at 150, 200 and 250 °C and a pressure of approximately 12 bars in quartz reactors prepared by fusing quartz tubing (OD = 12 mm, ID = 10 mm) supplied by National Scientific Inc. (Figure 2.1). Prior to being used, the quartz reactors were cleaned with

nitric acid (~75% HNO<sub>3</sub>) for 24 hours, rinsed with Milli-Q™ water and dried at 100°C for 2 hours. The palladium was introduced in the form Pd(0) wire, and was placed in a fused quartz ampoule (OD = 9 mm, ID = 7 mm) that had been cleaned using the method employed for the quartz reactors. The ampoule was then placed in the reactor. Aliquots (~0.5 ml) of the three different types of crude oil (A, B, and C) were placed in separate reactors, which were sealed using an oxyhydrogen flame. All weights, namely, those of the quartz reactor before and after introduction of the Pd(0) wire-bearing quartz ampoule and the crude oil, before and after an experiment, were carefully determined using a high precision Mettler M3 analytical balance. The reactors were then placed in a Thermo Scientific™ Thermolyne™ tabletop muffle furnace oven that had been preheated to the desired temperature. The temperature was controlled to ± 1 °C.

After an experiment, the reactor was quenched to room temperature in water, opened with a diamond cutter and the Pd(0) wire-bearing ampoule removed with disposable tweezers. The reactor was then prepared for analysis by being stoppered with clean quartz wool to prevent loss of material.

### **2.3.2 Analytical Method**

The unreacted and reacted crude oils were analysed using a method similar to that described by Sugiyama and Williams-Jones (2018). The crude oils were ashed using a combination of thermal combustion and chemical oxidation, and the residues leached with HCl and analysed using Inductively Coupled Plasma Mass Spectrometry (ICP-MS; Fig. 2.1). Refer to Supplementary Materials for further details on the ICP-MS dilutions and data correction.

After an experiment, the Pd(0) wires were retrieved from their reactors, rinsed in toluene and vacuum-dried at room temperature for 24 hours (Fig. 2.1). The surface composition of the wires was characterized by X-ray Photoelectron Spectroscopy (XPS) on a Thermo Scientific  $K\alpha$  spectrometer, using Al  $K\alpha$  radiation (1486 eV) and an X-ray spot size of 200  $\mu\text{m}$ . Scans were made with a pass energy of 50eV and a resolution of 0.1 eV. The curve fitting analysis was performed using Avantage software version 4.60 with Gaussian–Voigt curves functions and background removal through the Smart method (Castle and Salvi, 2001).

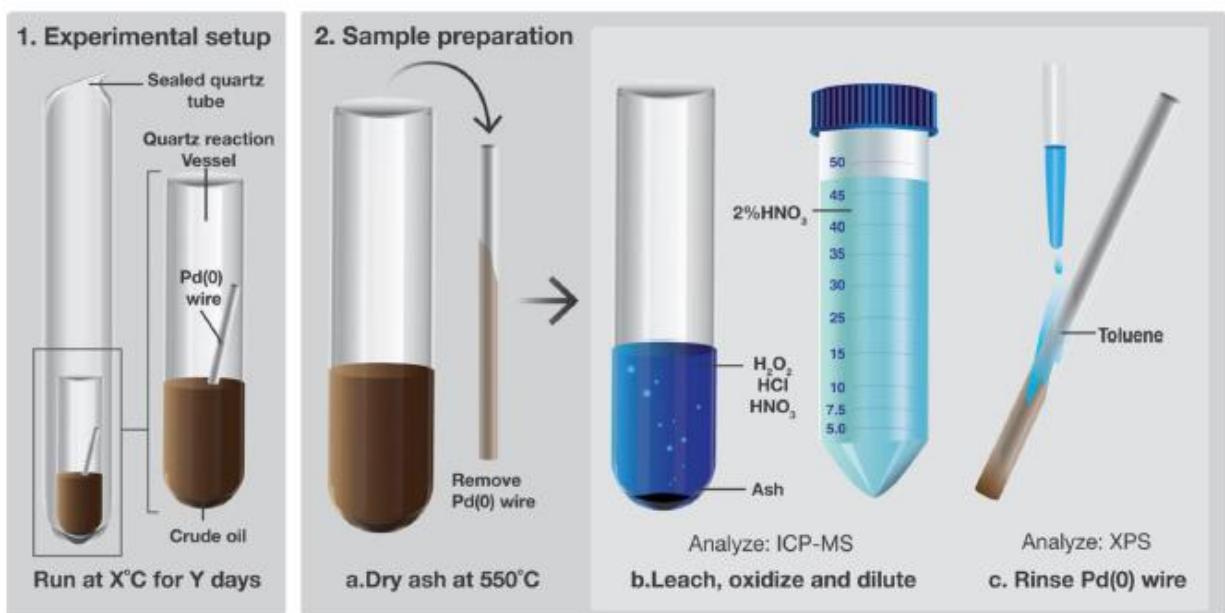


**Figure 2.1** The experimental protocol employed for the investigation of Pd solubility and speciation in oils A, B, and C at 150, 200 and 250  $^\circ\text{C}$ .

## **2.4 Experimental Parameters**

### **2.4.1 Temperatures of the experiments**

Although the oil window extends from 80 to 160 °C (Peters et al., 2004), it is known from pyrolysis experiments (Price and Wenger, 1992), and the entrapment of liquid hydrocarbons in black smokers (Peter and Scott, 1988), that liquid hydrocarbons are stable for protracted periods of time at temperatures above 300 °C. We therefore elected to conduct the experiments at temperatures of 150, 200 and 250 °C. The lowest temperature of the range was chosen for kinetic reasons, i.e., to ensure that equilibrium was reached in a reasonable amount of time and the upper temperature limit to avoid any risk of thermal degradation of the crude oils.

### **2.4.2 Duration of the experiments**

To establish the time required for the experiments to reach equilibrium, kinetic experiments were conducted at 150, 200 and 250 °C using crude oils A, B and C. Aliquots of these crude oils were reacted with Pd(0) wire for durations ranging from 1 to 30 days at 150 °C and 1 to 15 days at 200 and 250 °C, as discussed in Section 2.5.1, and the Pd concentrations in the crude oils were determined as described in Section 2.4.2. As is evident from Figure 2.2, Pd concentrations in the crude oils start to plateau after approximately 5 days. This is taken to be the steady-state concentration of Pd in crude oil. Accordingly, experiments designed to determine the steady-state concentration of Pd in crude oils were conducted for durations of 10 or more days at temperatures of 150, 200 and 250 °C.

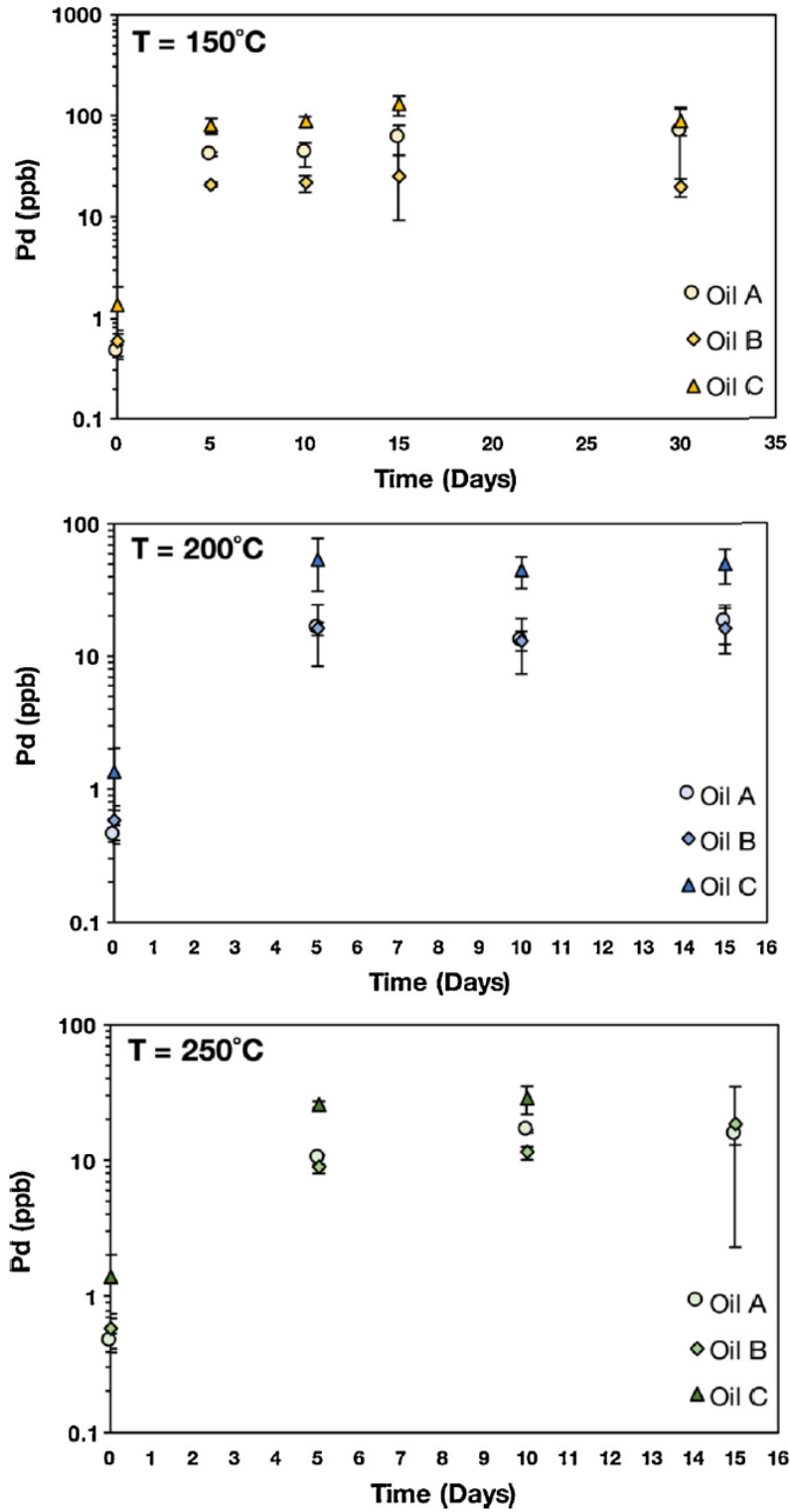


**Figure 2.2** Concentration of Pd in oils A, B and C at 150, 200 and 250 °C as a function of the duration of the experiments.

## 2.5 Results

### 2.5.1 Results from the Palladium Solubility Experiments

From Table 2.2, it is evident that the Pd concentration in each crude oil decreased progressively with increasing temperature. It is also evident that the composition of the crude oil plays a key role in controlling Pd solubility. These differences in Pd concentration can be accounted for largely by differences in the thiol content and perhaps also the asphaltene content of the oils. Oil C is the heaviest and most asphaltene-rich oil; it also has the highest thiol content of the all the oils and dissolved the highest concentration of Pd at each temperature tested. Oils A and B are lighter oils, which have lower asphaltene contents than Oil C. Of these lighter oils, Oil A has the higher thiol content and dissolved more Pd than its light counterpart, Oil B. Oil B contains no detectable thiols but still dissolved 19.5 ppb of Pd at 150 °C, which means that Pd dissolution in crude oil is not determined solely by the thiol content (See Section 2.6.1 for more detail). Nevertheless, it is evident from Figure 2.3, which compares the maximum Pd concentration dissolved by each oil with its thiol content, that the decreasing trend in maximum Pd concentration is mirrored by a decreasing trend in thiol concentration. Of all the compositional parameters measured in our crude oils, only the sulfur content and more broadly the asphaltene content correlate positively with Pd concentration.

**Table 2.2** A summary of the experimentally determined solubility of Pd in oils A, B and C at 150, 200 and 250 °C. The palladium concentration at 25 °C is the background concentration in the unreacted oils.

Temp.	Oil A			Oil B			Oil C		
	n*	Pd (ppb)	Error (%)	n*	Pd (ppb)	Error (%)	n*	Pd (ppb)	Error (%)
25 °C	3	0.5 ± 0.1	15	3	0.6 ± 0.2	29	3	1.4 ± 0.7	49
150 °C	3	60 ± 20	32	3	20 ± 4	21	3	130 ± 30	22
200 °C	3	18 ± 6	33	3	20 ± 6	37	3	50 ± 10	29
250 °C	3	16 ± 3	16	3	11 ± 1	11	3	26.0 ± 2	5.8

n\* is the number of experiments conducted

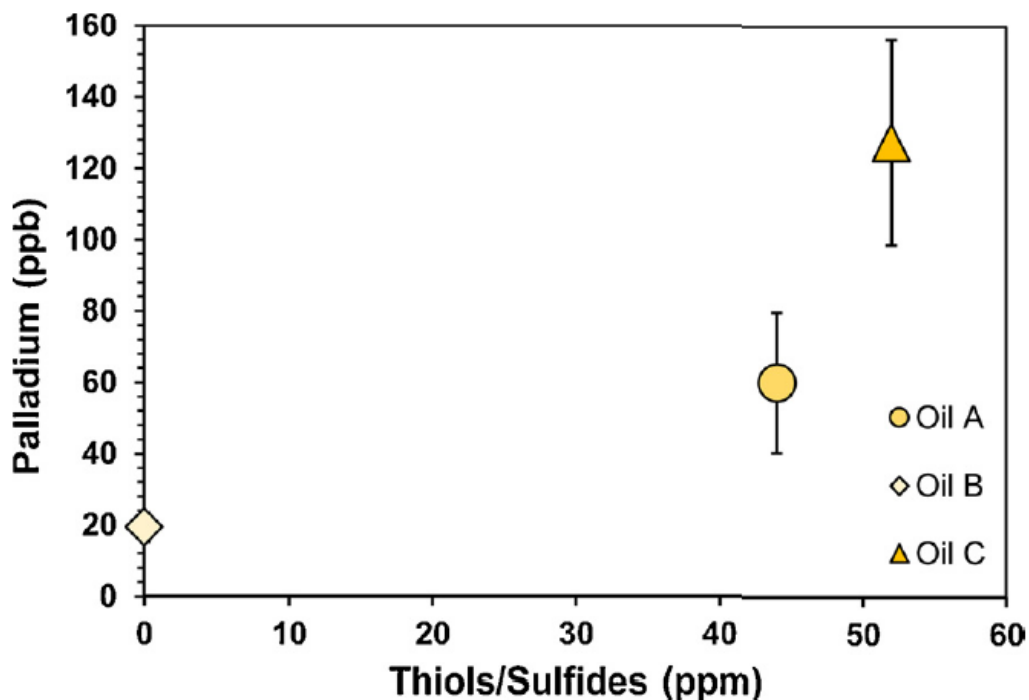


**Figure 2.3** The maximum Pd solubility (ppb) in crude oils A, B and C versus their thiol content (ppm).

## 2.5.2 Results of XPS Analyses

X-ray Photoelectron Spectroscopy (XPS) was employed to determine the composition of the residual oil coating the surface of the palladium wire. Sulfur is the most abundant element coating the wire and accounts for approximately 6 atom% of the wire surface as determined by XPS. Figure 2.4 is an XPS spectrum for the sulfur compounds coating the Pd wire after reaction with Oil C at 150 °C. The prominent sulfur (S2p) peak, indicated by the dotted line, is centered at a binding energy of 163 eV corresponding to the thiol functional group (Castner et al., 1996). This indicates that most of the sulfur coating the wire is in the form of thiols, implying that palladium has a strong affinity for the reduced sulfur in oil.

The thiol peak in Figure 2.4 is relatively broad and can be resolved into two separate peaks. The peak at 164.7 eV indicated by the yellow line represents free thiols, whereas the green peak located at 162.4 eV corresponds to palladium-thiolate. The latter interpretation assumes that the binding energy for gold-thiolate is similar to that for palladium-thiolate, for which there are no data (Castner et al., 1996). This means that, whereas some thiols remain unbound, a large proportion of the thiols are chemically bonded to the palladium wire. A less prominent sulfur peak at 168 eV corresponds to the sulfate functional group. The much smaller size of the sulfate peak relative to the thiol peaks provides evidence that oxidized sulfur is a much less important ligand for palladium, consistent with HSAB principles (Pearson, 1963); sulfate is a hard base and palladium a soft acid.

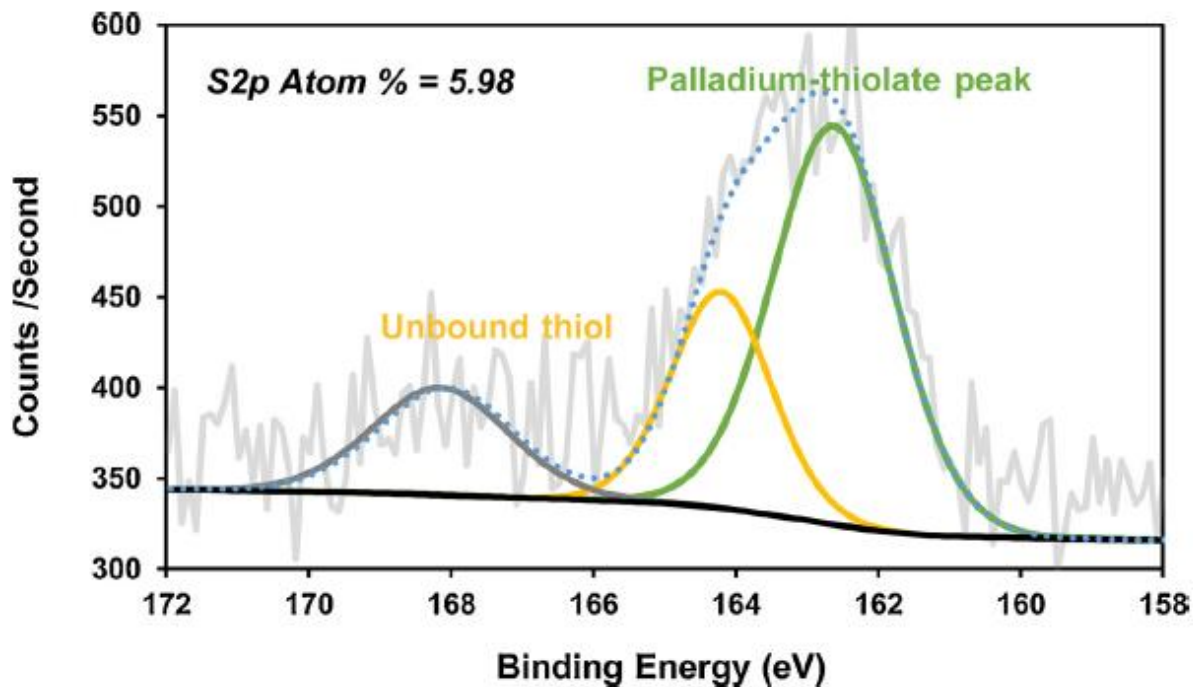


**Figure 2.4** An XPS spectrum illustrating the sulfur speciation of residual oil on a palladium wire after reaction with oil C at 150 °C. The thiol peak is resolved into an unbound thiol peak in yellow (~164eV) and a palladium-thiolate peak in green (~162eV).

In Figure 2.5, we show an XPS spectrum for palladium after reaction with crude Oil C at 150 °C. Deconvolution of the spectrum reveals that the wire is coated in a mixture of native Pd metal and Pd(II). The XPS spectrum for the native Pd metal consists of a doublet (in green) with the Pd 3d<sub>5/2</sub> and 3d<sub>3/2</sub> peaks centered at 335.7 and 340.9 eV, respectively. The Pd(II) doublet (in purple) is shifted to slightly higher binding energies than the doublet of its non-oxidized counterpart. Thus, the palladium wire was oxidized by reaction with the crude oil, whereas thiols in the oil were reduced to form palladium-thiolate. In this reaction the hydrogen atom of the thiol group is replaced by a Pd atom ( $2 \text{ RSH} + \text{Pd}(0) \Rightarrow (\text{RS})_2\text{-Pd}^{++}$ ). Palladium-thiolates are clearly stable in crude oil up to 150 °C and are important in controlling palladium solubility in liquid hydrocarbons. This is consistent with the predictions of HSAB theory (Pearson, 1963).

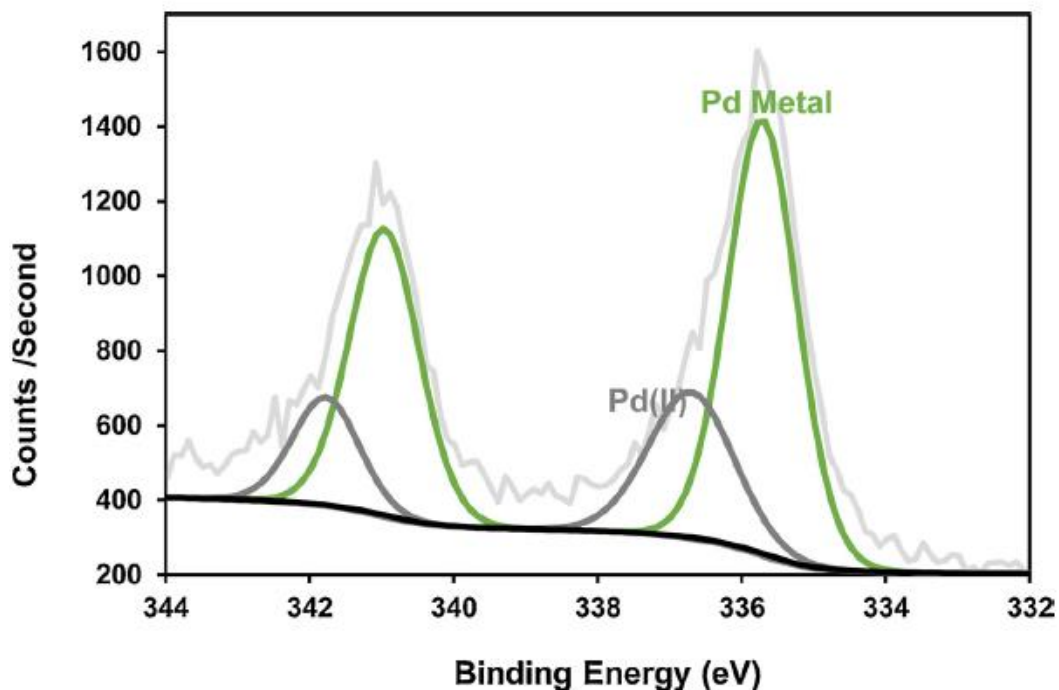


**Figure 2.5** An XPS spectrum of the palladium wire after reaction with crude oil C at 150 °C. The grey doublet corresponds to the Pd(II) species whilst the green doublet corresponds to Pd(0).

## 2.6 Discussion

### 2.6.1 Factors determining Pd concentration and speciation in crude oil

Sulfur compounds in mature crude oils evolve during the mobilization of hydrocarbons through oil-rock interaction. Our results suggest that thiol-rich crude oils can dissolve appreciable concentrations of Pd, with Oil C, our most thiol-rich oil, dissolving up to 127 ppb Pd at 150°C. This oil contains 52 ppm of thiols, which is a low concentration compared to that reported for some crude oils. For example, the “Rodney Crude” described in Ho et al. (1974) has a thiol content of 3179 ppm based on an API gravity of 32 and a mercaptan number of 275 (refer to Supplementary Materials, Section B for a calculation of the thiol content of the Rodney Crude oil). Similarly, the “Light Mixed B.C.” oil, also described by Ho et al. (1974), has a thiol content of 1310 ppm. Based

on the results of our experiments, an oil such as the Rodney Crude or the Light Mixed B.C. oil would be expected to dissolve substantial amounts of Pd. Mature thiol-rich crude oils of this type come from deep carbonate reservoirs, which contain elevated concentrations of hydrogen sulfide and are typically associated with sulfate-bearing carbonate sequences (Ho et al., 1974; Cai et al., 2003; Wei et al., 2011; Nguyen et al., 2013). Orr et al. (1974) proposed that thermochemical sulfate reduction (TSR) was responsible for the large concentrations of hydrogen sulfide and polysulfides in oils hosted by carbonate reservoirs. Reactions between hydrogen sulfide and organic compounds from oil, gas or condensates can produce an elevated steady-state concentration of thiols, leading to thiol-enriched oils (Ho et al., 1974, Wei et al., 2011, Cai et al., 2003, Nguyen et al., 2013). In contrast, oils that mature in the absence of sulfate have low total sulfur and thiol contents (Ho et al., 1974; Orr et al., 1974).

Another compositional parameter that may control Pd dissolution in high specific gravity crude oil is the asphaltene content; asphaltenes comprise a variety of very high molecular weight compounds including porphyrins, which are effective metal chelators (Filby et al., 1987). As they form stable complexes with Pd (Kostas et al., 2007), porphyrins could play an important role in the dissolution of PGEs in crude oils. This is supported by the observation that the metalation of porphyrins during diagenesis by chalcophile elements such as Ni is promoted by ion transfer compounds like carboxylic acids (Lipiner et al., 1988). Since Pd is a  $d_{10}$  transition metal and a chalcophile element like Ni, it should display an analogous chemical behavior. If we assume this to be the case, then an oil with a high carboxylic acid content can potentially form Pd porphyrin complexes under diagenetic conditions. Interestingly, Oil B has the highest TAN (an indicator of high carboxylic acid content) of the three crude oils considered in this study (2.9 mg KOH/g).

Furthermore, although Oil B contains no detectable thiols, it has a moderate asphaltene content (0.3 wt.%). Thus, Oil B has the potential to form Pd porphyrins, which may explain why it was able to dissolve significant Pd despite the absence of thiols. In contrast, Oil A has the lowest TAN and asphaltene content of the oils tested but contains 44 ppm thiols and so is likely to dissolve Pd as a thiolate complex rather than as a porphyrin complex. Oil C has the highest thiol content of the three crude oils tested (52 ppm thiol S), displays a strong chemical affinity for thiols according to our XPS analyses and also dissolved much more Pd metal than the other two oils. However, Oil C also has the largest asphaltene fraction (1.4 wt.%) of the three oils and a high TAN (2.3 mg KOH/g), suggesting that the very high concentration of dissolved Pd may be due partly to the formation of Pd porphyrins.

## **2.6.2 The environment of hydrocarbon-associated palladium ore formation**

The Kupferschiefer, Zunyi and Boss deposits all exhibit notable Pd enrichment and lie in close spatial proximity to sulfate-bearing carbonate sequences. For example, the Permian Kupferschiefer is overlain by an anhydrite-rich carbonate sequence (Oszczepalski, 1999) and, consequently, some researchers have suggested that TSR may have played a role in the mineralization of the Kupferschiefer deposit, although this continues to be debated (Bechtel and Püttmann, 1991; Jowett et al., 1991; Oszczepalski et al., 2012). In contrast, the Zunyi deposit in Southern China consists of a thin layer of transition metal sulfides within a sequence of black shales. The black shales locally contain barite deposits and unconformably overlie a thick sequence of Precambrian dolomite (Lott et al., 1999; Mao et al., 2002). Moreover, barite is commonly observed in the Zunyi deposit (Murowchick et al., 1994), an important precondition for the production of reduced sulfur by thermochemical sulfate reduction. Finally, it is noteworthy that sulfate-bearing minerals

(plumbojarosite and hydronium jarosite) are also observed in close association with bitumen in the Boss deposit (Jedwab et al., 1999).

Although, there is no agreement on the genesis of black-shale-hosted PGE deposits, most researchers favor one of two models, a synsedimentary model, in which the metals precipitate from the seawater column and accumulate at the seawater-sediment interface, and a hydrothermal model in which the metals are deposited by sea-floor vent fluids (Jowitt and Keays, 2011; Kucha and Przybylowicz, 1999). These models, however, do not adequately account for the fact that a significant proportion of the Pd in black-shale-hosted deposits occurs as metal organic bituminous material (Kucha, 1993; Mitkin et al., 2000). Indeed, the currently favored genetic models do not consider this observation, proposing only that hydrocarbons act as chemical reduction fronts which aid in the precipitation of redox sensitive elements from a metalliferous hydrothermal fluid or from seawater (Disnar and Sureau, 1990). A hypothesis that therefore needs to be considered is that the metals were transported to the site of deposition in liquid hydrocarbons. In the case of the Zunyi deposit in southern China (Ni-Mo-PGE), support for liquid hydrocarbons as alternatives to a hydrothermal ore fluid is provided by the fact that the principal ore metal, Ni, is sparingly soluble in aqueous liquids. Indeed, chemical analyses of modern petroleum and bitumen from over-mature reservoirs and analyses of petroleum in modern hydrothermal seafloor vents all indicate that the major metals concentrated in the ore zone at Zunyi are all very soluble in petroleum (Emsbo et al., 2005). This conclusion led Emsbo et al. (2005) to propose that petroleum, rather than a hydrothermal fluid, was responsible for the metal enrichment of the Zunyi Deposit.

Platinum group element enrichment is associated with organic matter potentially derived from petroleum in a number of black-shale-hosted deposits, i.e., Zunyi, Nick, the Polish Kupferschiefer and the Boss deposit. At Zunyi, particles of migrabitumen, indicative of brecciation by petroleum, have been found in the ore zone (Křibek et al, 2007). Large bituminous veins underlie the mineralized horizon of the Nick Prospect, potentially documenting the passage of a liquid hydrocarbon fluid into the black shales from below (Hulbert et al, 1992). Polyaromatic sulfur hydrocarbons (PASH), which are common constituents of crude oils, are abundant in organic matter associated with the sulfide ore of the Polish Kupferschiefer and are interpreted by Püttmann and Goßel (1990) to have been transported into the Kupferschiefer from the underlying Carboniferous strata. Finally, the PGE-ore of the Boss Deposit is hosted by bitumen in breccias that almost certainly represents the residues of petroleum (Jedwab et al., 1999).

The ability of a crude oil to dissolve Pd is dependent on the abundance of key ligands in the oil, of which thiols appear to be the most important (this study). Metals and thiols can be incorporated into hydrocarbon source rocks by sulfate reducing bacteria during sedimentation (Vairavamurthy and Mopper, 1987). As shales undergo diagenesis, the metal and sulfur content of the nascent oil will reflect that of the source rocks (Caumette et al., 2009). The thiol content of the oil, however, may be increased to unusually high levels through catagenetic reactions like TSR that occur when the oil encounters sulfate minerals at temperatures in excess of 100°C (Machel, 2001). These thiol-rich oils, of which the Rodney crude and Light Mixed B.C. oils (see above) are examples, in turn, would have greatly enhanced capacity to leach ‘soft’ metals like Pd from the surrounding sediments, potentially leading to orders of magnitude higher Pd concentrations than those of our experiments, which employed comparatively thiol-poor oils. We propose that such metalliferous,

thiol-enriched oils eventually accumulate in traps where, through continued heating, form carbonaceous, PGE-rich sulfide seams exemplified by the deposits referred to in this paper.

### **2.6.3 Evaluation of the potential of crude oils to act as ore fluids for palladium**

In the previous section, we discussed evidence for the association of petroleum with PGEs in several deposits, among which, the Kupferschiefer is the most important. Because of its location at the edge of the Carboniferous-Rotliegend petroleum system, which occupies a large part of the southern North Sea and adjacent onshore parts of Europe (Gautier, 2003), it is therefore reasonable to propose that the Kupferschiefer was infiltrated by hydrocarbons from this source. Moreover, this hypothesis is supported by the observation that the source rocks (Carboniferous Coal Measures), reservoir rocks (Permian Rotliegend sandstones), and evaporite seals (Zechstein formation) of the Carboniferous-Rotliegend petroleum system (Gautier, 2003) are reproduced by the Kupferschiefer stratigraphy, i.e., the Kupferschiefer shales are overlain by the Zechstein evaporites and underlain by the Permian Rotliegend sandstones (Kucha and Przybyłowicz, 1999).

A key question for the present discussion is whether the Carboniferous-Rotliegend petroleum system could have supplied sufficient petroleum to the Kupferschiefer shales to account for the mass of Pd that accumulated in this deposit. To answer this question, we calculated the size of the Pd resource in the Polish Kupferschiefer (Supplementary materials; Section C) by integrating the annual production of Pd from the start of mining in 1995 to present and the projected annual production to 2054, when the last reserves are predicted to be exhausted. According to this calculation, the Polish Kupferschiefer initially contained ~ 1000 kg of Pd. Assuming that the

putative petroleum ore fluid contained 100 ppb of Pd (Oil C dissolved a maximum of 127 ppb Pd), it follows that 10 billion kg of oil would have been required to form the Kupferschiefer resource of 1000 kg of Pd ore. By comparison, the Carboniferous-Rotliegend petroleum system in Western Europe hosts estimated mean undiscovered resources of 144 million barrels of oil which, given an oil density of  $940 \text{ kg/m}^3$  (comparable to Oil C), is equivalent to 21.5 billion kg of oil. Thus, the Carboniferous-Rotliegend petroleum system would have been more than sufficient to form the Pd resource of the Polish Kupferschiefer. We note also that our estimate of the amount of oil needed to form the Kupferschiefer is conservative, because of the relatively modest thiol content of Oil C compared to that reported for many other crude oils (Ho et al., 1974).

In assessing the potential of petroleum as an ore fluid, it is important to compare the Pd solubility to its solubility in hydrothermal fluids, which as discussed earlier, also have been invoked to explain Pd enrichment in black shales. The solubility of Pd in hydrothermal fluids at temperatures comparable to those considered in this study is controlled mainly by the formation of chloride and bisulfide complexes and depends on the ligand concentration, oxygen fugacity and pH. As a chloride complex, the solubility of Pd exceeds 1 ppb only under highly oxidised conditions (above the magnetite-hematite oxygen buffer), at relatively low pH ( $< 4$ ) and at unusually high salinity ( $> 3 \text{ m NaCl}_{\text{eq}}$ ) (Gammons and Bloom, 1992). The solubility of Pd is similarly low as a bisulfide complex; for a geologically realistic reduced sulfur concentration of 0.01 m, the solubility of Pd at  $200^\circ\text{C}$  is  $< 1 \text{ ppb}$  (Gammons and Bloom, 1993). For comparison, the highest concentration of Pd that has been measured in a hydrothermal fluid is 2 ppb, which was for a geothermal fluid at  $300^\circ\text{C}$  (McKibben et al., 1990), considered to be an analogue for epithermal ore-forming fluids (Clark and Williams-Jones, 1990). In summary, the solubility of Pd in Oil C at  $150^\circ\text{C}$  (our thiol-

rich oil) is at least two orders of magnitude higher than the solubility of Pd in hydrothermal fluids that might have been present during the formation of black shale-hosted Pd deposits, further strengthening the case that hydrocarbon liquids rather than aqueous fluids are the main agents of Pd transport for black-shale-hosted Pd deposits.

## **2.7 Conclusions**

We have demonstrated that crude oils can serve as effective Pd ore fluids for black shale-hosted deposits. X-ray Photoelectron Spectroscopy analyses of Pd wires reacted in crude oil at 150 °C indicate that Pd has a strong chemical affinity for the reduced sulfur fraction of crude oil causing Pd to be preferentially dissolved as thiolate complexes. Heavy crude oils that mature in the presence of sulfate at the interface between a black shale and a carbonate sequence at temperatures between 100 and 140°C are likely to undergo thermochemical sulfate reduction. This leads to hydrogen sulfide production and the formation of a thiol-rich oil. Palladium concentrations in our most thiol-rich oil reached 127 ppb at 150°C, which is considerably higher than the solubility of Pd in hydrothermal fluids of the type that have been invoked as possible ore fluids.

Despite the clear link between thiol and Pd concentrations in crude oil, one of our oils dissolved 19 ppb Pd at 150°C yet contained no detectable thiols. We attribute this to the formation of Pd porphyrin complexes in the asphaltene fraction of the oil. Given that carboxylic acids promote the metalation of porphyrin complexes by metals such as Pd, we propose that the transport of Pd as Pd-porphyrins is likely to be important in heavy oils with a large asphaltene fraction and a high carboxylic acid to thiol ratio. Lastly, we note that in crude oils with truly anomalous thiol contents, Pd concentrations are expected to far exceed the concentrations reported in this study.

## **2.8 Acknowledgements**

We express our gratitude to Anna Jung for her assistance with our ICP-MS analyses, to Dr. Scott Bohle for bringing the XPS technique to our attention as a method to gain insight into metal speciation in oil and to Statoil for providing us with the crude oil samples required to perform our experiments. The research was funded by a NSERC-CRD grant to AEW-J.

## **2.9 References**

Barthauer, G.L., Rulfs, C.L. and Pearce, D.W., 1953. Investigation of thucholite. *Am. Mineralogist*, 38.

Bechtel, A. and Püttmann, W., 1991. The origin of the Kupferschiefer-type mineralization in the Richelsdorf Hills, Germany, as deduced from stable isotope and organic geochemical studies. *Chemical Geology*, 91(1), p.1-18.

Buchler, J.W., 1978, Syntheses and properties of metalloporphyrins, in *The Porphyrins*, Academic Press, Inc., p. 389–483.

Cai, C., Worden, R.H., Bottrell, S.H., Wang, L. and Yang, C., 2003. Thermochemical sulphate reduction and the generation of hydrogen sulphide and thiols (mercaptans) in Triassic carbonate reservoirs from the Sichuan Basin, China. *Chemical Geology*, 202(1-2), p.39-57.

Castle, J.E. and Salvi, A.M., 2001. Interpretation of the Shirley background in x-ray photoelectron

spectroscopy analysis. *Journal of Vacuum Science & Technology A: Vacuum, Surfaces, and Films*, 19(4), p.1170-1175.

Castner, D.G., Hinds, K. and Grainger, D.W., 1996. X-ray photoelectron spectroscopy sulfur 2p study of organic thiol and disulfide binding interactions with gold surfaces. *Langmuir*, 12(21), p.5083-5086.

Caumette, G., Lienemann, C.P., Merdrignac, I., Bouyssiere, B. and Lobinski, R., 2009. Element speciation analysis of petroleum and related materials. *Journal of Analytical Atomic Spectrometry*, 24(3), p.263-276.

Clark, J.R. and Williams-Jones, A.E., 1990. Analogues of epithermal gold–silver deposition in geothermal well scales. *Nature*, 346(6285), p.644.

Coveney, R.M., 1991, Ni-Mo-PGE-Au-rich ores in Chinese black shales and speculations on possible analogues in the United States: *Mineralium Deposita*, 26, p. 83–88.

Coveney, R.M., Murowchick, J.B., Grauch, R.I., Glascock, M.D., and Denison, J.R., 1992, Gold and platinum in shales with evidence against extraterrestrial sources of metals: *Chemical Geology*, 99, p. 101–114.

Disnar, J.R. and Sureau, J.F., 1990. Organic matter in ore genesis: Progress and perspectives. *Organic Geochemistry*, 16(1-3), p.577-599.

Emsbo, P., Hofstra, A.H., Johnson, C.A., Koenig, A., Grauch, R., Zhang, X.C., Hu, R.Z., Su, W.C. and Pi, D.H., 2005. Lower Cambrian metallogenesis of South China: Interplay between diverse basinal hydrothermal fluids and marine chemistry. In *Mineral deposit research: Meeting the global challenge* (p. 115-118). Springer, Berlin, Heidelberg.

Eugster, H.P., 1985. Oil shales, evaporites and ore deposits. *Geochimica et Cosmochimica Acta*, 49(3), p.619-635.

Falk, J.E., 1964. *Porphyry and Metalloporphyry* (J. E. Falk, Ed.): Elsevier Publishing Company.

Filby, R.H. and Van Berkel, G.J., 1987. Geochemistry of metal complexes in petroleum, source rocks and coals: an overview. In *Metal complexes in fossil fuels* (344, p. 2-39). American Chemical Society Washington, DC.

Gammons, C.H. and Bloom, M.S., 1993. Experimental investigation of the hydrothermal geochemistry of platinum and palladium: II. The solubility of PtS and PdS in aqueous sulfide solutions to 300 C. *Geochimica et Cosmochimica Acta*, 57(11), p.2451-2467.

Gautier, D.L., 2003. *Carboniferous-Rotliegend total petroleum system description and assessment results summary* (p. 29). USGS Bulletin, 2211.

Giordano, T.H., 1994. Metal Transport in Ore Fluids by Organic Ligand Complexation, in Pittman, E.D. and Lewan, M.D. eds., *Organic Acids in Geological Processes*, Springer-Verlag, p. 320 – 354.

Hardardóttir, V., Brown, K.L., Fridriksson, T., Hedenquist, J.W., Hannington, M.D. and Thorhallsson, S., 2009. Metals in deep liquid of the Reykjanes geothermal system, southwest Iceland: Implications for the composition of seafloor black smoker fluids. *Geology*, 37(12), p.1103-1106.

Ho, T.Y., Rogers, M.A., Drushel, H.V. and Koons, C.B., 1974. Evolution of sulfur compounds in crude oils. *AAPG Bulletin*, 58(11), p.2338-2348.

Hulbert, L.J., Gregoire, D.C., Paktunc, D. and Carne, R.C., 1992. Sedimentary nickel, zinc, and platinum-group-element mineralization in Devonian black shales at the Nick property, Yukon, Canada: a new deposit type. *Exploration and Mining Geology*, 1(1), p.39-62.

Jedwab, J., Badaut, D. and Beaunier, P., 1999. Discovery of a palladium-platinum-gold-mercury bitumen in the Boss Mine, Clark County, Nevada. *Economic Geology*, 94(7), p.1163-1172.

Jones, P. (1975). Trace metals and other elements in crude oil: a literature review. Sunbury: British Petroleum Co. Ltd.

Jowett, E.C., Roth, T., Rydzewski, A. and Oszczepalski, S., 1991. "Background"  $\delta^{34}\text{S}$  values of Kupferschiefer sulphides in Poland: pyrite-marcasite nodules. *Mineralium Deposita*, 26(2), p.89-98.

Jowitt, S.M. and Keays, R.R., 2011. Shale-hosted Ni–(Cu–PGE) mineralisation: a global overview. *Applied Earth Science*, 120(4), p.187-197.

Knopf, A., 1915. A gold-platinum-palladium lode in southern Nevada (pp. 1-18). *USGS Bulletin*, 620A.

Kostas, I.D., Coutsolelos, A.G., Charalambidis, G. and Skondra, A., 2007. The first use of porphyrins as catalysts in cross-coupling reactions: a water-soluble palladium complex with a porphyrin ligand as an efficient catalyst precursor for the Suzuki–Miyaura reaction in aqueous media under aerobic conditions. *Tetrahedron Letters*, 48(38), p.6688-6691.

Kotarba, M.J., Peryt, T.M., Kosakowski, P. and Więclaw, D., 2006. Organic geochemistry, depositional history and hydrocarbon generation modelling of the Upper Permian Kupferschiefer and Zechstein Limestone strata in south–west Poland. *Marine and Petroleum Geology*, 23(3), p.371-386.

Kříbek, B., Sýkorová, I., Pašava, J. and Machovič, V., 2007. Organic geochemistry and petrology of barren and Mo–Ni–PGE mineralized marine black shales of the Lower Cambrian Niutitang Formation (South China). *International Journal of Coal Geology*, 72(3-4), p.240-256.

Kucha, H., 1993. Noble metals associated with organic matter, Kupferschiefer, Poland. In *Bitumens in Ore Deposits* (p. 153-170). Springer, Berlin, Heidelberg.

Kucha, H., and Przybylowicz, W., 1999. Noble Metals in Organic Matter and Clay-Organic Matrices, Kupferschiefer, Poland: *Economic Geology*, 94, p. 1137–1162.

Lewan, M., 1984. Factors controlling the proportionality of vanadium to nickel in crude oils: *Geochimica et Cosmochimica Acta*, 48, p. 2231 – 2238.

Lipiner, G., Willner, I. and Aizenshtat, Z., 1988. Correlation between geochemical environments and controlling factors in the metallation of porphyrins. *Organic geochemistry*, 13(4-6), p.747-756.

Liu, W., Migdisov, A. and Williams-Jones, A., 2012. The stability of aqueous nickel(II) chloride complexes in hydrothermal solutions: Results of UV–Visible spectroscopic experiments. *Geochimica et Cosmochimica*, p. 276-290.

Lott, D., Coveney, R., and Murowchick, J., 1999. Sedimentary exhalative nickel-molybdenum ores in South China: *Economic Geology*, 94, p. 1051–1066.

Machel, H.G., 2001. Bacterial and thermochemical sulfate reduction in diagenetic settings—old and new insights. *Sedimentary Geology*, 140(1-2), p.143-175.

Manning, D.A.C., and Gize, A.P., 1993. The Role of Organic Matter in Ore Transport Processes, in Engel, M.H. and Macko, S.A. eds., *Organic Geochemistry*, p. 547 – 563.

Mao, J., Lehmann, B., Du, A., Zhang, G., Ma, D., Wang, Y., Zeng, M. and Kerrich, R., 2002. Re-Os dating of polymetallic Ni-Mo-PGE-Au mineralization in Lower Cambrian black shales of South China and its geologic significance. *Economic Geology*, 97(5), p.1051-1061.

McKibben, M.A., Williams, A.E. and Hall, G.E., 1990. Solubility and transport of platinum-group elements and Au in saline hydrothermal fluids; constraints from geothermal brine data. *Economic Geology*, 85(8), p.1926-1934.

Mitkin, V.N., Galizky, A.A. and Korda, T.M., 2000. Some Observations on the Determination of Gold and the Platinum-Group Elements in Black Shales. *Geostandards and Geoanalytical Research*, 24(2), p.227-240.

Murowchick, J.B., Coveney Jr, R.M., Grauch, R.I., Eldridge, C.S. and Shelton, K.L., 1994. Cyclic variations of sulfur isotopes in Cambrian stratabound Ni-Mo-(PGE-Au) ores of southern China. *Geochimica et Cosmochimica Acta*, 58(7), p.1813-1823.

Nguyen, V.P., Burklé-Vitzthum, V., Marquaire, P.M. and Michels, R., 2013. Thermal reactions between alkanes and H<sub>2</sub>S or thiols at high pressure. *Journal of analytical and applied pyrolysis*, 103, p.307-319.

Orr, W.L., 1974. Changes in sulfur content and isotopic ratios of sulfur during petroleum maturation--study of Big Horn basin Paleozoic oils. AAPG bulletin, 58(11), p.2295-2318.

Oswald, A.A., 1961. Organic Sulfur Compounds. III. Co-Oxidation of Mercaptans with Styrenes and Indene. The Journal of Organic Chemistry, 26(3), p.842-846.

Oszczepalski, S., 1999. Origin of the Kupferschiefer polymetallic mineralization in Poland. Mineralium Deposita, 34(5-6), p.599-613.

Oszczepalski, S., Nowak, G., Bechtel, A. and Zák, K., 2012. Evidence of oxidation of the Kupferschiefer in the Lubin-Sieroszowice deposit, Poland: implications for Cu-Ag and Au-Pt-Pd mineralisation. Geological Quarterly, 46(1), p.1-24.

Pearson, G., 1963. Hard and Soft Acids and Bases: Journal of the American Chemical Society, 85, p. 3533–3539.

Peter, J.M., and Scott, S.D., 1988. Mineralogy, composition, and fluid-inclusion microthermometry of seafloor hydrothermal deposits in the Southern Trough of Guaymas Basin, Gulf of California: Canadian Mineralogist, 26, p. 567–587.

Peters, K.E., Walters, C.C., and Moldowan, J.M., 2004. The Biomarker Guide: Volume 1, Biomarker and Isotopes in the Environment and Human History: Cambridge University Press.

Plyusnina, L. P., Kyz'mina, T. V., Likhoidov, G. G., & Narnov, G. A., 2000. Experimental modeling of platinum sorption on organic matter. *Applied geochemistry*, 15(6), 777-784.

Price, L.C., and Wenger, L.M., 1992. The influence of pressure on petroleum generation and maturation as suggested by aqueous pyrolysis: *Organic Geochemistry*, 19, p. 141–159.

Püttmann, W. and Goßel, W., 1990. The Permian Kupferschiefer of southwest Poland: a geochemical trap for migrating, metal-bearing solutions. *Applied Geochemistry*, 5(1-2), pp.227-235.

Simmons, S.F. and Brown, K.L., 2006. Gold in magmatic hydrothermal solutions and the rapid formation of a giant ore deposit. *Science*, 314(5797), p.288-291.

Speight, J.G., 2001. *Handbook of Petroleum Analysis* (J. G. Speight, Ed.): John Wiley & Sons Inc.

Sugiyama, I., & Williams-Jones, A. E., 2018. An approach to determining nickel, vanadium and other metal concentrations in crude oil. *Analytica chimica acta*, 1002, p. 18-25.

Sun, Y. and Püttmann, W., 1997. Metal accumulation during and after deposition of the Kupferschiefer from the Sangerhausen Basin, Germany. *Applied Geochemistry*, 12(5), p.577-592.

Tissot, B.P., and Welte, D.H., 1978. *Petroleum Formation and Occurrence*: Berlin, Germany,

Springer-Verlag.

Vairavamurthy, A. and Mopper, K., 1987. Geochemical formation of organosulphur compounds (thiols) by addition of H<sub>2</sub>S to sedimentary organic matter. *Nature*, 329(6140), p.623.

Wei, Z., Mankiewicz, P., Walters, C., Qian, K., Phan, N.T., Madincea, M.E. and Nguyen, P.T., 2011. Natural occurrence of higher thiadiamondoids and diamondoidthiols in a deep petroleum reservoir in the Mobile Bay gas field. *Organic geochemistry*, 42(2), p.121-133.

**Supplementary Materials for**  
The Solubility of Palladium (Pd) in Crude Oil at 150, 200 and 250 °C and its Application to Ore Genesis

Sanz-Robinson et al.

## A. ICP-MS sample preparation and data correction

The crude oils were ashed using reusable Pyrex™ culture tubes and glass wool that was cleaned with HNO<sub>3</sub> for 24 hrs, rinsed with Mili-Q® water for two hours, and then dried in an oven for one hour at 150 °C. Three mL aliquots of oil were placed in three separate culture tubes, which were capped with glass wool to prevent loss of ash. The capped culture tubes were then combusted at 550 °C in a muffle furnace for 12 hours. After combustion, 0.25 ml of 75% Optima™ grade HNO<sub>3</sub>, 0.5 ml of Optima™ grade H<sub>2</sub>O<sub>2</sub> and Trace metal grade 0.25 ml HCl were placed in each culture tube to oxidize the ash and leach the metals. The crude oils, acids, and culture tubes were weighed at each of the steps outlined above.

We measured <sup>105</sup>Pd and <sup>89</sup>Y counts in digested samples (crude oils from Table A), Pd standards (0.1, 0.5, 1, 5, 10, 15, 20 and 50 ppb standards diluted from 1000 ppm Pd aqueous standards supplied by SCP Science Ltd.) and a blank solution (1 ppb Yttrium (Y) diluted from 1000 ppm Y aqueous standards supplied by SCP Science, 2% Optima grade HNO<sub>3</sub>, and Mili-Q® water). The blank solution was also used as a diluent for the digested acid samples and the standards. Digested acid samples were diluted ~80x in 50 ml centrifuge tubes, and then analysed with an ICP-MS using Y as an internal standard. To convert the counts to concentrations, we constructed calibration curves for each metal by plotting the corrected <sup>105</sup>Pd/<sup>89</sup>Y ratios (<sup>105</sup>Pd/<sup>89</sup>Y ratios subtracted from the blank <sup>105</sup>Pd/<sup>89</sup>Y ratios; Eq. A.1) with known standard concentrations (Eq. A.2). All the calibration curves regressed linearly through the origin with a R<sup>2</sup> > 99.9%. Finally, the metal concentrations in the samples were determined by converting counts to concentrations using the slope from Eq. A.2, and then corrected by multiplying dilution factors

and density factors to account for dilutions and acid-oil density differences between the digested acid samples and the original oil samples (Eq. A.3).

$$\left(\frac{^{105}\text{Pd}}{^{89}\text{Y}}\right)_{\text{Corrected}} = \left(\frac{^{105}\text{Pd}}{^{89}\text{Y}}\right)_{\text{Sample}} - \left(\frac{^{105}\text{Pd}}{^{89}\text{Y}}\right)_{\text{blank}} \quad \text{Equation A.1}$$

$$\left(\frac{^{105}\text{Pd}}{^{89}\text{Y}}\right)_{\text{Corrected standard}} = \text{slope} \times \text{Known Pd Standard Concentration (C1)} \quad \text{Equation A.2}$$

A.2

$$\text{Metal Concentration in Crude Oil} = \text{C1} \times \text{Dilution factor} \times \frac{\text{acid (in grams)}}{\text{oil (in grams)}} \quad \text{Equation A.3}$$

## B. Calculation of the thiol content of the Rodney Crude oil

$API = \frac{141.5}{SG} - 131.5$ , where API is a measure of the weight of petroleum liquids and SG is the specific gravity of the oil.

$$\text{Therefore, } SG = \frac{141.5}{API + 131.5}$$

The API value for the Rodney Crude is 32. (Ho et al., 1974)

$$SG_{\text{Rodney Crude}} = \frac{141.5}{32 + 131.5} = 0.865$$

$$SG = \frac{\rho_{\text{Oil}}}{\rho_{\text{H}_2\text{O}}} \text{ where } \rho \text{ denotes density.}$$

Assuming  $\rho_{\text{H}_2\text{O}} = 1.0 \text{ g/mL}$

$$\rho_{\text{Rodney Crude}} = SG_{\text{Rodney Crude}} = 0.865 \text{ g/mL}$$

$$\text{Mercaptan Number} = \frac{\text{mg of thiol S}}{100\text{mL}} \quad (\text{Oswald, 1961})$$

The Mercaptan number for the Rodney Crude is 275 (Ho et al., 1974)

$$\text{Mercaptan Number} = \frac{275 \text{ mg of thiol S}}{100\text{mL}} = \frac{275 \text{ mg thiol S} \times \frac{1000\mu\text{g}}{\text{mg}}}{100\text{mL} \times \rho_{\text{Rodney Crude}}} = \frac{275000 \mu\text{g}}{100\text{mL} \times \frac{0.865\text{g}}{\text{mL}}} = 3179 \text{ ppm}$$

Thus, the Rodney Crude contains 3179 ppm of thiol S.

#### References:

Ho, T.Y., Rogers, M.A., Drushel, H.V. and Koons, C.B., 1974. Evolution of sulfur compounds in crude oils. *AAPG Bulletin*, 58(11), p.2338-2348.

Oswald, A.A., 1961. Organic Sulfur Compounds. III. Co-Oxidation of Mercaptans with Styrenes and Indene. *The Journal of Organic Chemistry*, 26(3), pp.842-846.

### **C. Calculating size of the Pd resource at Polish Kupferschiefer and the petroleum reserves of the Carboniferous-Rotliegend petroleum system**

#### Calculating Pd resource of the Polish Kupferschiefer

Pt and Pd are extracted together as a by-product of copper mining at the Polish Kupferschiefer.

Pd + Pt produced in 1995: 95 kg (Piestrzyński and Sawlowicz, 1999)

Pd + Pt produced in 2011 = 2505 oz x 0.0284kg/oz = 71kg (Bartlett et al, 2013)

Working mines of Polish Kupferschiefer have average concentrations of **0.2ppm Pt** and **0.1ppm Pd**. (Piestrzyński and Sawlowicz, 1999)

Pt:Pd = 2:1

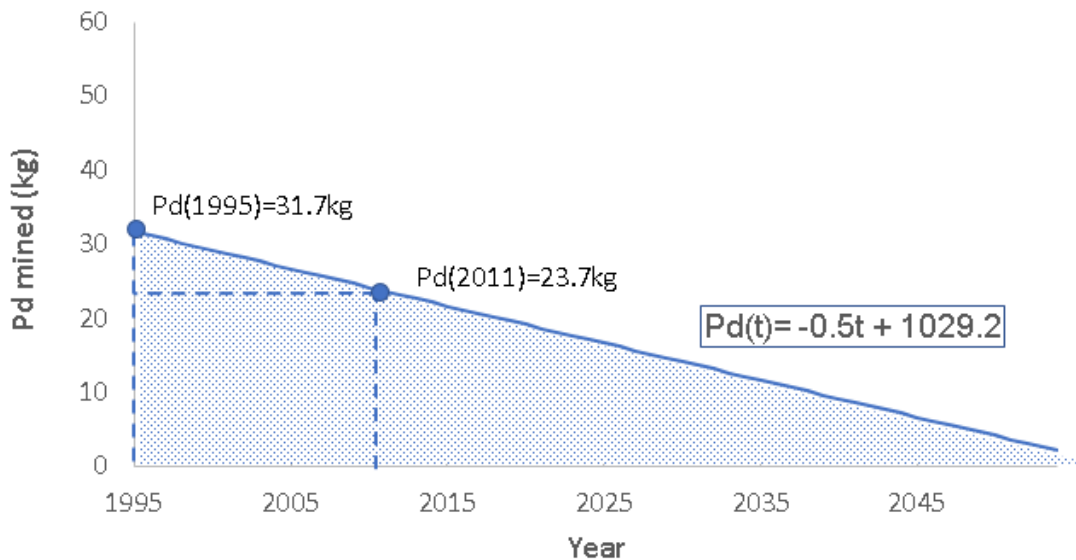
We can use this ratio to estimate how much Pd was extracted in each year

$$\text{Pd (1995)} = 95\text{kg}/3 = \mathbf{31.7 \text{ kg}}$$

$$\text{Pd (2011)} = 71\text{kg}/3 = \mathbf{23.7 \text{ kg}}$$

The earliest available report of Pd production at the Polish Kupferschiefer that we could find dates to **1995** (Piestrzyński and Sawłowicz, 1999) and mining is expected to last until **2054** at the latest (Speczik et al, 2013).

Now we can use these data to linearly extrapolate the amount of Palladium mined in any given year.



**Supplementary Figure 2.1** Linear extrapolation showing the amount of Pd extracted from the Polish Kupferschiefer every year.

#### Estimation of total Pd resource at the Polish Kupferschiefer

$$\text{Total Pd} = \int_{1995}^{2054} 1029.2 - 0.5t \, dt = 1000\text{kg}$$

#### Quantity of oil required to form the Pd mineralization at the Polish Kupferschiefer

Assuming oil is transporting 127ppb Pd.

$$127\text{ppb} = 127 \times 10^{-9} \text{kg Pd/kg oil} = 1.27 \times 10^{-7} \text{kg Pd/kg oil}$$

$$\text{Amount of oil} = 1000 \text{kg Pd} / \frac{1.27 \times 10^{-7} \text{kg Pd}}{\text{kg oil}} = \mathbf{7.87 \text{ billion kg oil}}$$

Mean undiscovered resources in Carboniferous Rotliegend petroleum system.

Mean undiscovered resources of the Carboniferous-Rotliegend petroleum system: 144 million barrels of oil

Assuming oil density is equal to Oil C

$$\text{Density oil C } (\rho) = \text{Specific Gravity Oil C} \times \frac{1000 \text{kg}}{\text{m}^3} = 0.94 \times \frac{1000 \text{kg}}{\text{m}^3} = 940 \text{kg/m}^3$$

$$\text{Volume of oil barrel} = 0.159 \text{ m}^3/\text{barrel}$$

$$\text{Mass of oil in petroleum system} = 144 \times 10^6 \text{barrels} \times \frac{0.159 \text{ m}^3}{\text{barrel}} \times \frac{940 \text{ kg}}{\text{m}^3} = \mathbf{21.5 \text{ billion kg oil}}$$

References:

Bartlett, S.C., Burgess, H., Damjanovic, B., Gowans, R.M. and Lattanzi, C.R.(2013). *Technical report on the copper-silver production operations of KGHM Polska Miedź SA in the Legnica-Głogów copper belt area of southwestern Poland*: Micon International Limited.

Gautier, D.L., 2003. *Carboniferous-Rotliegend total petroleum system description and assessment results summary* (p. 29). USGS Bulletin, 2211.

Piastryński, A. and Sawlowicz, Z., 1999. Exploration for Au and PGE in the Polish Zechstein copper deposits (Kupferschiefer). *Journal of Geochemical Exploration*, 66(1-2), p.17-25.

Speczik, S., Oszczepalski, S. and Chmielewski, A., 2013, August. Exploration and mining perspective of the Kupferschiefer series in SW Poland: digging deeper?. In *Mineral deposit research for a high-tech world. Proceedings of the 12th Biennial SGA Meeting* (pp. 12-15).

### Preface to Chapter 3

---

The results presented in Chapter 2 demonstrate that crude oil can serve as an effective ore fluid for the transport of Pd in sediment-hosted deposits. Furthermore, it was shown that the entire Pd resource in the Kupferschiefer deposit in Poland could have been supplied by crude oil sourced from the underlying Carboniferous strata. Nonetheless, arguably the most compelling evidence for the transport of metals by petroleum is found in the sediment-hosted Pb-Zn deposits of the Mississippi Valley Type (MVT) class. Chapter 3 reports the results of experiments designed to evaluate the solubility and speciation Zn in the same crude oils that were considered in Chapter 2. It also discusses the factors that contribute to the formation of Zn-rich crude oils as well as the geochemical conditions required to precipitate Zn from metalliferous crude oil to form an ore deposit. Wires of Zn(0) were reacted in crude oils at 150, 200 and 250°C and the steady-state concentration of Zn in these oils was determined. This was accomplished by digesting the reacted oils and analyzing them by ICP-MS. The surface of the Zn wires was analyzed by XPS to identify the ligands in crude oil that have a high affinity for Zn. An experiment was also conducted that had been devised to precipitate sphalerite, ZnS, from crude oil by mimicking the geochemical conditions found in the ore zones of Mississippi Valley Type (MVT) deposits.

### **3. Zinc solubility, speciation and deposition: A role for liquid hydrocarbons as ore fluids for Mississippi Valley Type Pb-Zn deposits.**

---

**J. Sanz-Robinson\*<sup>a</sup> and A.E. Williams-Jones<sup>a</sup>**

<sup>a</sup> Department of Earth and Planetary Sciences, McGill University, 3450 University Street,  
Montreal, QC, H3A 0E8, Canada

Published in Chemical Geology, 2019

DOI: <https://doi.org/10.1016/j.chemgeo.2019.05.002>

## Abstract

Although the ore fluid for Mississippi Valley Type (MVT) deposits is universally considered to be a basinal brine, the common occurrence of liquid hydrocarbons as inclusions in one of the ore minerals (sphalerite) raises the question of whether liquid hydrocarbons could play a role in metal transport. Here, we explore the potential of liquid hydrocarbons to act as an ore fluid by determining the steady-state concentration of zinc in crude oil and evaluating the factors that promote its dissolution. To this end, zinc wires were reacted with a series of oils (labelled oils A, B and C) at 150, 200 and 250 °C, and the steady-state concentration of Zn was determined. Zinc concentrations were observed to increase with temperature and with the Total Acid Number (TAN) of the oils, the latter of which is strongly correlated to the carboxylic acid content of crude oil. Crude oil B, the highest TAN oil, dissolved  $1700 \pm 0.8$  ppm of Zn at 250 °C, which is comparable to the highest Zn concentration inferred to have been dissolved in brines interpreted to represent MVT ore fluids. X-ray Photoelectron Spectroscopic (XPS) analyses performed on the residual oil coating the zinc wires after the reaction supported the conclusion that Zn has a strong chemical affinity for carboxylic acids in crude oil. Finally, an experiment designed to precipitate sphalerite crystals from a Zn-rich synthetic oil at room temperature showed that sphalerite precipitation from liquid hydrocarbons proceeds efficiently in a carbonate-buffered, H<sub>2</sub>S -rich environment.

### 3.1 Introduction

Zinc ( $[\text{Ar}] 3d^{10} 4s^2$ ) is the 24th most abundant element in the Earth's crust and the second most abundant metal in the human body after iron (Huang and Gitschier, 1997). Unlike the transition metals, the  $\text{Zn}(2+)$  ion has a full d-orbital and so does not participate in redox reactions but rather acts as a Lewis acid accepting electrons to form stable complexes with variety of ligands and in varied geometries. This makes Zn a metal of noteworthy biological significance, serving as an essential enzymatic co-factor for the growth, development and differentiation of all types of life, including micro-organisms, plants and animals (McCall et al., 2000). It also explains its accumulation and retention to significant levels in organic matter (Jones, 1975; Shuman, 1999), including liquid hydrocarbons (see below).

Since Roman times, when it was alloyed with copper to form brass, zinc has been an important metal in human development (Craddock, 1978), and currently some 13 million tons of the metal are used annually in a large variety of industrial applications (Thomas, 2018). Much of the current production of zinc is from the mining of deposits hosted by carbonate-rich sedimentary rocks, in which it occurs as the mineral sphalerite ( $\text{ZnS}$ ), making zinc a chalcophile or “sulphur loving” element (Lee and Saunders, 2003). Many of these deposits belong to the Mississippi Valley Type (MVT) deposit class (Anderson and Macqueen, 1982; Leach et al., 2010), and are epigenetic, typically occurring on the flanks of sedimentary basins, orogenic forelands, or foreland thrust belts inboard of clastic rock-dominated passive margin sequences (Leach et al., 2010). Nearly all of them are dolomite-hosted with the zinc and lead ore minerals (sphalerite and

galena) occurring commonly within cavities or as breccia cements in the carbonate rocks (Anderson and Macqueen, 1982).

The generally accepted hypothesis for the formation of MVT deposits is that the metals are transported in basinal brines (oil field brines) that migrate into carbonate reservoirs (limestone reefs) formerly occupied by liquid hydrocarbons; the hydrocarbons, which have lower density than the brines, precede the latter. There, the brines deposit the metals as a result of mixing with fluids from the backreef, in which sulphate is thermally reduced to H<sub>2</sub>S by interacting with the hydrocarbon residues (Leach et al., 2010). This hypothesis is supported by the close association of MVT deposits with hydrocarbons, such as bitumen (Anderson and Macqueen, 1982).

However, hydrocarbons are also commonly present as fluid inclusions in the sphalerite ores (Roedder, 1979; Anderson and Macqueen, 1982; Etminan and Hoffmann, 1989), which raises the possibility that instead of acting solely as reductants, the hydrocarbons could also have served as agents of metal transport. This latter hypothesis would be consistent with the observation that the oil window (80–160 °C; Peters et al., 2004) overlaps with the temperatures at which MVT deposits commonly form (100–150 °C; Anderson and Macqueen, 1982; Parnell, 1988). It is also supported by the observation that crude oils commonly contain high concentrations of Zn (up to 160 ppm, Jones, 1975).

In this paper, we examine the hypothesis that, in some cases, liquid hydrocarbons can dissolve enough Zn to act as ore fluids for MVT deposits. To this end, we experimentally investigated the solubility of zinc in crude oils of variable composition at temperatures up to 250 °C. As sulphur in these deposits is generally considered to come from evaporites and to be supplied for mineral

precipitation as H<sub>2</sub>S through the process of bacterial sulphate reduction (BSR) or thermochemical sulphate reduction (TSR), we also report the results of experiments designed to precipitate sphalerite from a synthetic liquid hydrocarbon fluid.

## **3.2 Materials and methods**

### **3.2.1 Crude oil characterization**

The crude oils A, B and C used in this study, as well as data on their compositions and physical properties, were supplied by Statoil Canada. These oils differ markedly from one to another, both compositionally and with respect to their physical properties (Table 3.1). For example, the oils vary greatly in their sulphur content and the proportions of different sulphur compounds (thiols, polysulphides, thiophenes, benzothiophenes). Certain sulphur compounds, notably thiols, are well known for their ability to form metal organic complexes with chalcophile elements (Lewan, 1984; Giordano, 1994; Speight, 2001) and so are of particular interest when studying metal solubility in oil. Our oils also differ considerably in their Total Acid Number (TAN), a measure of oil acidity, which is strongly correlated to the carboxylic acid content (Meredith et al., 2000). Significantly, short-chain carboxylic acids have been proposed as potentially effective ligands for the transport of Zn in aqueous fluids, such as those thought to be responsible for the formation of MVT deposits (Giordano, 1985; Sverjensky, 1986; Giordano and Kharaka, 1994). Consequently, the carboxylic acid content of an oil, which is reflected in its TAN, may also play an important role in controlling zinc solubility in liquid hydrocarbons. Lastly, the nitrogen and

asphaltene content of the oils are parameters that should be considered because of their association with nitrogen-bearing ligands such as porphyrins, which are well-known for their ability to form metal organic complexes. Indeed, nickel and vanadium porphyrins are very commonly present in crude oil, and chromium, titanium, cobalt and zinc porphyrins have all been identified in oil shales (Duyck et al., 2007).

**Table 3.1** The characteristics and compositions of the three crude oils, A, B and C, employed in our experimental study.

<b>Parameters</b>	<b>Oil A</b>	<b>Oil B</b>	<b>Oil C</b>
<b>API Gravity</b>	26.6	25	19
<b>Specific Gravity</b>	0.895	0.904	0.94
<b>Sulfur (wt.%)</b>	0.84	0.52	0.82
<b>Thiols/sulfides (ppm)</b>	44	0	52
<b>Thiophenes/Disulfides (ppm)</b>	1401	37	1052
<b>Benzothiophenes (ppm)</b>	3892	1884	3164
<b>Dibenzothiophenes (ppm)</b>	2575	2737	2024
<b>Benzonaphthothiophenes (ppm)</b>	490	549	109
<b>Nitrogen (wt.%)</b>	---	0.2	0.44
<b>TAN (mgKOH/g)</b>	0.2	2.9	2.3
<b>Paraffins (wt.%)</b>	---	37	19
<b>Naphthenes (wt.%)</b>	---	49	65
<b>Aromatics (wt.%)</b>	---	13	15
<b>Asphaltenes (wt.%)</b>	1.6	0.3	1.4

### 3.2.2 The solubility and speciation of zinc in liquid hydrocarbons

In order to determine the steady-state concentration of elemental zinc in crude oil, zinc wires were reacted in crude oils A, B and C at 150, 200 and 250 °C. This involved reacting a zinc wire in oil inside a sealed quartz tube for variable durations (5, 10, 15 and 30 days). After the experiments, the tubes were quenched in water at room-temperature and the metal wire was removed. The oil was then combusted in a furnace at 550 °C for 24 h and the resulting char was

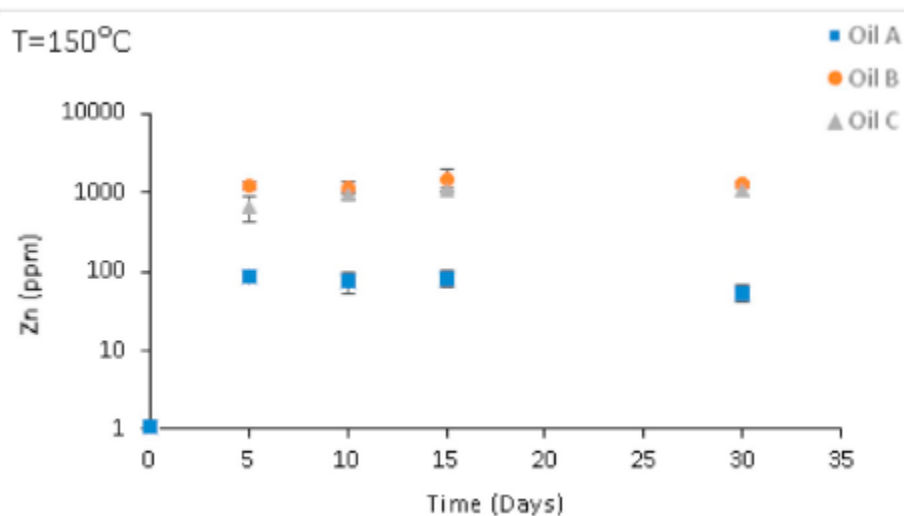
leached in a solution composed of 2:1:1 parts H<sub>2</sub>O<sub>2</sub>:HNO<sub>3</sub>: HCl for a further 24 h. The leaching solution was diluted in a 2% HNO<sub>3</sub> solution and analysed by ICPMS using Y as an internal standard. Further details of the experimental and analytical methods are given in Sanz-Robinson et al. (2019) and Sugiyama and Williams-Jones (2018).

After reaction with oil, the zinc wires were removed, rinsed in toluene and vacuum dried for 24 h. The residual oil coating the wires was analysed by X-ray Photoelectron Spectroscopy (XPS) to gain insight into the types of ligands in oil, which preferentially bind to zinc. The surface composition of the wires was characterized by XPS on a Thermo Scientific K $\alpha$  spectrometer, using Al K $\alpha$  radiation (1486 eV) and an X-ray spot size of 100  $\mu$ m. Scans were made with a pass energy of 50 eV and a resolution of 0.1 eV. We used the Thermo Scientific K $\alpha$  spectrometer etching capability to progressively etch the zinc wire with an argon (Ar<sup>+</sup>) ion beam and analyse the freshly exposed zinc surface. Progressive etching removes ligands that are weakly bound to the surface of the wire, thereby exposing ligands that have a greater chemical affinity for zinc and are more deeply embedded in the wire.

### **3.2.2.1 Temperature and duration of the experiments**

The oil window extends from 80 to 160 °C (Peters et al., 2004). Pyrolysis experiments (Price and Wenger, 1992) and evidence from liquid hydrocarbons entrapped in black smokers (Peter and Scott, 1988), however, both suggest that oil remains stable to temperatures above 300 °C for protracted periods of time ( $\geq 30$  days). Thus, the range of experimental temperatures selected for this study (150–250 °C) was based on oil window temperatures and oil stability considerations.

In order to determine the steady-state concentration of zinc in an oil at a given temperature, zinc wires were left to react in the oil for different durations (see Fig. 3.1). Zinc concentrations were measured after reaction with the oils for 5, 10, 15 and 30 days. Every data point in Fig. 1 is the average of three trials performed at the same temperature and duration and the associated error bars represent the standard deviation of the three trials. As is evident from Fig.3.1, a steady-state concentration was reached in <30 days, and in some cases in as little as 5 days. Nevertheless, the experimental errors for oils B and C decreased, if reaction times were prolonged to the full 30 days. Experimental errors for oil A remained the same for all durations. Zinc concentration in the crude oils was deemed to have reached a steady state when the concentration reached a plateau value and the experimental error was at a minimum. All subsequent experiments were conducted for durations predicted to produce a steady-state concentration.



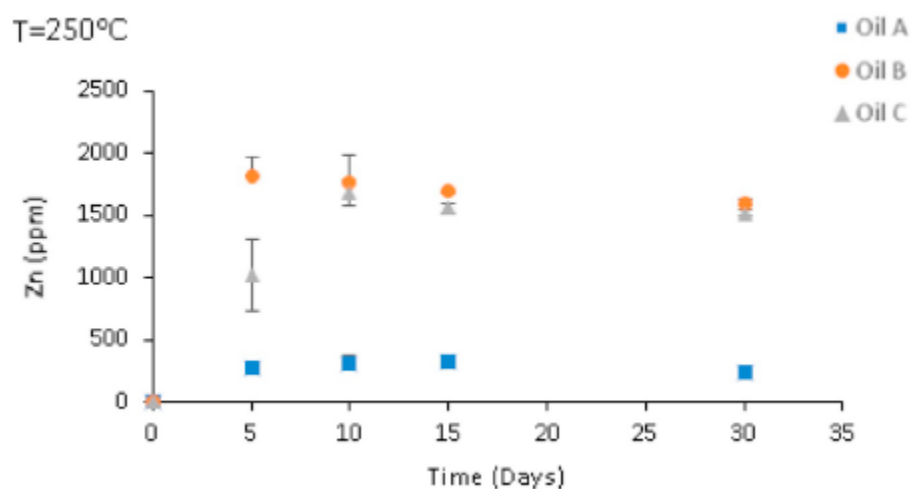
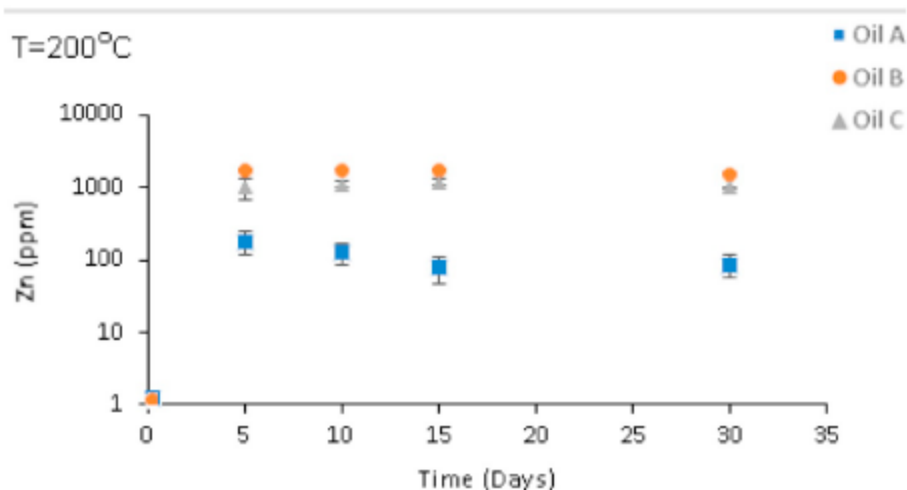


**Figure 3.1** Concentration of Zn in crude oils A, B and C at 150, 200 and 250 °C as a function of the duration of the experiments. The vertical lines are error bars indicating the experimental uncertainty.

### 3.2.3 Precipitation of sphalerite from a synthetic zinc-rich oil

The Conostan® 1000 ppm Zn oil standard (Catalogue #CB7–100-032), which is composed of Zn-alkylaryl sulphonate (1000 ppm Zn) dissolved in crude oil (compositional information for this Zn oil standard is provided in Supplementary materials, Section A), was injected into a reaction vessel atop a layer of calcite-buffered, 15 wt% NaCl brine. Hydrogen sulphide gas was

generated in an external flask by dripping 38% hydrochloric acid onto sodium sulphide. The hydrogen sulphide gas was pumped through the reaction vessel under positive pressure for five (5) minutes to ensure a hydrogen sulphide atmosphere (Sup. Fig. 3.1). The reaction vessel was then sealed and left to rest for 24 h at room temperature. Sphalerite crystals were seen to precipitate from the oil after 10 min. The crystals were separated by centrifuging the brine, and their composition was confirmed using a Rigaku SmartLab X-ray diffractometer (XRD) with Cu K $\alpha$  radiation ( $\lambda=0.154$  nm).

### **3.3 Results**

#### **3.3.1 Solubility and speciation of Zinc in crude oil**

The Zn solubility increases with temperature for the three oils tested (Table 3.2). In addition, zinc solubility increases with TAN concentration at the three temperatures considered (Fig.3.2). Oil B, our highest TAN oil (Table 3.2), with a TAN value of 2.9 mgKOH/g, dissolved 1700 ppm Zn at 250 °C, the highest Zn concentration dissolved in any of our experiments. At the same temperature, Oil C, with a TAN value of 2.3 mgKOH/g, dissolved 1520 ppm Zn and Oil A, with a TAN value of 0.2 mgKOH/g, dissolved 244 ppm. Steady-state concentrations of Zn in the crude oil were observed to correlate strongly and exclusively with oil TAN values.

**Table 3.2** The experimentally determined steady-state concentration of Zn in crude oils A, B and C at 150,200 and 250 °C. The Zn concentration at 25 °C is the background concentration in the unreacted oil.

	<u>Oil A</u>			<u>Oil B</u>			<u>Oil C</u>		
	n*	Zn (ppm)	Error (ppm)	n*	Zn (ppm)	Error (ppm)	n*	Zn (ppm)	Error (ppm)
<b>25°C</b>	3	0.1	0.1	3	0.2	0.2	3	0.15	0.09
<b>150 °C</b>	3	50	10	3	1300	100	3	1080	50
<b>200 °C</b>	3	90	30	3	1600	50	3	1200	90
<b>250 °C</b>	3	240	20	3	1700.0	0.8	3	1520	30

n\* is the number of experiments conducted.

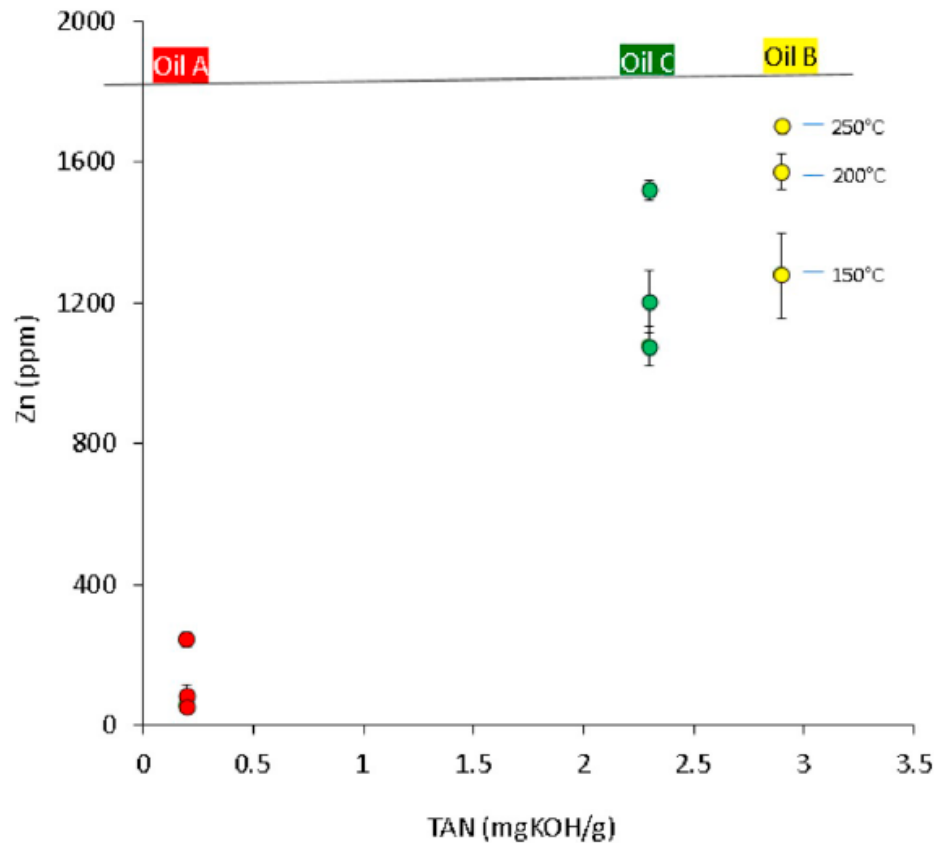


**Figure 3.2** Zn solubility (ppm) in crude oils A, B and C versus the oil TAN (mgKOH/g).

As noted earlier, X-ray Photoelectron Spectroscopy analyses were performed on the residual oil coating the zinc wires after reaction with crude oil (see Fig. 3.3). The zinc wires were covered in a layer of carbon (C), oxygen (O) and sulphur (S). Progressive etching of the Zn wires led to an increase in the relative abundance of Zn and O and a decrease in the relative abundance of C as detected by XPS. The relative abundance of S did not change significantly during etching. This indicates that Zn has a strong chemical affinity for the oxygen-bearing fraction of crude oil, a weaker affinity for S and a weaker affinity still for C in crude oil.

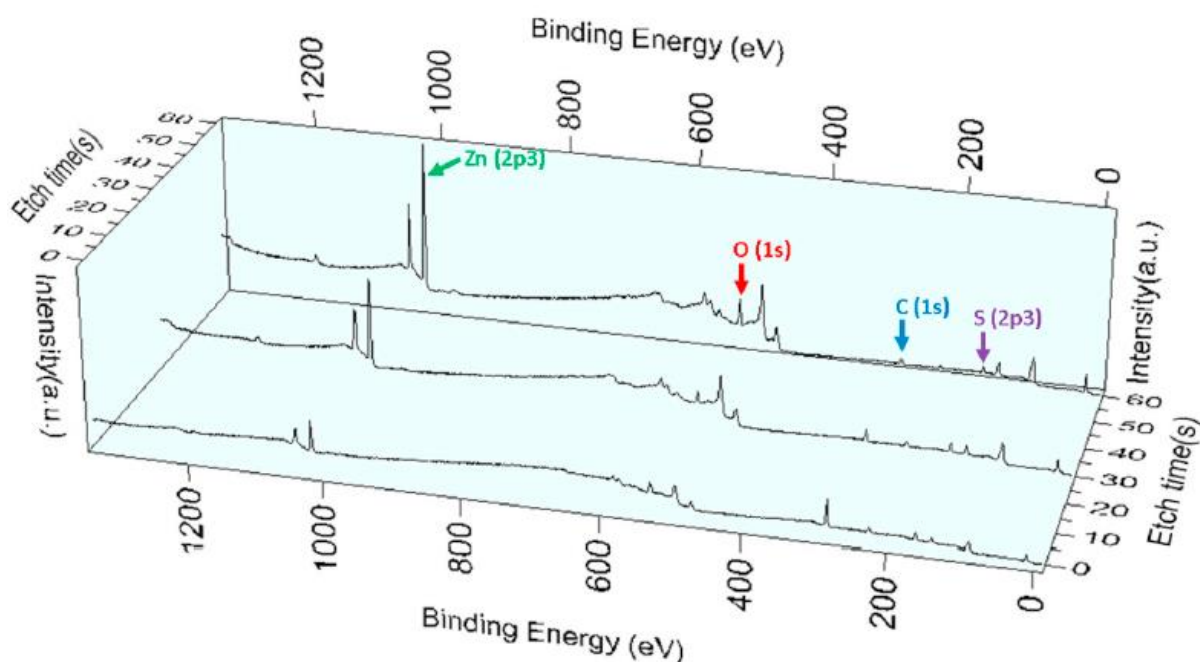


**Figure 3.3** An XPS spectrum identifying the major elements bound to the Zn wire after reaction with Oil C at 200 °C. The relative abundances of these elements changed as the wire was progressively etched.

### 3.3.2 Precipitation of sphalerite from a Zn-rich oil

A reaction designed to precipitate Zn from oil in the presence of hydrogen sulphide gas was carried out successfully (details of the experimental setup are provided in Section 3.2.3).

Although the reaction was allowed to proceed for 24 h, sphalerite crystals were seen to precipitate at the oil-brine interface as a cloud of small, white crystals after just 10 min (Fig. 3.4).

The composition of the crystals was confirmed using XRD (see Fig. 3.5). The mass of sphalerite that precipitated was measured and shown to represent for 44% of the Zn initially present in the oil (see Supplementary materials, Section B for details of the calculation).

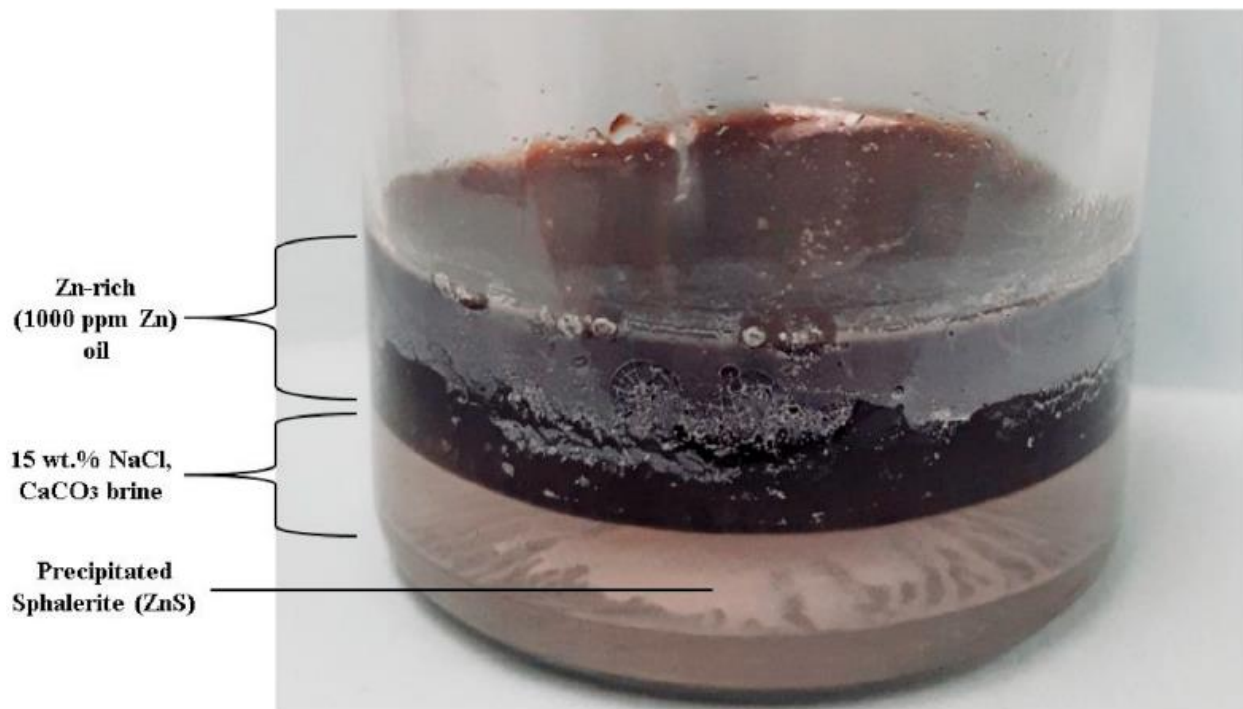


**Figure 3.4** Reaction vessel containing sphalerite that was precipitated from a 1000 ppm zinc-sulphonate oil.

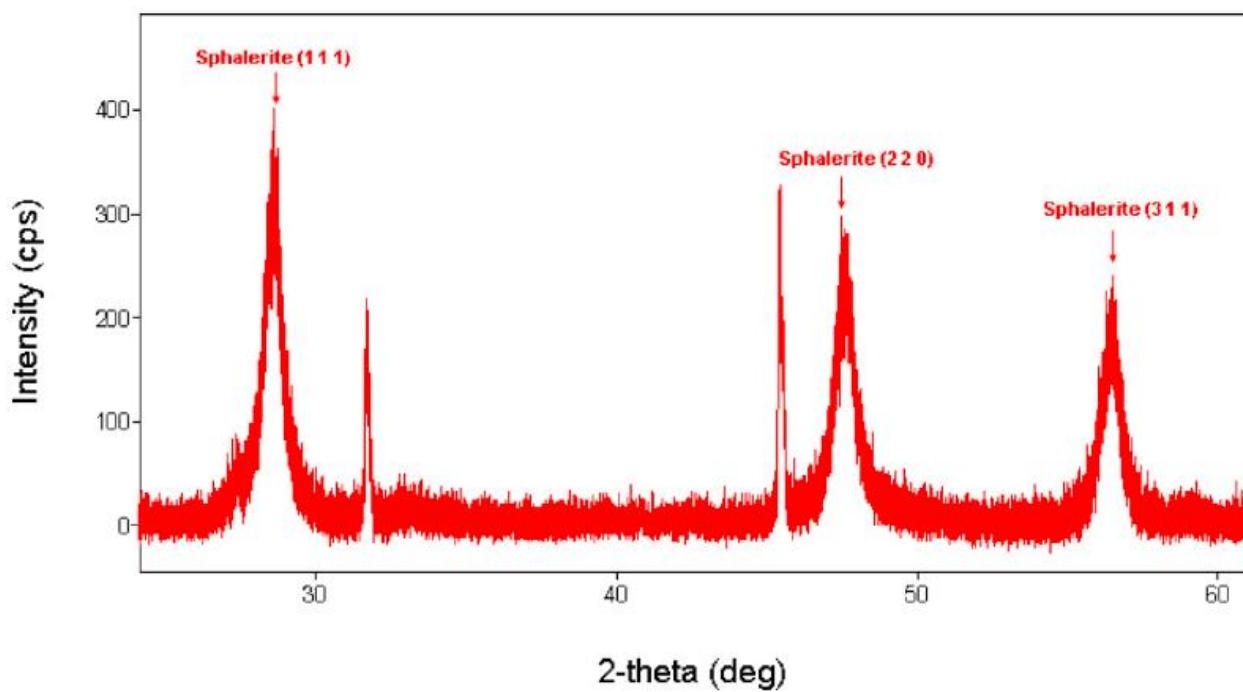


**Figure 3.5** An XRD spectrum of the sphalerite precipitated from a 1000 ppm zinc-sulphonate oil.

## 3.4 Discussion

### 3.4.1 Factors affecting the solubility and speciation of Zn in crude oil

The results of the experiments illustrated in Fig. 3.2 show that zinc solubility in crude oil increases with the TAN value at all temperatures investigated. The total acid number (TAN) is a variable, that quantifies the acidity of an oil and is strongly correlated to its carboxylic acid content (Meredith et al., 2000). Thus, the carboxylic acid content appears to exert an important control on Zn solubility in crude oil. In addition, as is evident from Fig. 3.3, the results of XPS analyses of the Zn wires reacted in crude oil show that Zn has a strong chemical affinity for oxygen compounds in the oil. This is reflected by the growth of the Zn peak and the O peak upon etching of the wire. As most of the oxygen in petroleum is contained in carboxylic acids (Seifert, 1975), this independently reinforces the hypothesis that Zn is complexed primarily by carboxylic acids in crude oil. In contrast, the carbon peak in Fig. 3.3 shrinks upon etching, which indicates that carbon is only loosely bound to the zinc wire. The observation that the sulphur peak changes little upon etching indicates that the chemical affinity of Zn for S in oil may be very limited. This is confirmed by the fact that Oil B, our most Zn-rich oil, has the lowest sulphur content of the three oils. In addition, thiols were not detected in Oil B. This contrasts sharply with the conclusion that thiols form the dominant organic complexes with Zn in aqueous ore fluids (Giordano, 1994).

Heavy crude oils from geologically young formations tend to have the highest carboxylic acid contents. This high content is due primarily to bacterial biodegradation (Meredith et al., 2000; Li et al., 2010). Redox processes during late diagenesis involving the reaction of kerogen or hydrocarbons with mineral oxidants, such as hematite ( $\text{Fe}_2\text{O}_3$ ) in red beds, however, may also be a significant source of carboxylic acids (Surdam et al., 1993).

### **3.4.2 The potential of liquid hydrocarbons to act as zinc ore fluids.**

It has long been thought that water-soluble carboxylic acids, such as acetic acid, may be effective ligands for the transport of Zn in oilfield brines (Giordano, 1985; Sverjensky, 1986; Giordano and Kharaka, 1994) but little consideration has been given to the possibility that liquid hydrocarbons may act as ore fluids for Zn. High TAN crude oils can contain as much as 3 wt% carboxylic acids, making these acids potentially important ligands for complexation with Zn (Seifert, 1975). Oil B, our highest TAN oil (2.9 mg KOH/g, corresponding to a carboxylic acid content of 8.6 mg/g; See Appendix C for calculation), dissolved 1700 ppm Zn at 250 °C, which is comparable to the maximum amount of Zn inferred to have been dissolved in brines trapped as fluid inclusions in sphalerite from MVT deposits based on thermodynamic modeling (Stoffell et al., 2008). It is important to note, however, that the TAN of Oil B is much lower than that of some oils reported in the literature. For example, the Muglad basin and Great Palogue Field in Sudan are known to produce oils with TAN values of up to 16.2 mgKOH/g (Li et al., 2010) and 10.4 mgKOH/g (Dou et al., 2008), respectively. Lower but still significant TAN values (up to 3.6 mgKOH/g) have been reported for crude oils from offshore oilfields along the Brazilian coast (Barbosa et al., 2016). Based on the results of our experiments, all these oils have the potential to transport significantly greater concentrations of Zn than Oil B.

It is noteworthy that not only can crude oils dissolve significant quantities of Zn but in some MVT deposits, e.g., San Vicente in Peru, Laisvall and Vassbo in Sweden, those of the Canning Basin in Western Australia and Gays River in Nova Scotia, there is evidence for the epigenetic injection of petroleum into the ore zone from an underlying shale sequence (Gize and Barnes, 1987; Etminan and Hoffmann, 1989; Spangenberg et al., 1999; Saintilan et al., 2016). In the case of the Cadjebut deposit, one of the largest Pb and Zn deposits in the Canning Basin, brine inclusions commonly coexist with hydrocarbon inclusions in sphalerite from the ore zone. Hydrocarbon inclusions appear as areas of purple zoning in the sphalerite, which can constitute up to 30% volume of the crystals (Etminan and Hoffmann, 1989). This is consistent with the observation from stratigraphic reconstruction, seismic depth mapping and basin modeling, that large portions of the Ordovician-Devonian source rock sequence below the Cadjebut deposit were within the oil window when the deposit formed at  $350 \text{ Ma} \pm 15 \text{ Ma}$  (Warren and Kempton, 1997; Wallace et al., 2002). Significantly, this also coincided with a time of extension and subsidence in the region (Wallace et al., 2002). It has, therefore, been proposed that the MVT-related hydrocarbons were driven up from the source rocks into the ore zone through compaction-induced flow and compactional dewatering (Wallace et al., 2002). If, as seems plausible from the scenario described above, the hydrocarbons were generated at the same time as the brines and traveled with them to the site of ore deposition, then it is reasonable to speculate that the hydrocarbons may have played a role in transporting the zinc.

Before concluding that liquid hydrocarbons could play a role in the transport of Zn in MVT ore-forming systems, it is necessary to establish whether it is possible to mobilise petroleum in the quantities required to form a MVT deposit. The Cadjebut deposit has reserves of 3.5 million metric tons of 17% combined Zn+Pb (Tompkins et al., 1994). Assuming that the ore fluid was an oil with a density  $850 \text{ kg/m}^3$  (similar to the oil used in our sphalerite precipitation experiments), it would require  $0.7 \text{ km}^3$  of oil with a concentration of 1000 ppm Zn to form 3.5 million tonnes of ore grading at 17 wt% Zn. Given the oil productivity of the Canning Basin, this volume of oil could have been easily supplied (refer to Supplementary materials, section D for relevant calculations). For example, the Ordovician, organic-rich Goldwyer Shale in the Canning Basin has risked oil and condensate reserves in place of  $38.8 \text{ km}^3$  (EIA, 2015), and this probably only constitutes a small fraction of the original hydrocarbon producing potential of the basin. These observations, when considered in light of the results of our experiments showing that carboxylic acid-rich crude oils can transport very large concentrations of Zn, strengthens the case for a hypothesis involving the transport of Zn by liquid hydrocarbons during MVT ore formation.

### **3.4.3 Precipitation of sphalerite from zinc-rich oils**

The calculations described above have shown that it should be possible, in principle, to form a MVT deposit from a liquid hydrocarbon ore fluid. These calculations, however, assume that a mechanism is available for efficiently precipitating sphalerite from the hydrocarbon liquid. In MVT deposits, the sphalerite (and galena) is commonly precipitated from the ore fluid as a result of the reduction of sulphate by organic matter (Thom and Anderson, 2008). This generates large amounts of  $\text{H}_2\text{S}$  gas, which is postulated to react with the dissolved Zn species in the ore fluid, thereby inducing deposition of sphalerite and other base metals (Machel, 2001). Sulphate

reduction can occur at low temperature (from 0 to 80 °C) through a microbially-mediated process known as Bacterial Sulphate Reduction (BSR) but can also start to occur abiotically at temperatures between 100 and 140 °C through a process referred to as Thermochemical Sulphate Reduction (TSR) (Machel, 2001).

We evaluated the potential for sphalerite deposition experimentally for the case in which the ore fluid is a hydrocarbon liquid rather than a brine by placing a 1000 ppm Zn synthetic oil in contact with a calcite-equilibrated, 15 wt% NaCl brine. The resulting fluid was purged with hydrogen sulphide gas to simulate the geochemical conditions imposed by BSR or TSR inside a carbonate reservoir. The experiment was conducted at room temperature and led to the precipitation of 44 wt% of the Zn initially contained in the oil as sphalerite, indicating that Zn dissolved in crude oil will precipitate readily in the presence of H<sub>2</sub>S. Although this is an extremely efficient process at ambient temperature, it does not follow that the process would be similarly efficient at the temperature of MVT ore-formation. The results of calculations reported by Williams-Jones and Migdisov (2014), however, show that any Zn present in brines at temperatures corresponding to those of MVT deposits will precipitate entirely in the presence of an equivalent amount of H<sub>2</sub>S. Thus, if any of the Zn dissolved in the oil were to partition into the coexisting brine, a process that would be favoured by elevated temperatures, it would precipitate spontaneously in the presence of H<sub>2</sub>S. This supports the hypothesis that liquid hydrocarbons could play a significant role in the formation of MVT deposits as an agent for metal transport.

Bacterial sulphate reduction and TSR take place spatially at the confluence of organic matter (kerogen, bitumen or oil) with sulphate rich brines. The aqueous sulphate for this reaction is

thought to be derived locally from gypsum in the carbonate host rocks (Machel, 2001). In MVT systems, such as those that formed the Cadjebut deposit, there is evidence for multiple ore fluid pulses due to regional extension and subsidence (Tompkins et al., 1997). During the initial pulses, Zn-rich fluids (petroleum and water) would migrate into the carbonate-sulphate reservoir, where, in the presence of minerals such as gypsum and magnesite, sulphate reduction leads to the precipitation of an early generation of sphalerite ore. Subsequent fluid pulses may not only be enriched in Zn but may also re-dissolve some of the pre-existing ore and reprecipitate it higher up in the stratigraphy. Thus, it is likely that the locus of sulphate reduction, which coincides with the organic phase-water interface, mobilises Zn with each fluid pulse and so the ore in these systems becomes progressively enriched in a pulse-wise manner, thereby providing further support for the hypothesis that liquid hydrocarbons may play a role in Zn transport in MVT ore-forming systems.

### **3.5 Conclusion**

The solubility of Zn in crude oil correlates positively with their Total Acid Number (TAN), and XPS analyses performed on zinc wires after reaction in crude oil indicate that Zn has a strong chemical affinity for the oxygen ligands in crude oil. Both the oxygen content and TAN correlate with the carboxylic acid content of crude oil, indicating that carboxylic acids are likely the main enabling ligands for Zn dissolution in crude oils. Most importantly, from the perspective of MVT ore-genesis, the concentrations of Zn dissolved in our high TAN crude oils are comparable to the inferred concentration of zinc in sphalerite-saturated brines representative of MVT deposits; even higher concentrations are predicted for oils reported to have TAN considerably higher than

the highest one (Oil B) in our study. This, and the preservation of liquid hydrocarbons in MVT ores, support the hypothesis that these hydrocarbons play an important role in transporting the zinc required for the formation of some MVT deposits. Finally, the results of our experiments simulating the geochemical conditions imposed by Thermochemical Sulphate Reduction (TSR) show that sphalerite is precipitated efficiently from liquid hydrocarbons through interaction with H<sub>2</sub>S in exactly the same way as it is proposed to precipitate from hydrothermal fluids.

### **3.6 Acknowledgements**

The research described in this paper was funded by a grant from Statoil Canada and a collaborative research and development grant from NSERC. The crude oil samples used in the experiments were supplied by Statoil Canada. Ichiko Sugiyama helped with the set-up of the experiments and developed the methodology that we employed in analysing our samples. Finally, we acknowledge the constructive comments of two anonymous reviewers that helped us to improve the manuscript significantly.

### **3.7 References**

Anderson, G.M. and Macqueen, R.W., 1982. Ore deposit models-6. Mississippi Valley-type lead-zinc deposits. *Geoscience Canada*, **9(2)**.

Ayuso, R.A., Kelley, K.D., Leach, D.L., Young, L.E., Slack, J.F., Wandless, J.F., Lyon, A.M. and Dillingham, J.L., 2004. Origin of the red dog Zn-Pb-Ag deposits, Brooks Range, Alaska: evidence from regional Pb and Sr isotope sources. *Economic Geology*, **99(7)**, pp.1533-1553.

Barbosa, L.L., Sad, C.M., Morgan, V.G., Figueiras, P.R. and Castro, E.R., 2016. Application of low field NMR as an alternative technique to quantification of total acid number and sulphur content in petroleum from Brazilian reservoirs. *Fuel*, **176**, pp.146-152.

Cooke, D.R., Bull, S.W., Large, R.R. and McGoldrick, P.J., 2000. The importance of oxidized brines for the formation of Australian Proterozoic stratiform sediment-hosted Pb-Zn (Sedex) deposits. *Economic Geology*, *95*(1), pp.1-18.

Craddock, P.T., 1978. The composition of the copper alloys used by the Greek, Etruscan and Roman civilizations: 3. The origins and early use of brass. *Journal of Archaeological Science*, **5**(1), pp.1-16.

Dou, L., Cheng, D., Li, M., Xiao, K., Shi, B. and Li, Z., 2008. Unusual high acidity oils from the great palogue field, melut basin, Sudan. *Organic Geochemistry*, **39**(2), pp.210-231.

Duyck, C., Miekeley, N., da Silveira, C.L.P., Aucelio, R.Q., Campos, R.C., Grinberg, P. and Brandao, G.P., 2007. The determination of trace elements in crude oil and its heavy fractions by atomic spectrometry. *Spectrochimica Acta Part B: Atomic Spectroscopy*, **62**(9), pp.939-951.

EIA (2015). Technically recoverable Oil and Shale Gas Resources: Australia. Washington D.C.

Etminan, H. and Hoffmann, C.F., 1989. Biomarkers in fluid inclusions: A new tool in constraining source regimes and its implications for the genesis of Mississippi Valley-type deposits. *Geology*, **17(1)**, pp.19-22.

Evans, T.L., Campbell, F.A. and Krouse, H.R., 1968. A reconnaissance study of some western Canadian lead-zinc deposits. *Economic Geology*, **63(4)**, pp.349-359.

Giordano, T.H., 1985. A preliminary evaluation of organic ligands and metal-organic complexing in Mississippi Valley-type ore solutions. *Economic Geology*, **80(1)**, pp.96-106.

Giordano, T.H., 1994, Metal Transport in Ore Fluids by Organic Ligand Complexation, in Pittman, E.D. and Lewan, M.D. eds., *Organic Acids in Geological Processes*, Springer-Verlag, p. 320 – 354.

Giordano, T.H. and Kharaka, Y.K., 1994. Organic ligand distribution and speciation in sedimentary basin brines, diagenetic fluids and related ore solutions. *Geological Society, London, Special Publications*, **78(1)**, pp.175-202.

Gize, A.P. and Barnes, H.L., 1987. The organic geochemistry of two Mississippi Valley-type lead-zinc deposits. *Economic Geology*, **82(2)**, pp.457-470.

Huang, L. and Gitschier, J., 1997. A novel gene involved in zinc transport is deficient in the lethal milk mouse. *Nature genetics*, **17(3)**, p.292.

Ireland, T., Bull, S.W. and Large, R.R., 2004. Mass flow sedimentology within the HYC Zn–Pb–Ag deposit, Northern Territory, Australia: evidence for syn-sedimentary ore genesis. *Mineralium Deposita*, 39(2), pp.143-158.

Jones, P. (1975). *Trace Elements and Other Elements in Crude Oil—a Literature Review*. Sunbury: Report of British Petroleum Research Centre.

Kennard, J.M., Jackson, M.J., Romine, K.K., Shaw, R.D. and Southgate, P.N., 1994, August. Depositional sequences and associated petroleum systems of the Canning Basin, WA. In *The Sedimentary Basins of Western Australia. Proceedings, PESA Symposium, Perth. Perth: PESA*.

Leach, D.L., Taylor, R.D., Fey, D.L., Diehl, S.F. and Saltus, R.W., 2010. *A deposit model for Mississippi Valley-Type lead-zinc ores: Chapter A in Mineral deposit models for resource assessment* (No. 2010-5070-A). US Geological Survey.

Lee, M.K. and Saunders, J.A., 2003. Effects of pH on metals precipitation and sorption. *Vadose Zone Journal*, 2(2), pp.177-185.

Lewan, M., 1984, Factors controlling the proportionality of vanadium to nickel in crude oils: *Geochimica et Cosmochimica Acta*, v. 48, p. 2231 – 2238.

Li, M., Cheng, D., Pan, X., Dou, L., Hou, D., Shi, Q., Wen, Z., Tang, Y., Achal, S., Milovic, M. and Tremblay, L., 2010. Characterization of petroleum acids using combined FT-IR, FT-ICR-MS and GC-MS: Implications for the origin of high acidity oils in the Muglad Basin, Sudan. *Organic Geochemistry*, **41(9)**, pp.959-965.

Machel, H.G., 2001. Bacterial and thermochemical sulfate reduction in diagenetic settings—old and new insights. *Sedimentary Geology*, **140(1-2)**, p.143-175.

McCall, K.A., Huang, C.C. and Fierke, C.A., 2000. Function and mechanism of zinc metalloenzymes. *The Journal of nutrition*, **130(5)**, pp.1437S-1446S.

Meredith, W., Kelland, S.J. and Jones, D.M., 2000. Influence of biodegradation on crude oil acidity and carboxylic acid composition. *Organic Geochemistry*, **31(11)**, pp.1059-1073.

Perkins, W.G. and Bell, T.H., 1998. Stratiform replacement lead-zinc deposits; a comparison between Mount Isa, Hilton, and McArthur River. *Economic Geology*, **93(8)**, pp.1190-1212.

Peter, J.M., and Scott, S.D., 1988, Mineralogy, composition, and fluid-inclusion microthermometry of seafloor hydrothermal deposits in the Southern Trough of Guaymas Basin, Gulf of California: *Canadian Mineralogist*, v. **26**, p. 567–587.

Peters, K.E., Walters, C.C., and Moldowan, J.M., 2004, *The Biomarker Guide: Volume 1, Biomarker and Isotopes in the Environment and Human History*: Cambridge University Press.

Price, L.C., and Wenger, L.M., 1992, The influence of pressure on petroleum generation and maturation as suggested by aqueous pyrolysis: *Organic Geochemistry*, v. **19**, p. 141–159.

Roedder, E., 1979. Fluid inclusion evidence on the environments of sedimentary diagenesis, a review. SPEM special publication No. 26, p. 89-107

Saintilan, N.J., Spangenberg, J.E., Samankassou, E., Kouzmanov, K., Chiaradia, M., Stephens, M.B. and Fontboté, L., 2016. A refined genetic model for the Laisvall and Vassbo Mississippi Valley-type sandstone-hosted deposits, Sweden: constraints from paragenetic studies, organic geochemistry, and S, C, N, and Sr isotope data. *Mineralium Deposita*, **51**(5), pp.639-664.

Sanz-Robinson, J., Sugiyama I., Williams-Jones, A.E., (in review). The Solubility of Palladium (Pd) in Crude Oil at 150, 200 and 250°C and its Application to Ore Genesis ms. *Chemical Geology*

Schenk, C.J., Tennyson, M.E., Mercier, T.J., Woodall, C.A., Finn, T.M., Le, P.A., Brownfield, M.E., Gaswirth, S.B., Marra, K.R. and Leathers-Miller, H.M., 2018. *Assessment of undiscovered oil and gas resources in the Canning Basin Province, Australia, 2017* (No. 2018-3023). US Geological Survey.

Seifert, W.K., 1975. Carboxylic acids in petroleum and sediments. In *Fortschritte der Chemie Organischer Naturstoffe/Progress in the Chemistry of Organic Natural Products* (pp. 1-49). Springer, Vienna.

Shah, B. and Hambright, P., 1970. Acid catalyzed solvolysis reactions of zinc porphyrins. *Journal of Inorganic and Nuclear Chemistry*, 32(10), pp.3420-3422.

Shuman, L.M., 1999. Effect of organic waste amendments on zinc adsorption by two soils. *Soil Science*, **164**(3), pp.197-205.

Spangenberg, J.E., Fontbote, L. and Macko, S.A., 1999. An evaluation of the inorganic and organic geochemistry of the San Vicente mississippi valley-type zinc-lead district, central Peru; implications for ore fluid composition, mixing processes, and sulfate reduction. *Economic Geology*, **94**(7), pp.1067-1092.

Speight, J.G., 2001, *Handbook of Petroleum Analysis* (J. G. Speight, Ed.): John Wiley & Sons, Inc.

Stoffell, B., Appold, M.S., Wilkinson, J.J., McClean, N.A. and Jeffries, T.E., 2008. Geochemistry and evolution of Mississippi Valley-type mineralizing brines from the Tri-State and northern Arkansas districts determined by LA-ICP-MS microanalysis of fluid inclusions. *Economic Geology*, **103**(7), pp.1411-1435.

Sugiyama, I. and Williams-Jones, A.E., 2018. An approach to determining nickel, vanadium and other metal concentrations in crude oil. *Analytica chimica acta*, 1002, pp.18-25.

Surdam, R.C., Jiao, Z.S. and MacGowan, D.B., 1993. Redox reactions involving hydrocarbons and mineral oxidants: A mechanism for significant porosity enhancement in sandstones. *AAPG Bulletin*, 77(9), pp.1509-1518.

Sverjensky, D.A., 1984. Oil field brines as ore-forming solutions. *Economic Geology*, 79(1), pp.23-37.

Sverjensky, D.A., 1986. Genesis of Mississippi Valley-type lead-zinc desposits. *Annual Review of Earth and Planetary Sciences*, 14(1), pp.177-199.

Thom, J. and Anderson, G.M., 2008. The role of thermochemical sulfate reduction in the origin of Mississippi Valley-type deposits. I. Experimental results. *Geofluids*, 8(1), pp.16-26.

Thomas C.L. (2018). Mineral Commodity Summaries 2018: Zinc. United States Geological Survey. Retrieved May 17, 2018.

Tompkins, L.A., Rayner, M.J., Groves, D.I. and Roche, M.T., 1994. Evaporites; in situ sulfur source for rhythmically banded ore in the Cadjebut mississippi valley-type Zn-Pb deposit, Western Australia. *Economic Geology*, 89(3), pp.467-492.

Tompkins, L.A., Eisenlohr, B., Groves, D.I. and Raetz, M., 1997. Temporal changes in mineralization style at the Cadjebut mississippi valley-type deposit, Lennard Shelf, WA. *Economic Geology*, 92(7-8), pp.843-862.

Wallace, M.W., Middleton, H.A., Johns, B. and Marshallsea, S., 2002, October. Hydrocarbons and Mississippi Valley-type sulfides in the Devonian reef complexes of the eastern Lennard Shelf, Canning Basin, Western Australia. In *The sedimentary basins of Western Australia 3. Proceedings of the West Australian basins Symposium: Perth, Petroleum Exploration Society of Australia* (pp. 795-815).

Warren, J.K. and Kempton, R.H., 1997. Evaporite Sedimentology and the Origin of Evaporite-Associated Mississippi Valley-Type Sulfides in the Cadjebut Mine Area Lennard Shelf, Canning Basin, Western Australia.

Williams-Jones, A.E. and Migdisov, A.A., 2014. Experimental constraints on the transport and deposition of metals in ore-forming hydrothermal systems. *Society of Economic Geologists*, 18, pp.77-96.

## Supplementary Materials for

Zinc solubility, speciation and deposition: A role for liquid hydrocarbons as ore fluids for  
Mississippi Valley Type Pb-Zn deposits.

Sanz-Robinson and Williams-Jones

### **A. Composition of the zinc oil standard used in experiments designed to precipitate sphalerite from a zinc-rich oil**

Sphalerite was successfully precipitated from a Conostan® 1000 ppm Zn oil standard (Catalogue #CB7-100-032) using the technique detailed in Section 3.4.2. of our methodology. Zinc is dissolved in the oil standard as a Zn-alkylaryl sulfonate (1000 ppm Zn). The sulfonate functional group binds stably to zinc, whereas the alkylaryl component facilitates the dissolution of the compound in oil. The oil is composed of a blend of light mineral oil (short-chain alkanes) and Hibernia crude oil. Compositional information pertaining to the Hibernia crude oil used in the oil standard is detailed below (Table A1).

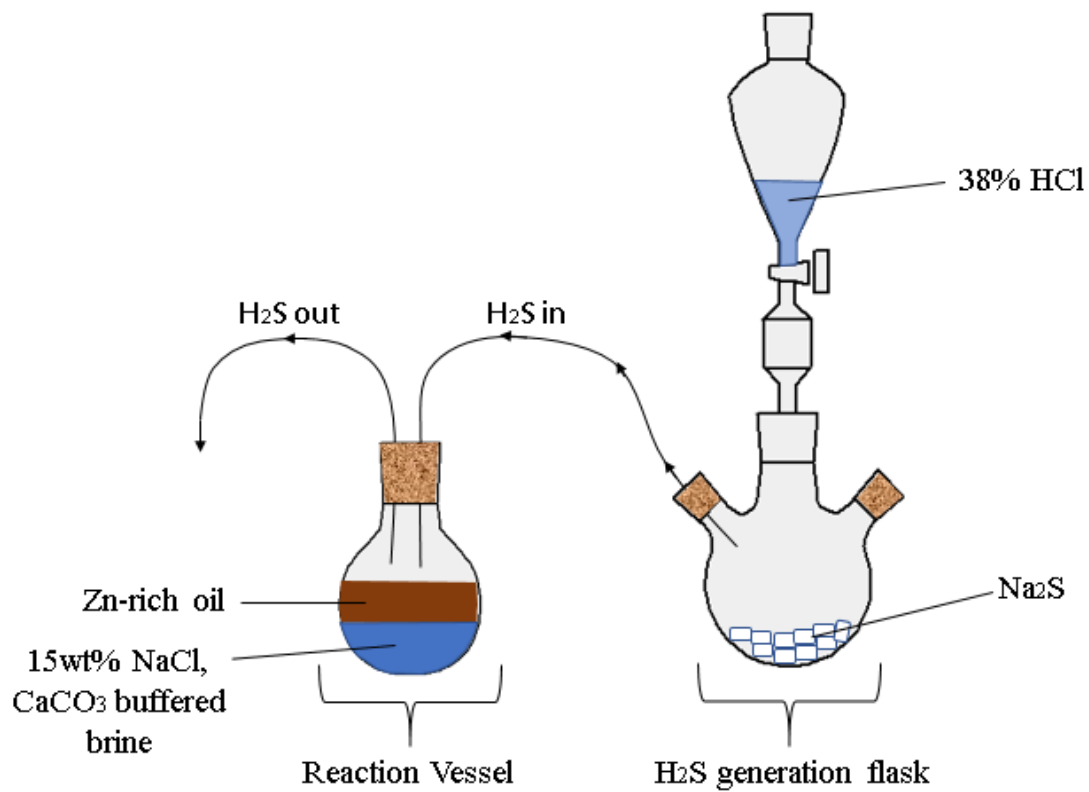
**Supplementary Table 3.1** The composition and properties of the Hibernia Crude oil used in the Conostan® Zn oil standard.

#### **Parameters**

<b>Specific gravity</b>	0.84-0.86
<b>Carbon (wt%)</b>	86
<b>Hydrogen (wt%)</b>	13
<b>Nitrogen (wt%)</b>	0
<b>Saturates (wt%)</b>	79
<b>Aromatics (wt%)</b>	15

<b>Resins (wt%)</b>	4
<b>Asphaltenes (wt%)</b>	3
<b>Waxes (wt%)</b>	8

**B. Experimental setup for the precipitation of sphalerite from a Zn-rich oil**



**Supplementary Figure 3.1** The experimental setup for the precipitation of sphalerite from a zinc-rich oil

### Calculating experimental yield

The experiment was performed with 20g of 1000ppm Zn oil.

$$\text{Total Zinc} = \left( \left( \frac{1000g \text{ Zn}}{10^6g \text{ oil}} \right) \times 20g \text{ oil} \right) \times \frac{1000 \text{ mg}}{g} = 20mg \text{ Zn}$$

Our experiment precipitated 13.11 mg of Sphalerite (ZnS)

$$\text{Zinc in sphalerite} = \left( \left( \frac{13.11 \times 10^{-3}g \text{ ZnS}}{M_{\text{ZnS}}} \right) \times M_{\text{Zn}} \right) \times \frac{1000mg}{g} \quad \text{where } M_{\text{ZnS}} \text{ is the molecular weight}$$

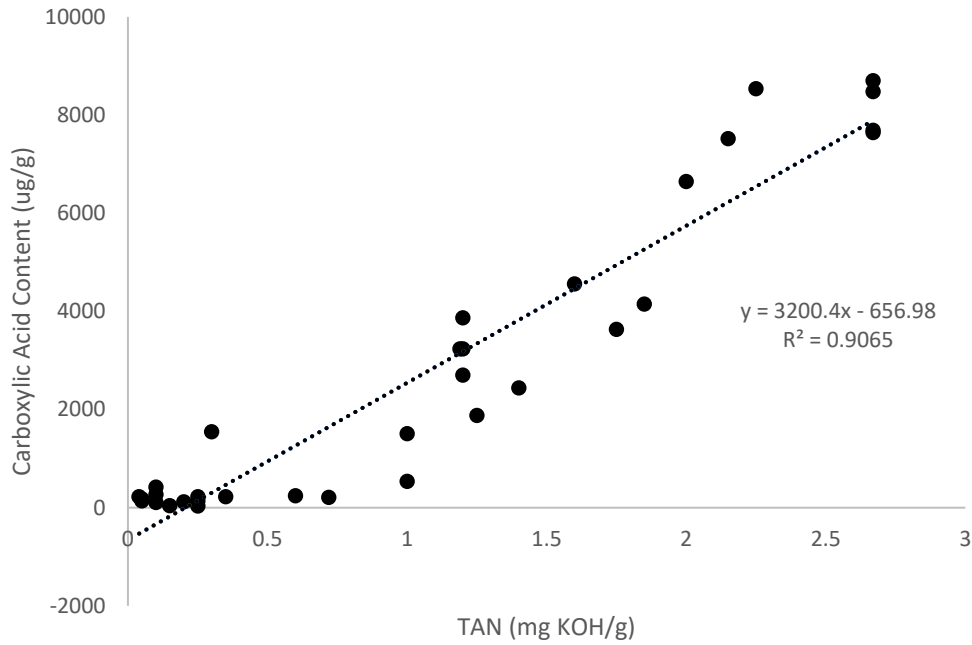
of ZnS and  $M_{\text{Zn}}$  is the atomic mass of Zn.

$$\text{Zinc in Sphalerite} = \left( \left( \frac{13.11 \times 10^{-3}g \text{ ZnS}}{97.47 \frac{g}{mol}} \right) \times 65.38 \frac{g}{mol} \right) \times \frac{1000mg}{g} = 8.794 \text{ mg Zn}$$

$$\text{Experimental yield} = \left( \frac{\text{Zinc in Sphalerite}}{\text{Total Zinc}} \right) \times 100\% = \left( \frac{8.794 \text{ mg Zn}}{13.11 \text{ mg Zn}} \right) \times 100\% = 44\%$$

44% of Zn contained in the oil was precipitated as sphalerite

### C. Estimating the carboxylic acid content of crude oil from TAN values



**Supplementary Figure 3.2** Oil TAN versus carboxylic acid content (modified from Meredith et al., 2000)

$$\text{Carboxylic acids } \left( \frac{\mu\text{g}}{\text{g}} \right) = 3200.4 \times \text{TAN} \left( \frac{\text{mg KOH}}{\text{g}} \right) - 656.98$$

Empirical equation derived from the data of Meredith et al. (2000).

Our most metalliferous oil has a TAN = 2.9 mg KOH/g.

This corresponds to a carboxylic acid content of **8620 µg/g**

**D. Mass balance calculation to determine the amount of Zn-rich oil required to form Zn deposit as large as the Cadjebut deposit in the Canning Basin, Australia.**

The Cadjebut deposit has reserves of 3.5 million tonnes of ore grading at 17wt% Pb + Zn.

$$\text{Mass of metal} = 3.5 \times 10^{12} \text{ g} \times 0.17 = \mathbf{5.95 \times 10^{11} \text{ g Pb + Zn.}}$$

Calculating amount of oil required to form a Cadjebut sized deposit assuming all the metal is Zn and assuming that the oil has a density ( $\rho$ ) of 850 kg/m<sup>3</sup> and dissolves 1000 ppm Zn (equivalent to the density and Zn concentration of the oil used in our sphalerite precipitation experiments).

$$\text{Concentration of Zn in oil} = 1000 \text{ ppm Zn} = \frac{1000 \text{ kg Zn}}{10^6 \text{ kg oil}} = \frac{1000 \text{ kg Zn}}{10^6 \text{ kg} / 850 \text{ kg m}^{-3}} = \frac{0.85 \text{ kg Zn}}{\text{m}^3 \text{ oil}}$$

$$\text{Amount of oil} = \frac{\text{Mass of Zn deposit}}{\text{Concentration of Zn in oil}} = \frac{5.95 \times 10^8 \text{ kg Zn}}{0.85 \text{ kg/m}^3} = 0.7 \text{ km}^3$$

Calculating volume of oil reserves (in cubic kilometers) of the Goldwyer Shale in the Canning Basin

$$\text{Oil reserves} = 244 \times 10^9 \text{ barrels} \times \frac{0.159 \text{ m}^3}{\text{barrel}} \times \frac{1 \text{ km}^3}{10^9 \text{ m}^3} = 38.8 \text{ km}^3$$

## Preface to Chapter 4

---

The previous chapters demonstrated that petroleum is a potentially effective ore fluid for Pd and Zn in the context of sediment-hosted deposits. Both metals can be dissolved to high concentrations in liquid hydrocarbons. The research presented in Chapter 4 deals with the solubility and speciation of Ni in petroleum. Some highly viscous oils naturally contain large amounts of Ni (in excess of 100 ppm), a considerable proportion of which (as much as 50%) is bound to a family of nitrogen-bearing ligands known as porphyrins, which are derived from porphyrin-like molecules such as chlorophyll and heme present in living organisms. Little is known, however, about the other classes of compounds in petroleum that may bind to Ni. Therefore, in this chapter, the physical and geochemical factors that control the dissolution of Ni in liquid hydrocarbons are discussed. The data required for this discussion were obtained using the methodology described in Chapters 2 and 3. As in these chapters, the research findings are linked to observations of sediment-hosted deposits which, in addition to containing high concentrations of Ni, appear to have been infiltrated by petroleum.

## **4. The solubility of Nickel (Ni) in crude oil at 150, 200 and 250°C and its Application to Ore Genesis**

---

**J. Sanz-Robinson\*<sup>a</sup> and A.E. Williams-Jones<sup>a</sup>**

<sup>a</sup> Department of Earth and Planetary Sciences, McGill University, 3450 University Street,  
Montreal, QC, H3A 0E8, Canada.

Published in *Chemical Geology*, 2019

DOI: <https://doi.org/10.1016/j.chemgeo.2019.119443>

## Abstract

The very low solubility of Ni in saline brines and the correspondingly high concentration of Ni in some crude oils raises the possibility that liquid hydrocarbons may be the ore fluids for black-shale-hosted Ni deposits. To test the feasibility of this hypothesis, Ni wires were reacted with three crude oils of differing composition at 150, 200 and 250°C for up to 30 days, and the concentration of Ni in the oil determined. At 150°C, Ni concentrations in the three oils remained relatively low. Above 200°C, however, Ni concentrations were elevated and correlated positively with the thiol content of the oil. Our most thiol-rich oil dissolved  $217 \pm 40.4$  ppm Ni after 30 days at 250°C. X-ray photoelectron spectroscopic (XPS) analyses performed on the residual oil coating the Ni wires after reaction independently corroborate the conclusion that Ni has a strong chemical affinity for thiols in crude oil. Furthermore, in crude oils with no thiols, the Ni reacted with other sulfur compounds (potentially sulfonic acids) in oil to form thiols. Significantly, our XPS analyses show that iron (Fe) from the oil was embedded in the Ni wire concomitantly with the attachment of thiols. This suggests that Fe has an affinity for Ni and that the thiolation of Ni by crude oil may depend on the availability of Fe in the oil. In addition to thiols, porphyrins also likely play an important role in the dissolution of Ni, the oil in which Ni was most soluble has a high nitrogen content, whereas in the other oil, which is characterized by a high thiol content, the Ni solubility was relatively low and the nitrogen content of this oil was below the detection limit. Immature biodegraded oils that are sourced from carbonate rocks generally tend to be enriched in asphaltenes, Ni and sulfur. Nevertheless, some mature oils acquire anomalously large thiol

contents through Thermochemical Sulphate Reduction (TSR), a high temperature (100 to 140°C) reaction occurring commonly in carbonate reservoirs, which involves the abiotic reduction of sulfate minerals at the expense of oil or bitumen. Thus, given the affinity of Ni for thiols, large volumes of Ni-poor oil can potentially be altered by TSR to produce smaller volumes of residual oil enriched in thiols and Ni.

## 4.1 Introduction

Nickel (Ni) commonly forms metal organic complexes with nitrogen-bearing ligands such as tetrapyrroles and sulfur-bearing ligands, e.g., thiols in living organisms, organic sediments, oil and bitumen (Parnell, 1988). For example, the Ni-F<sub>430</sub> co-enzymes present in methanogens are Ni-tetrapyrrole complexes (Diekert et al., 1981) and the most common form of hydrogenase enzyme present in anaerobic microorganisms consists of metal organic iron-nickel (Fe–Ni) complexes bound together by cysteinyl thiolate ligands (Ohki and Tatsumi, 2011). Nickel and sulfur are also enriched in the asphaltene phase in bitumen and petroleum (Parnell, 1988; Yu et al., 2015), which is composed of large (500-1000 Da) heterocyclic molecules such as tetrapyrroles (Groenzin and Mullins, 1999).

Occurrences of Ni-rich bitumen veins in Peru, Argentina and Venezuela and high levels of Ni and Vanadium (V) in Venezuelan oils and coals, according to Kapo (1978), may be genetically related to Ni and V ore deposits in the watershed. Moreover, several ore grade Ni deposits elsewhere, notably the Zunyi Deposit in Southern China, the Nick and related prospects in the Yukon, Canada and the Talvivaara deposit in Finland, are hosted in sediments, which may have been infiltrated by petroleum. The relationship between petroleum and anomalous Ni enrichment in organic-rich sedimentary rocks is intriguing.

The Zunyi deposit in Southern China and the prospects of Yukon, Canada, are metalliferous black shales that share many similarities, most notably that the ore horizon in both localities consists of a thin (between 10 and 30 cm thick), stratiform layer of sulfide minerals with weight percent enrichments of Ni (Jowitt and Keays, 2011). Both deposits also display signs of having

interacted with liquid hydrocarbons. For example, evidence of migrabitumen in the Zunyi deposit may indicate that the latter was brecciated during late diagenesis, allowing it to act as an “oil collector” (Křibek et al., 2007). Similarly, large, bituminous veins in the Nick Prospect in Yukon Canada, have been interpreted as evidence for the passage of hydrocarbon-rich fluids through the mineralized horizon (Hulbert et al., 1992, Henderson et al., 2019). Unlike the aforementioned metalliferous shales, the Talvivaara deposit, located in the central part of the Fennoscandian Shield, has a considerably thicker ore horizon (up to 330m thick) and contains 300 million metric tons (Mt) of ore averaging 0.26 wt.% Ni, 0.14 wt.% Cu, and 0.53 wt.% Zn with minor concentrations (10-30 ppm) of uranium (U) (Loukola-Ruskeeniemi and Heino, 1996; Lecomte et al, 2014). The presence of bitumen rims on uraninite crystals from the Talvivaara deposit suggests a close association with liquid hydrocarbons (Lecomte et al., 2014).

As discussed above, liquid hydrocarbons may have interacted with the black shales hosting several Ni-rich deposits. Here, we examine the physical and compositional parameters that control Ni solubility in oil to determine the potential of crude oil to act as a Ni ore fluid. We do so, using the results of experiments designed to determine the solubility of Ni wire in crude oil at temperatures of 150, 200 and 250 °C, a range consistent with conclusions from pyrolysis experiments (Price and Wenger, 1992) and studies of liquid hydrocarbons entrapped in black smokers (Peter and Scott, 1988) that liquid hydrocarbons remain stable to temperatures above 300°C for protracted periods of time. Finally, we use the results of this study to examine the hypothesis that Ni-enriched deposits in sedimentary basins may be the products of Ni-rich oils.

## 4.2 Materials and Methods

### 4.2.1 Crude Oil Characterization

The crude oils selected for this investigation and compositional data were provided by Statoil Canada. These oils have markedly different compositions and physical properties (Table 4.1). This is important for isolating the compositional parameters, which affect the dissolution of Ni in crude oil. The selected oils vary in specific gravity from 0.90 to 0.94 and have varying asphaltene contents. The asphaltene phase of petroleum is composed of large heterocyclic molecules and is particularly important to the context of this investigation given that Ni is commonly concentrated in the asphaltene fraction of petroleum (Parnell, 1988; Groenzin and Mullins, 1999). In our oils, the asphaltene content ranges from below 0.3 wt.% up to 1.6 wt. %. The selected oils also differ in their Total Acid Number (TAN), a measure of their carboxylic acid content (Seifert, 1975) and contain sulfur compounds (e.g., thiols, thiophenes, benzothiophenes, dibenzothiophenes and benzonaphthothiophenes) in varying abundances. Certain sulfur species, such as thiols, are recognized for their ability to form metal organic complexes (Lewan, 1984; Giordano, 1994; Speight, 2001). Finally, the nitrogen content of our oils varies between 0.2 and 0.44 wt. %. Nitrogen is an important compositional parameter as certain nitrogen bearing species in petroleum, such as porphyrins, are known to bind stably to Ni (Barwise, 1990). Compounds, such as pyrroles, pyridines and saturated amines, also contribute to the nitrogen budget of crude oil (Mitra-Kirtley et al., 1993).

**Table 4.1** The composition and properties of the three crude oils, A, B and C, employed in our experiments.

<b>Parameters</b>	<b>Oil A</b>	<b>Oil B</b>	<b>Oil C</b>
<b>API Gravity</b>	26.6	25	19
<b>Specific Gravity</b>	0.895	0.904	0.94
<b>Sulfur (wt.%)</b>	0.84	0.52	0.82
<b>Thiols/sulfides (ppm)</b>	44	0	52
<b>Thiophenes/Disulfides (ppm)</b>	1400	37	1050
<b>Benzothiophenes (ppm)</b>	3890	1880	3160
<b>Dibenzothiophenes (ppm)</b>	2580	2740	2020
<b>Benzonaphthothiophenes (ppm)</b>	490	549	109
<b>Nitrogen (wt.%)</b>	---	0.2	0.44
<b>TAN (mgKOH/g)</b>	0.2	2.9	2.3
<b>Paraffins (wt.%)</b>	---	37	19
<b>Naphthenes (wt.%)</b>	---	49	65
<b>Aromatics (wt.%)</b>	---	13	15
<b>Asphaltenes (wt.%)</b>	1.6	0.3	1.4
<b>Background Ni (ppm)</b>	5.59	4.05	6.22
<b>Background Fe (ppm)</b>	0.343	8.71	16.5

#### 4.2.2 Solubility and speciation of Nickel in liquid hydrocarbons

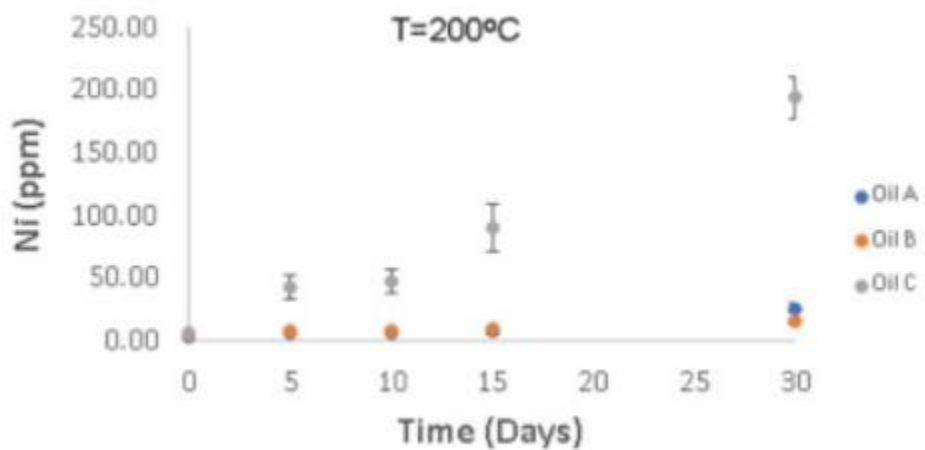
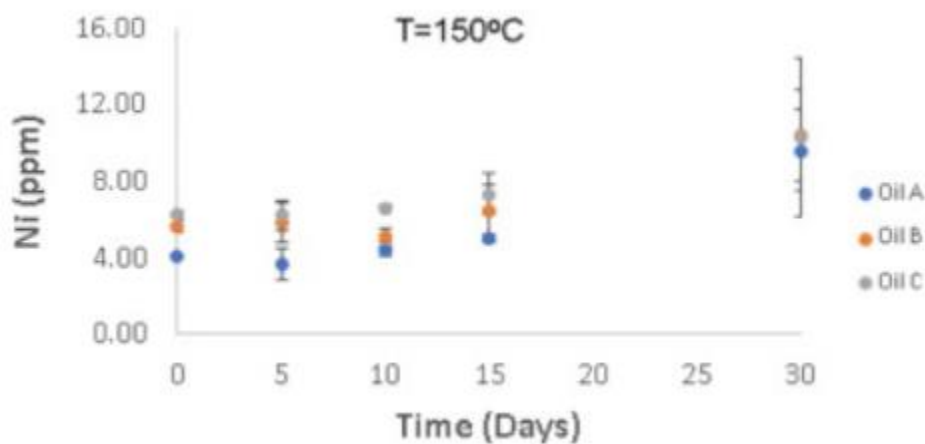
In order to determine the solubility of elemental Ni in crude oil, Ni(0) wires ( $\geq 99.9\%$ ) from Sigma-Aldrich<sup>®</sup> were reacted in crude oils A, B and C for varying lengths of time following the procedure described in Sanz-Robinson and Williams-Jones (2019). This involved reacting a Ni wire in oil inside a sealed quartz tube. Prior to being used, the quartz tubes were cleaned with trace-metal grade nitric acid ( $\sim 75\%$  HNO<sub>3</sub>) for 24 hours, rinsed with Milli-Q<sup>™</sup> water and dried at 100 °C for 2 hours. A Ni wire was placed in the reaction tube and an aliquot of crude oil ( $\sim 0.5$ ml) was pipetted into the tube. The loaded reactors were then placed in a Thermo Scientific<sup>™</sup> Thermolyne<sup>™</sup> tabletop muffle furnace oven that had been preheated to the desired

temperature. This procedure was repeated for varying periods of time (5, 10, 15 and 30 days) at 150°C, 200°C and 250°C.

After each experiment, the reaction vessel was removed from the furnace and quenched immediately in a beaker of tap-water at room temperature. The tubes were then opened using a file and the Ni wire was removed. The reacted oil was combusted in a muffle furnace at 550°C for 24 h and the resulting char was digested in a solution of 0.25 ml of 75% Optima™ grade HNO<sub>3</sub>, 0.5 ml of Optima™ grade H<sub>2</sub>O<sub>2</sub> and 0.25 ml of Optima™ grade HCl for a further 24h in order to oxidize the remaining char and dissolve the metal. The leaching solution was diluted with a solution of 2% Optima™ grade HNO<sub>3</sub> and analysed with the Thermo Scientific™ iCAP™ Q inductively coupled plasma mass spectrometer (ICPMS) in the ICP Laboratory of the Department of Earth and Planetary Sciences at McGill University. Yttrium was used as an internal standard for the ICPMS analyses. The instrument response was calibrated by using dilute external standard Ni solutions in 2% HNO<sub>3</sub>.

The reacted Ni wires were rinsed in toluene (≥99.5%) purchased from Fischer Scientific, vacuum-dried for 24 h and analyzed by X-ray photoelectron spectroscopy (XPS) to determine the composition of the residual oil bound to the wire. For the purpose of comparison, the procedure was repeated for Ni wires that had been immersed in the three oils at ambient temperature. The analyses were conducted with a Thermo Scientific Kα™ spectrometer at the McGill Institute for Advanced Materials (MIAM). Analyses were performed using Al Kα™ radiation (1486 eV) and an X-ray spot size of 100 μm, and scans were made with a pass energy of 50 eV at a resolution of 0.1 eV. The C1S, C-C peak at 284.8eV was used as a charge-

reference peak to ensure adequate peak alignment. The Thermo Scientific  $K\alpha^{\text{TM}}$  spectrometer etching function was used to progressively etch the Ni wire, thereby removing weakly bound surficial ligands and exposing deeply embedded ligands with a strong chemical affinity for Ni.



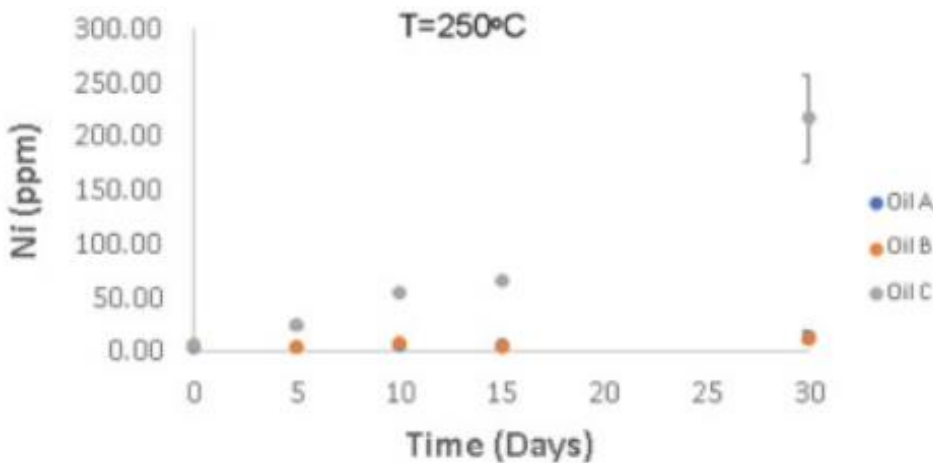


**Figure 4.1** The concentration of Ni (3 S.D.) in crude oils A, B and C at 150, 200 and 250 °C as a function of the duration of the experiments. The vertical lines are error bars indicating the experimental uncertainty.

## 4.3 Results

### 4.3.1 Nickel solubility

Nickel wires were reacted with crude oils A, B and C for 5, 10, 15 and 30 days at 150, 200 and 250°C in order to establish the steady-state Ni concentrations. Three experiments were performed for each oil at each temperature and for each duration, and the average temperature and standard deviation for each set of experiments determined. As the Ni concentrations increased with time and were highest after 30 days (Fig. 4.1), we consider the average concentrations obtained for this duration to represent the minimum solubility of Ni in the corresponding oils (Table 4.2).

Nickel concentrations in the crude oil were relatively low at 150°C, with all oils dissolving approximately 10 ppm Ni. Progressive heating, however, resulted in a significantly higher solubility of Ni in Oil C (Figure 4.1) relative to the other oils; Oil C dissolved 194±17 ppm Ni at 200°C and 217 ppm Ni at 250°C, whereas Oil A dissolved 25.7 and 13.8 ppm at these temperatures and Oil B dissolved 15.6 and 12.3 ppm, respectively (Table 4.2). Oil C has the highest thiol and iron content of the three oils considered, followed by Oil A, which dissolved the second largest amount of Ni, albeit a considerably lower amount than Oil C. The asphaltene and sulfur content of Oils A and C are similar, but Oil A has a considerably smaller TAN and Fe content. Oil B dissolved the least Ni of the three crude oils. It has the largest TAN number but a much smaller asphaltene fraction than Oils A and B, has a moderate Fe content and contains no detectable thiols.

**Table 4.2** Results of experiments designed to determine the solubility of Ni in crude oils A, B and C at 150, 200 and 250 °C. The Ni concentration at 25°C is the background concentration in the unreacted oil.

Temp	Oil A			Oil B			Oil C		
	n*	Ni (ppm)	Error (ppm)	n*	Ni (ppm)	Error (ppm)	n*	Ni (ppm)	Error (ppm)
25 °C	3	5.6	0.3	3	4.05	0.03	3	6.2	0.2
150 °C	3	10	2	3	10	2	2	10	4
200 °C	3	26	4	3	16	3	2	190	20
250 °C	3	14	6	3	12	2	3	220	40

n\* is the number of experiments conducted

### 4.3.2 Results of X-ray Photoelectron Spectroscopy Analyses

An XPS scan (Figure 4.2) performed on the residue of oil on a Ni wire after reaction with Oil C (Ni solubility is highest in this oil) at 200°C, showed that the wire is coated mainly with carbon (C), sulfur (S) and oxygen (O). The wire was etched with an argon ion beam to remove weakly bound surficial ligands. After etching, the amounts of C and O decreased, whereas the relative proportions of Ni and S increased. This shows that Ni has a strong chemical affinity for S in crude oil. An enlargement of the S peak (Figure 4.3a) shows that it is centered at a binding energy of ~163 eV, which corresponds to the thiol functional group (Castner et al., 1996). This indicates that S, and more specifically thiols in Oil C, have a strong chemical affinity for Ni. The XPS scan of the wire that had been immersed in Oil C at ambient temperature also yielded a spectrum with a thiol peak (~ 163 eV) but, in addition, the spectrum contained a peak at ~168 eV corresponding to an oxidized sulfur species, possibly a sulfonic acid (Figure 4.3b). Similar results were obtained for Oil A after reaction at 200 °C and ambient temperature, respectively (Supplementary materials, Sup. Fig. 1a and b).

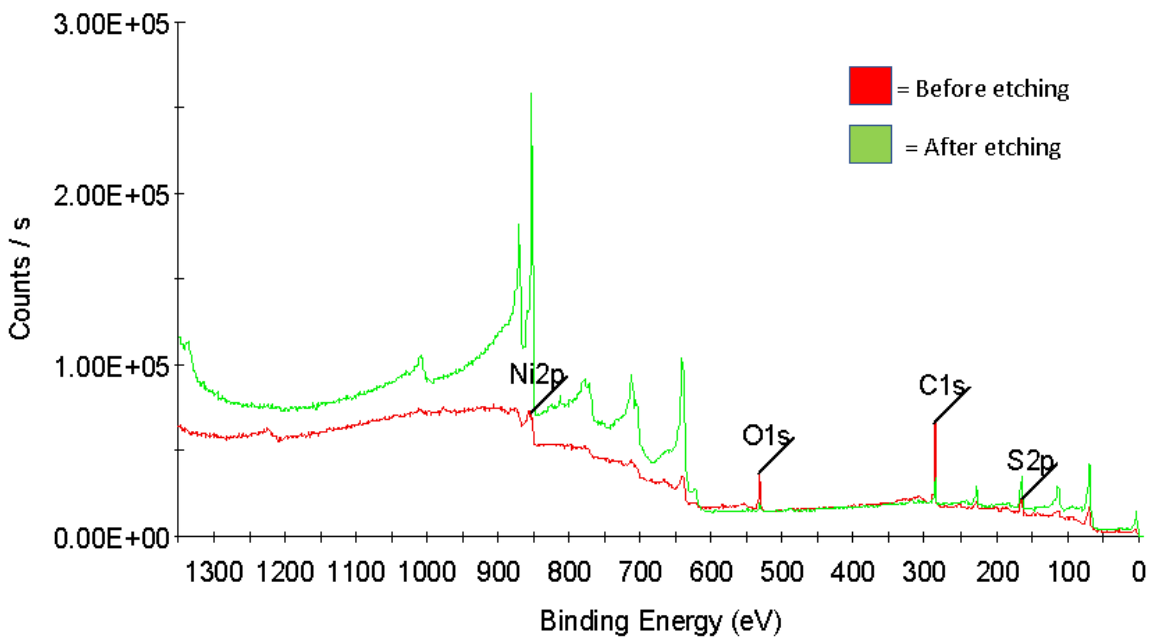


**Figure 4.2** A XPS spectrum identifying the major elements bound to the Ni wire after reaction with Oil C at 200°C. The relative abundances of these elements changed as the wire was progressively etched. Peak binding energies for the different elements are as follows: S 2p =163eV, C 1S= 285eV, O 1S = 532eV and Ni 2p = 853eV. The peaks between 650eV and 750eV that appear after etching are Ni Auger Lines, resulting from the relaxation of core Ni electrons (Wagner, 1972, Potočnik et al., 2016)

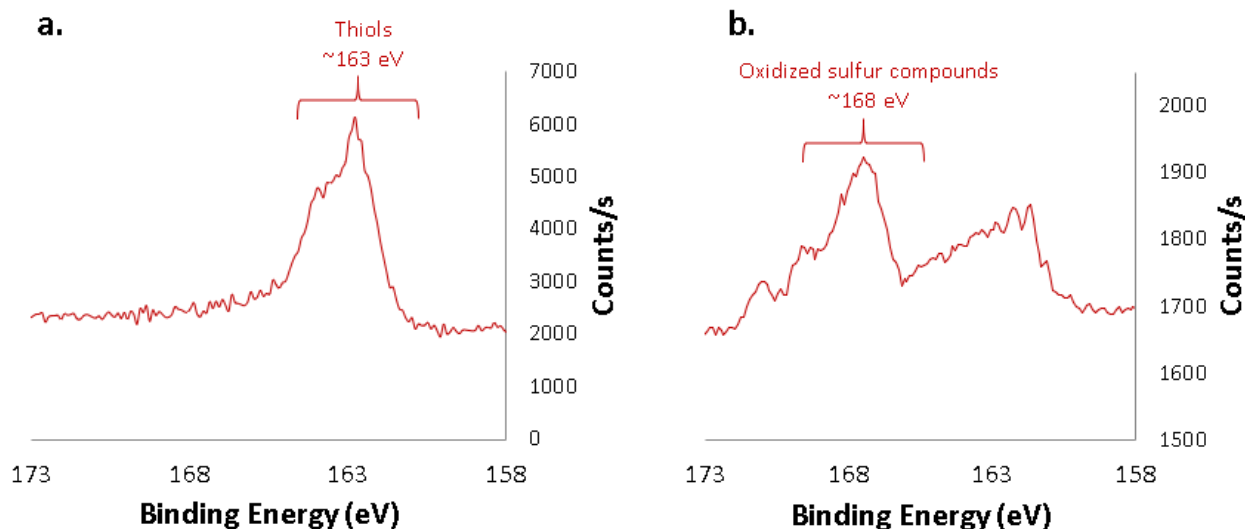


**Figure 4.3** An XPS spectrum illustrating the sulfur speciation of residual oil on a nickel wire after reaction with Oil C at a) 200°C and b) ambient temperature. The sulfur 2p peak centered at a binding energy of 163eV corresponds to the thiol functional group whereas the sulfur 2p peak centered at 168eV corresponds to oxidized sulfur compounds.

Predictably, and in contrast to the spectra for Oils A and C at ambient temperature, the Ni wire spectrum soaked in Oil B (which does not contain detectable thiols) at ambient temperature did not display a thiol peak ( $\sim 163$  eV), although, like the other oils it did contain a peak for an oxidized sulfur species ( $\sim 168$  eV) (Figure 4.4a). Unexpectedly, however, the spectrum obtained for Ni wire after reaction with Oil B at  $200^\circ\text{C}$  contained a thiol peak ( $\sim 163$  eV) (Figure 4.4b). We interpret this finding to indicate that the Ni wire catalytically reduced oxidized forms of sulfur in the oil like sulfonic acids to thiols (Kelemen et al., 1990).

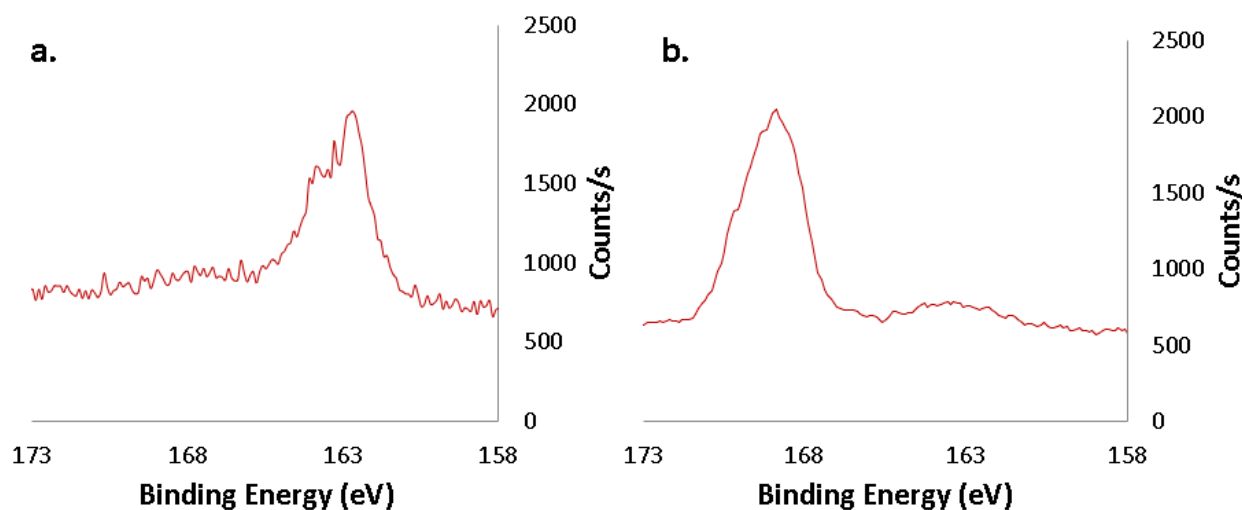


**Figure 4.4** An XPS spectrum illustrating the sulfur speciation of residual oil on a nickel wire after reaction with Oil B at a)  $200^\circ\text{C}$  and b) ambient temperature.

The thiolation of the Ni wires and the dissolution of Ni in Oil B and C also coincided with the incorporation of iron (Fe) from the oil into the Ni wires, albeit in trace amounts ( $< 1$  atom % of the Ni wire surface). This is evident in Figure 5 by the presence of an Fe doublet with peaks at 706 and 714 eV, which appeared after etching the Ni wire. Thus, Fe also displays a strong

chemical affinity for Ni and may participate in the redox reactions that occur between the Ni wire and sulfur compounds in the oil.

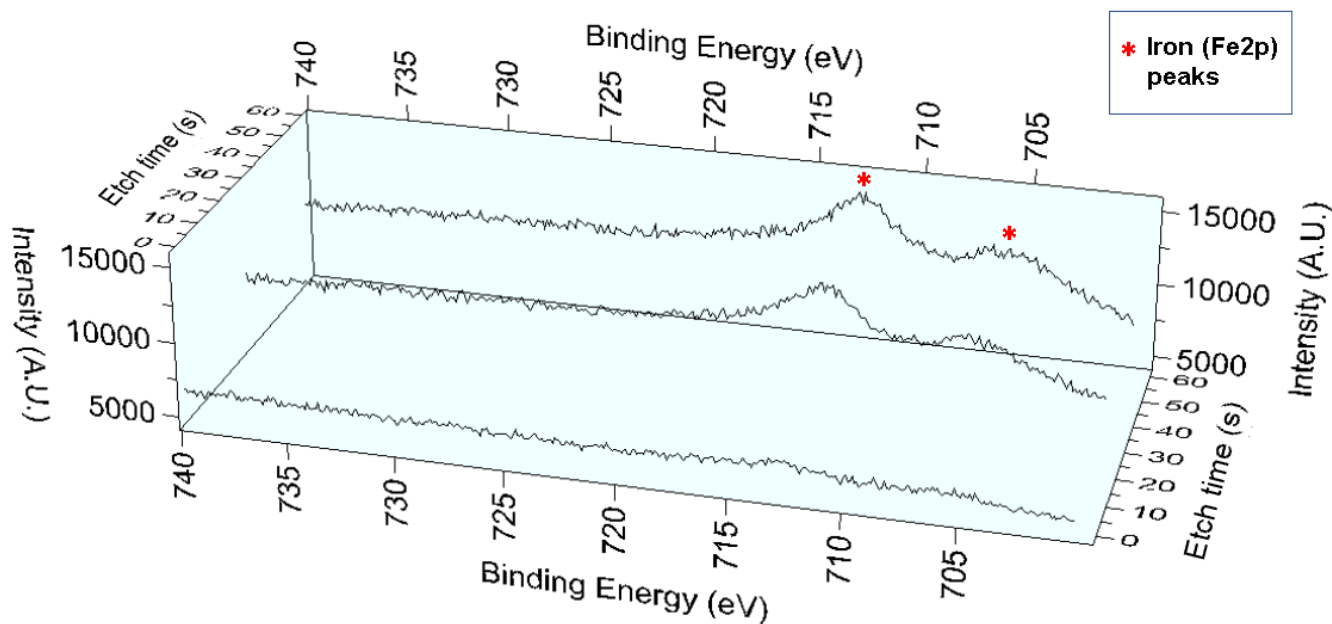


**Figure 4.5** An XPS spectrum of the nickel wire after reaction with Oil C at 200°C. Progressive etching revealed the presence of trace amounts of iron.

## 4.4 Discussion

### 4.4.1 Nickel solubility and speciation in liquid hydrocarbons as a function of petroleum composition.

In addition to testing the hypothesis that crude oils can dissolve significant amounts of Ni, the experiments described above were conducted to identify the compositional factors controlling the dissolution of Ni in liquid hydrocarbons. At 200°C and 250°C, Oil C has a much greater capacity to dissolve Ni than the other crude oils (Table 4.2), which in part reflects the fact that it

has the highest thiol content of the three oils. This high thiol content, however, does not explain the observation that the solubility of Ni in Oil C is nearly eight times higher than that of Oil A, whereas the thiol content of the latter oil is roughly 80% of that of Oil C (Table 4.1 and 4.2). The high Ni content of Oil C relative to Oil A also cannot be attributed to differences in the asphaltene content (Ni, like other metals has been shown to concentrate in the asphaltene fraction of crude oils; Marcano et al., 2011), because the asphaltene contents of the two oils are very similar and, indeed, the asphaltene content of Oil A is slightly higher than that of Oil C (1.6 versus 1.4 wt.%). The two oils do, however, differ in their nitrogen contents and TAN values. Oil C has the highest nitrogen content of the three oils (0.44 wt.%), whereas nitrogen was not detected in Oil A (Table 4.2). This may indicate that a significant proportion of the Ni in Oil C dissolved as porphyrin species, an observation that has been made for other crude oils (Ali et al., 1993). As the TAN value of Oil C is very much higher than that of Oil A (2.3 versus 0.2) and this value is an indicator of the carboxylic acid content, it is also possible that the binding of Ni by thiols in Oil C was greatly enhanced by the much higher acidity of this oil (Wenger et al., 2002. Clegg and Henderson, 2002). Notably, Oil B has the highest TAN value (2.9 wt.%), which may explain that it dissolved some Ni (15.6 ppm at 200 °C), despite being thiol-free initially (thiols formed during the experiments due to Ni catalyzed reduction of oxidized sulfur species; see above). Given that Oil A contains some nitrogen (0.2 wt.%), it is likewise possible that Ni in this oil was dissolved in large part as porphyrin species.

The thiolation of Ni may also involve Fe, which is the only other chemical component in the oil, aside from thiols that showed an affinity for the Ni wire. The intimate association of Ni, Fe and thiols on the wire surface indicates that Fe may be involved in the redox processes that helped

dissolve Ni into the oil. Oil C has the highest Fe content of all the oils and displays a strong Fe peak upon etching of the reacted Ni wire, whereas Oil A has the lowest Fe content and shows little evidence of complexing with Fe. This may also explain why these two oils dissolve very different amounts of Ni. In principle, Fe could enhance the dissolution of Ni by forming Ni-Fe-sulfur clusters, i.e., stable complexes of Fe and Ni bound together by thiolate ligands that are ubiquitous in nature (Ragsdale, 2009).

#### **4.4.2 Geochemical factors affecting oil composition and ore deposit formation**

The polar compounds in crude oil (also referred to as NSO compounds) contain one or more heteroatoms of nitrogen(N), sulfur(S) or oxygen(O) and, although they typically compose less than 10 wt% of petroleum, they are considered important ligands for metals in crude oil (Hughley et al., 2004). With the increasing maturity of oils, the NSO content generally decreases, whereas their gasoline content (the amount of short-chain, volatile aromatic and aliphatic compounds) increases (Meyer, 1989). Thus, Ni transport is favored by immature oils, particularly those that have experienced strong biodegradation, as these oils generally have higher NSO contents than less biodegraded oils of similar maturity (Meyer, 1989; Wenger et al., 2002; Head et al., 2003). Biodegraded immature oils are also characterized by high asphaltene contents. Nickel concentrations are highest in immature oils derived from carbonate source rocks with a low clay content and a high reduced sulfur content (this is likely due to Ni complexation by thiols). By comparison, marine and lacustrine shales generate oils with moderate amounts of Ni, and land-plant derived oils contain very little Ni (Meyer, 1989; Barwise, 1990). For example, crude oils generated in carbonate source rocks from the Gulf of Suez and Abu Dhabi have been documented to contain Ni in concentrations that range from 4 ppm to 148 ppm Ni, whereas oils

generated from non-carbonate source-rocks in the North Sea, mainland China, Indonesia and the Gippsland Basin in Australia have Ni concentrations in the 0.13 ppm Ni to 22 ppm Ni range (Barwise, 1990).

As noted above, nickel has an affinity for the asphaltene fraction of crude oil (Sugihara and Bean, 1962; Parnell, 1988; Yu et al., 2015). Indeed, the Boscan Crude oil from Venezuela, which has an asphaltene fraction corresponding to 20 wt% of the oil (Sugihara and Bean, 1962; Fish et al., 1984), contains up to 115 ppm Ni (Sugihara and Bean, 1962). Moreover, 78% of the Ni in this oil is contained within the asphaltene fraction (Fish et al., 1978). The asphaltene phase in petroleum is composed of large heterocyclic compounds, such as porphyrins (a form of tetrapyrrole), that are generated from the break-down of kerogen in the source rocks during catagenesis (Orr., 1986). Major precursors for porphyrins in oil are the chlorophylls present in photosynthetic organisms (Hodgson, 1973). In the Boscan Crude oil, 36 wt% of the metals in the asphaltene fraction are bound to porphyrins (Sugihara and Bean, 1962). Little is known, however, about the other kinds of metal organic complexes that form with Ni in petroleum, which are potentially more abundant than the Ni-porphyrins and may account for up to 50–80% of the metal being complexed in oil (Caumette et al., 2009).

In addition to its association with porphyrins, Ni possesses a strong chemical affinity for thiols, as has been shown in this study. Despite the decreasing trend in the proportion of NSO compounds with oil maturity, some very mature oils can contain anomalously high concentrations of thiols. These oils are typically sourced from deep, high temperature carbonate reservoirs with high partial pressures of hydrogen sulfide gas. The hydrogen sulfide in these

reservoirs is thought to be produced by thermochemical sulfate reduction (TSR) (Ho et al., 1974), a redox reaction between sulfate minerals and organic matter, which involves the high temperature, abiotic reduction of sulfate (see Equation 1 below). The hydrogen sulfide produced by TSR can react with organic compounds in liquid hydrocarbons, leading to the formation of thiol-enriched oils (Ho et al., 1974; Cai et al., 2003; Wei et al., 2011; Nguyen et al., 2013). Oil C, our most thiol-enriched oil (52 ppm thiol), has a relatively low thiol content compared to crude oils, described in the literature, that have undergone TSR. For example, the “Rodney Crude” and the “Light Mixed B.C.” oils described by Ho et al. (1974) have thiol contents of 3179 ppm and 1310 ppm, respectively, as calculated from their mercaptan numbers (refer to Supplementary materials, section A for a calculation of the thiol content of the Rodney Crude Oil). Anomalously thiol-rich oils, that have undergone TSR, therefore, may be expected to transport considerably greater concentrations of Ni than Oil C.

Thermochemical sulfate reduction:



(Machel, 2001)

Thermochemical sulfate reduction is a common source for the reduced sulfur responsible for the formation of Mississippi Valley Type (MVT) deposits (Machel, 2001) and is interpreted to be the source of reduced sulfur for the sulfide ores in other sediment-hosted deposits, such as the Kuperschiefer deposit in Poland (Bechtel and Püttmann, 1991; Jowett et al., 1991; Sun, 1998; Oszczepalski et al., 2012) and the Ni-rich sulfide ores in the Talvivaara deposit in Finland, which

displays mass-anomalous  $\Delta^{33}\text{S}$  fractionation similar to that of TSR laboratory experiments (Young et al., 2013). Thus, the genesis of some sediment-hosted sulfide deposits may be related through TSR to the production of a metalliferous, thiol-rich oil.

#### **4.4.3 Evidence for the involvement of liquid hydrocarbons in the genesis of shale-hosted nickel deposits.**

The two currently favored models for the formation of sedimentary Ni-rich deposits are: 1) synsedimentary mineralisation, with the metals being scavenged from seawater by organic matter close to the seawater-sediment interface (Lehman et al., 2007; and 2) exhalative hydrothermal mineralisation, with the metals being deposited from basinal brines as they are discharged into a euxinic, stratified water mass (Jowitt and Keays, 2011). Given that petroleum can dissolve considerable amounts of Ni, a petroleum exhalative (Petrex) model has also been proposed to describe the genesis of certain Ni-rich sedimentary deposits, e.g., the Zunyi deposits in China. In this model, petroleum is discharged into the basin and forms a sea-surface slick. Metals are then deposited as the oil is volatilized, water-washed, oxidized and biodegraded (Emsbo et al., 2005).

Here, we discuss the evidence for the involvement of liquid hydrocarbons in the genesis of shale-hosted nickel deposits. The principal examples of these deposits are the hyper-enriched black shale (HEBS) deposits in southern China as well as the Nick Prospect and related prospects in the Yukon, Canada. These deposits comprise thin highly enriched metal-sulfide layers, usually no more than 30 cm thick in southern China and 10 cm thick in the Yukon, with Ni grades of up to 7 wt% and 5.7 wt%, respectively (Jowitt and Keays, 2011; Henderson et al., 2019). They outcrop discontinuously for 2000 km in southern China and > 800 km in the Yukon. Organic

particles commonly fill voids and fissures in the mineralized black shale of southern China and most probably represent partly remobilized and solidified products of oil migration (migrabitumens) (Křibek et al., 2007). The restriction of migrabitumen to the ores and their absence in the barren shales likely reflect a higher primary porosity of the ore horizon (breccia) compared to the barren shale. Thus, the ore horizon probably played the role of an “oil collector” during late diagenesis and catagenesis (Křibek et al., 2007). At the Nick prospect, pyrobitumen occurs as centimetre-scale veinlets within the mineralized layer and meter-wide subvertical veins in the shales stratigraphically below this layer. Moreover, pyrobitumen within the mineralized layer contains 1300 ppm Ni on average and elevated concentrations of other metals. and one of the thicker veins below the layer contains 2000 ppm Ni (Henderson et al, 2019).

It is noteworthy that there are numerous oil and gas fields of Sinian to Cambrian age (Sichuan Basin) in relatively close proximity to some of the HEBS deposits in southern China (EIA 2011; Lan et al., 2017; Pages et al., 2018). The gas in these fields is interpreted to have formed through the thermal cracking of petroleum (Hao et al., 2008; Caineng et al., 2014; Zou et al., 2014; Zhu et al., 2015) and, in many cases, there is evidence that there was gas souring from TSR (Cai C. et al., 2003; Hao et al., 2008; Zhu et al., 2015). As crude oil starts to undergo TSR, it becomes oxidized at the expense of aqueous sulfate in the reservoir, which is reduced to hydrogen sulfide gas (Machel, 2001). The residual oil that has undergone TSR is anomalously enriched in thiols (Ho et al., 1974; Cai et al., 2003; Wei et al., 2011; Nguyen et al., 2013), that display a strong affinity for metals like Ni and Pd (Sanz-Robinson et al., 2019). These residual oils are therefore potentially effective ore fluids for the transport of Ni and Pd and perhaps other noble metals like Pt, Os and Au, all of which share similar electronegativity and therefore, according to hard-soft-

acid-base principles, are expected to bind to ‘soft’ ligands like thiols (Pearson, 1963).

Furthermore, the oxidation of petroleum by TSR can produce naphthenic acids (Machel, 2001), that are effective ligands for the complexation and transport of Zn in petroleum (Sanz-Robinson and Williams-Jones, 2019).

We propose that residual reduced sulfur-enriched hydrocarbons in the Sichuan basin supplied the Ni (and Pd, Pt, Os, Au, Zn and Mo) that formed the hyper-enriched black shale Ni deposits in southern China. The presence of highly enriched bituminous veins below the Nick prospect suggests that the HEBS in Yukon Canada had a similar history. According to the above hypothesis, the formation of HEBS is genetically related to a large petroleum system that undergoes pulses of thermal cracking and TSR (Cai et al., 2004; Hu et al., 2010) yielding natural gas, sour gas and residual petroleum enriched in thiols. With consumption of the petroleum by TSR, the volume of residual oil shrinks but becomes increasingly enriched in thiols and it is this oil that supplies the Ni (and other metals), which distinguishes hyper-enriched black shale deposits from other sediment-hosted metalliferous deposits.

Further evidence for the involvement of liquid hydrocarbons in the formation of HEBS, is provided by the (circa 2.0 – 1.9 Ga) Talvivaara deposit in Finland, which hosts significant Ni reserves and contains uraninite crystals rimmed by bitumen. The latter indicates that hydrocarbons, possibly from source rocks deeper in the stratigraphy deposited during the Shunga event (c. 2.0 Ga), migrated through the deposit (Lecomte et al, 2014). This event was marked by the global deposition of organic carbon-rich rocks and the development of vast petroleum resources such as those in the Zaonezhskaya Formation of the Onega Basin in Russian

Fennoscandia (Melezhik et al, 2009, Asael et al., 2013; Strauss et al., 2013; Lecomte et al, 2014). Thus, not only is the mineralization in the Talvivaara deposit associated with bitumen, but there was also a large reservoir of liquid hydrocarbons that could have transported the metals to the site of ore formation.

As mentioned above, one of the currently favored hypotheses for the HEBS of southern China and the Yukon, Canada is that they are syngenetic and formed as a result of the precipitation of the ore metals from seawater (seawater contains 2 ppb Ni on average; Kato et al., 1990) at the seawater-sediment interface through bacterially-mediated processes. It has been suggested that textures of the iron sulfides (i.e. framboidal pyrite) at the HEBS of Yukon, Canada reflect deposition during early-diagenesis (Gadd et al., 2018, and 2019). However, pyritic framboids could have also formed abiotically (Scott et al., 2009) and the millerite (NiS) mineralization at the Peel River HEBS in Yukon, show it mantling and replacing pyrite (Henderson et al., 2019), indicating that the nickel mineralization is epigenetic. Finally, the required concentration factor (~ 10 million; from 2 ppb to several wt%) seems unreasonably high. The other hypothesis for the formation of HEBS, namely that they are epigenetic but deposited from saline hydrothermal-vent brines (Lott et al., 1999, Steiner et al., 2001), is also problematic. This is because Ni is highly insoluble in hydrothermal fluids, even those with high chloride activity, making it unlikely that saline brines could have constituted an ore fluid for the mineralization in these rocks. For example, at 250 °C and  $fO_2$ -pH conditions buffered by the assemblage magnetite-pyrite-pyrrhotite, the solubility of millerite, the main Ni mineral in HEBS deposits, is 0.2 ppm; this solubility decreases with decreasing temperature (Liu et al., 2012). In view of the serious

weaknesses of the synsedimentary seawater and epigenetic brine models, the role of petroleum as an ore fluid for Ni and other metals in sediment-hosted deposits merits serious consideration.

#### 4.5 Conclusions

The potential of liquid hydrocarbons to act as ore fluids was evaluated by reacting Ni wires in crude oil at elevated temperatures (150-250°C). Below 150°C, Ni concentrations in the three crude oils considered in this study remained relatively low. Above, 200 °C, one of the oils, (Oil C) dissolved considerably more Ni than the other two oils (reaching a concentration of 217 ppm at 250°C). X-ray photoelectron spectroscopic analyses of the residual oil coating the Ni wires after reaction indicates that Ni has a strong chemical affinity for thiols. This is supported by the observation that Oil C, the most Ni-philic of the oils has the highest thiol content (52 ppm). Oil A, which has the second highest thiol concentration (44 ppm), dissolved the second largest amount of Ni (up to 26 ppm Ni at 200°C). The much lower capacity of Oil A to dissolve Ni compared to Oil C and its only slightly lower thiol content, however, indicate that a second species played an important role in Ni solubility. As Oil C has the highest nitrogen content (0.44 wt.%) of the three oils and Oil A contains no nitrogen, this second species is likely to be a Ni-porphyrin, which previous studies have linked to the high concentration of Ni in some crude oils. Oil C also has a high carboxylic acid content (indicated by its high TAN value), whereas that of Oil A is very low (very low TAN value). The much higher acidity of Oil C compared to Oil A may have promoted the stronger binding of Ni to thiol ligands and the formation of Ni-thiolate complexes, thereby further explaining the much higher capacity of Oil C to dissolve Ni; Ni-thiolation may also be promoted by the presence of Fe, as shown by the synchronous

incorporation of Fe in the Ni wires and the binding of thiols to them. The evidence that liquid hydrocarbons can dissolve high concentrations of Ni, that Ni is extremely insoluble in hydrothermal fluids and that Ni forms ore deposits (several wt.% Ni) in black shales, which have been infiltrated by petroleum, makes a compelling case that liquid hydrocarbons could be important ore fluids for nickel.

#### **4.6 Acknowledgments**

The research described in this paper was funded by a grant from Statoil Canada and a collaborative research and development grant from NSERC. The crude oil samples used in the experiments were supplied by Statoil Canada. We thank Scott Bohle and Danae Guerra for their assistance with our X-Ray Photoelectron Spectroscopy analyses and Ichiko Sugiyama for her help in setting-up the solubility experiments. Constructive comments by Mike Gadd and an anonymous Chemical Geology reviewer helped improve the manuscript substantially.

#### **4.7 References**

Ali, M.F., Perzanowski, H., Bukhari, A. and Al-Haji, A.A., 1993. Nickel and vanadyl porphyrins in Saudi Arabian crude oils. *Energy & Fuels*, 7(2), pp.179-184.

Asael, D., Tissot, F.L., Reinhard, C.T., Rouxel, O., Dauphas, N., Lyons, T.W., Ponzevera, E., Liorzou, C. and Chéron, S., 2013. Coupled molybdenum, iron and uranium stable isotopes as oceanic paleoredox proxies during the Paleoproterozoic Shunga Event. *Chemical Geology*, 362, pp.193-210.

Barwise, A.J.G., 1990. Role of nickel and vanadium in petroleum classification. *Energy & Fuels*, 4(6), pp.647-652.

Bechtel, A. and Püttmann, W., 1991. The origin of the Kupferschiefer-type mineralization in the Richelsdorf Hills, Germany, as deduced from stable isotope and organic geochemical studies. *Chemical Geology*, 91(1), p.1-18.

Belkin, H.E. and Luo, K., 2008. Late-stage sulfides and sulfarsenides in Lower Cambrian black shale (stone coal) from the Huangjiawan mine, Guizhou Province, People's Republic of China. *Mineralogy and Petrology*, 92(3-4), pp.321-340.

Cai, C., Worden, R.H., Bottrell, S.H., Wang, L. and Yang, C., 2003. Thermochemical sulphate reduction and the generation of hydrogen sulphide and thiols (mercaptans) in Triassic carbonate reservoirs from the Sichuan Basin, China. *Chemical Geology*, 202(1-2), pp.39-57

Cai, C., Xie, Z., Worden, R.H., Hu, G., Wang, L. and He, H., 2004. Methane-dominated thermochemical sulphate reduction in the Triassic Feixianguan Formation East Sichuan Basin, China: towards prediction of fatal H<sub>2</sub>S concentrations. *Marine and Petroleum Geology*, 21(10), pp.1265-1279.

Caineng, Z., Jinhu, D.U., Chunchun, X.U., Zecheng, W.A.N.G., Zhang, B., Guoqi, W., Tongshan, W., Genshun, Y., Shenghui, D., Jingjiang, L. and Hui, Z., 2014. Formation,

distribution, resource potential, and discovery of Sinian–Cambrian giant gas field, Sichuan Basin, SW China. *Petroleum Exploration and Development*, 41(3), pp.306-325.

Castner, D.G., Hinds, K. and Grainger, D.W., 1996. X-ray photoelectron spectroscopy sulfur 2p study of organic thiol and disulfide binding interactions with gold surfaces. *Langmuir*, 12(21), p.5083-5086.

Caumette, G., Lienemann, C.P., Merdrignac, I., Bouyssiere, B. and Lobinski, R., 2009. Element speciation analysis of petroleum and related materials. *Journal of Analytical Atomic Spectrometry*, 24(3), pp.263-276.

Clegg, W. and Henderson, R.A., 2002. Kinetic evidence for intramolecular proton transfer between nickel and coordinated thiolate. *Inorganic chemistry*, 41(5), pp.1128-1135.

Diekert, G., Konheiser, U., Piechulla, K. and Thauer, R.K., 1981. Nickel requirement and factor F430 content of methanogenic bacteria. *Journal of Bacteriology*, 148(2), pp.459-464.

EIA, 2011. World Shale Gas Resources: an Initial Assessment of 14 Regions Outside the United States. U.S. Department of Energy, Washington. DC.

Fish, R.H., Komlenic, J.J. and Wines, B.K., 1984. Characterization and comparison of vanadyl and nickel compounds in heavy crude petroleums and asphaltenes by reverse-phase and size-

exclusion liquid chromatography/graphite furnace atomic absorption spectrometry. *Analytical Chemistry*, 56(13), pp.2452-2460.

Gadd, M.G. and Peter, J.M., 2017. Field observations, mineralogy and geochemistry of Middle Devonian Ni-Zn-Mo-PGE hyper-enriched black shale deposits, Yukon. *Targeted Targeted Geoscience Initiative*.

Gadd, M. G., and Peter, J. M., 2018, Field observations, mineralogy and geochemistry of Middle Devonian Ni-Zn-Mo-PGE hyper-enriched black shale deposits, Yukon, in Rogers, N., ed., *Targeted Geoscience Initiative: 2017 report of activities, volume 1; Geological Survey of Canada*, Open File 8358, p. 193-206.

Gadd, M. G., Peter, J. M., Jackson, S. E., Yang, Z., and Petts, D., 2019, Platinum, Pd, Mo, Au and Re deportment in hyper-enriched black shale Ni-Zn-Mo-PGE mineralization, Peel River, Yukon, Canada: *Ore Geology Reviews*, v. 107, p. 600-614.

Giordano, T.H., 1994, Metal Transport in Ore Fluids by Organic Ligand Complexation, in Pittman, E.D. and Lewan, M.D. eds., *Organic Acids in Geological Processes*, Springer-Verlag, p. 320 – 354.

Groenzin, H. and Mullins, O.C., 1999. Asphaltene molecular size and structure. *The Journal of Physical Chemistry A*, 103(50), pp.11237-11245.

Grotzinger, J.P., Fike, D.A. and Fischer, W.W., 2011. Enigmatic origin of the largest-known carbon isotope excursion in Earth's history. *Nature Geoscience*, 4(5), p.285.

Hao, F., Guo, T., Zhu, Y., Cai, X., Zou, H. and Li, P., 2008. Evidence for multiple stages of oil cracking and thermochemical sulfate reduction in the Puguang gas field, Sichuan Basin, China. *AAPG bulletin*, 92(5), pp.611-637.

Hao, F., Zhang, X., Wang, C., Li, P., Guo, T., Zou, H., Zhu, Y., Liu, J. and Cai, Z., 2015. The fate of CO<sub>2</sub> derived from thermochemical sulfate reduction (TSR) and effect of TSR on carbonate porosity and permeability, Sichuan Basin, China. *Earth-Science Reviews*, 141, pp.154-177.

Head, I.M., Jones, D.M. and Larter, S.R., 2003. Biological activity in the deep subsurface and the origin of heavy oil. *Nature*, 426(6964), p.344.

Henderson, K.M., Williams-Jones, A.E., and Clark, J.R., 2019. Metal transport by liquid hydrocarbons: Evidence from metalliferous shale and pyrobitumen, Yukon; in *Targeted Geoscience Initiative: 2018 report of activities*, (ed.) N. Rogers; Geological Survey of Canada, Open File 8549, p. 179-187.

Ho, T.Y., Rogers, M.A., Drushel, H.V. and Koons, C.B., 1974. Evolution of sulfur compounds in crude oils. *AAPG Bulletin*, 58(11), p.2338-2348.

Hodgson, G.W., 1973. Geochemistry of porphyrins—reactions during diagenesis. *Annals of the New York Academy of Sciences*, 206(1), pp.670-684.

Hu, A., Li, M., Wong, J., Reyes, J., Achal, S., Milovic, M., Robinson, R., Shou, J., Yang, C., Dai, J. and Ma, Y., 2010. Chemical and petrographic evidence for thermal cracking and thermochemical sulfate reduction of paleo-oil accumulations in the NE Sichuan Basin, China. *Organic geochemistry*, 41(9), pp.924-929.

Hughey, C.A., Rodgers, R.P., Marshall, A.G., Walters, C.C., Qian, K. and Mankiewicz, P., 2004. Acidic and neutral polar NSO compounds in Smackover oils of different thermal maturity revealed by electrospray high field Fourier transform ion cyclotron resonance mass spectrometry. *Organic geochemistry*, 35(7), pp.863-880.

Hulbert, L.J., Carne, R.C., Gregoire, D.C. and Paktunc, D., 1992. Sedimentary nickel, zinc, and platinum-group-element mineralization in Devonian black shales at the Nick Property, Yukon, Canada; a new deposit type. *Exploration and Mining Geology*, 1(1), pp.39-62.

Hulen, J.B. and Collister, J.W., 1999. The oil-bearing, carlin-type gold deposits of Yankee Basin, Alligator Ridge District, Nevada. *Economic Geology*, 94(7), pp.1029-1049.

Jiang, G., Kaufman, A.J., Christie-Blick, N., Zhang, S. and Wu, H., 2007. Carbon isotope variability across the Ediacaran Yangtze platform in South China: Implications for a large

surface-to-deep ocean  $\delta^{13}\text{C}$  gradient. *Earth and Planetary Science Letters*, 261(1-2), pp.303-320.

Jowett, E.C., Roth, T., Rydzewski, A. and Oszczepalski, S., 1991. "Background"  $\delta^{34}\text{S}$  values of Kupferschiefer sulphides in Poland: pyrite-marcasite nodules. *Mineralium Deposita*, 26(2), p.89-98.

Jowitt, S.M. and Keays, R.R., 2011. Shale-hosted Ni-(Cu-PGE) mineralisation: a global overview. *Applied Earth Science*, 120(4), pp.187-197.

Kapo, G.: Vanadium: key to Venezuelan fossil hydrocarbons. In: Bitumens, asphalts and tar sands, G. V. Chilingarian, T. F. Yen, Eds., pp. 155-190. Amsterdam: Elsevier 1978.

Kato, T., Nakamura, S. and Morita, M., 1990. Determination of nickel, copper, zinc, silver, cadmium and lead in seawater by isotope dilution inductively coupled plasma mass spectrometry. *Analytical Sciences*, 6(4), pp.623-626.

Kelemen, S.R., George, G.N. and Gorbaty, M.L., 1990. Direct determination and quantification of organic sulfur forms by X-ray photoelectron spectroscopy (XPS) and sulfur k-edge absorption spectroscopy. *Fuel Processing Technology*, 24, pp.425-429.

Kelly, W.C. and Nishioka, G.K., 1985. Precambrian oil inclusions in late veins and the role of hydrocarbons in copper mineralization at White Pine, Michigan. *Geology*, 13(5), pp.334-337.

Kříbek, B., Sýkorová, I., Pašava, J. and Machovič, V., 2007. Organic geochemistry and petrology of barren and Mo–Ni–PGE mineralized marine black shales of the Lower Cambrian Niutitang Formation (South China). *International Journal of Coal Geology*, 72(3-4), pp.240-256.

Korsch, R.J., Huazhao, M., Zhaocai, S. and Gortler, J.D., 1991. The Sichuan basin, southwest China: a late proterozoic (Sinian) petroleum province. *Precambrian Research*, 54(1), pp.45-63.

Lambert, I.B., Walter, M.R., Wenlong, Z., Songnian, L. and Guogan, M.A., 1987. Palaeoenvironment and carbon isotope stratigraphy of Upper Proterozoic carbonates of the Yangtze Platform. *Nature*, 325(6100), p.140.

Lan, Z., Li, X.H., Chu, X., Tang, G., Yang, S., Yang, H., Liu, H., Jiang, T. and Wang, T., 2017. SIMS U-Pb zircon ages and Ni-Mo-PGE geochemistry of the lower Cambrian Niutitang Formation in South China: Constraints on Ni-Mo-PGE mineralization and stratigraphic correlations. *Journal of Asian Earth Sciences*, 137, pp.141-162.

Langevin, D., Poteau, S., Hénaut, I. and Argillier, J.F., 2004. Crude oil emulsion properties and their application to heavy oil transportation. *Oil & gas science and technology*, 59(5), pp.511-521.

Lecomte, A., Cathelineau, M., Deloule, E., Brouand, M., Peiffert, C., Loukola-Ruskeeniemi, K., Pohjolainen, E. and Lahtinen, H., 2014. Uraniferous bitumen nodules in the Talvivaara Ni–Zn–

Cu–Co deposit (Finland): influence of metamorphism on uranium mineralization in black shales. *Mineralium Deposita*, 49(4), pp.513-533.

Lehmann, B., Frei, R., Xu, L. and Mao, J., 2016. Early Cambrian black shale-hosted Mo-Ni and V mineralization on the rifted margin of the Yangtze Platform, China: reconnaissance chromium isotope data and a refined metallogenic model. *Economic Geology*, 111(1), pp.89-103.

Lewan, M., 1984, Factors controlling the proportionality of vanadium to nickel in crude oils: *Geochimica et Cosmochimica Acta*, v. 48, p. 2231 – 2238.

Liu, W., Migdisov, A. and Williams-Jones, A., 2012. The stability of aqueous nickel (II) chloride complexes in hydrothermal solutions: Results of UV–Visible spectroscopic experiments. *Geochimica et Cosmochimica Acta*, 94, pp.276-290.

Lott, D.A., Coveney, R.M., Murowchick, J.B. and Grauch, R.I., 1999. Sedimentary exhalative nickel-molybdenum ores in South China. *Economic Geology*, 94(7), pp.1051-1066.

Loukola-Ruskeeniemi, K. and Heino, T., 1996. Geochemistry and genesis of the black shale-hosted Ni-Cu-Zn deposit at Talvivaara, Finland. *Economic Geology*, 91(1), pp.80-110.

Lingang, X., Lehmann, B., Jingwen, M., Wenjun, Q. and Andao, D., 2011. Re-Os age of polymetallic Ni-Mo-PGE-Au mineralization in Early Cambrian black shales of South China—a reassessment. *Economic Geology*, 106(3), pp.511-522.

Machel, H.G., 2001. Bacterial and thermochemical sulfate reduction in diagenetic settings—old and new insights. *Sedimentary Geology*, 140(1-2), pp.143-175.

Marcano, F., Flores, R., Chirinos, J. and Ranaudo, M.A., 2011. Distribution of Ni and V in A1 and A2 asphaltene fractions in stable and unstable Venezuelan crude oils. *Energy & Fuels*, 25(5), pp.2137-2141.

McFadden, K.A., Huang, J., Chu, X., Jiang, G., Kaufman, A.J., Zhou, C., Yuan, X. and Xiao, S., 2008. Pulsed oxidation and biological evolution in the Ediacaran Doushantuo Formation. *Proceedings of the National Academy of Sciences*, 105(9), pp.3197-3202.

Melezhik, V.A., Fallick, A.E., Filippov, M.M., Lepland, A., Rychanchik, D.V., Deines, Y.E., Medvedev, P.V., Romashkin, A.E. and Strauss, H., 2009. Petroleum surface oil seeps from a Palaeoproterozoic petrified giant oilfield. *Terra Nova*, 21(2), pp.119-126.

Meyer, R. F. (1989). Heavy oil and natural bitumen. *The Petroleum System: Status of Research and methods, 1990*", U.S.G.P.O. pp 64.

Mitra-Kirtley, S., Mullins, O.C., Van Elp, J., George, S.J., Chen, J. and Cramer, S.P., 1993. Determination of the nitrogen chemical structures in petroleum asphaltene using XANES spectroscopy. *Journal of the American Chemical Society*, 115(1), pp.252-258.

Nguyen, V.P., Burklé-Vitzthum, V., Marquaire, P.M. and Michels, R., 2013. Thermal reactions between alkanes and H<sub>2</sub>S or thiols at high pressure. *Journal of analytical and applied pyrolysis*, 103, pp.307-319.

Ohki, Y. and Tatsumi, K., 2011. Thiolate-Bridged Iron–Nickel Models for the Active Site of [NiFe] Hydrogenase. *European Journal of Inorganic Chemistry*, 2011(7), pp.973-985.

Orberger, B., Vymazalova, A., Wagner, C., Fialin, M., Gallien, J.P., Wirth, R., Pasava, J. and Montagnac, G., 2007. Biogenic origin of intergrown Mo-sulphide-and carbonaceous matter in Lower Cambrian black shales (Zunyi Formation, southern China). *Chemical geology*, 238(3-4), pp.213-231.

Orr, W.L., 1986. Kerogen/asphaltene/sulfur relationships in sulfur-rich Monterey oils. *Organic geochemistry*, 10(1-3), pp.499

Oswald, A.A., 1961. Organic Sulfur Compounds. III. Co-Oxidation of Mercaptans with Styrenes and Indene. *The Journal of Organic Chemistry*, 26(3), pp.842-846.

Oszczepalski, S., Nowak, G., Bechtel, A. and Zák, K., 2012. Evidence of oxidation of the Kupferschiefer in the Lubin-Sierszowice deposit, Poland: implications for Cu-Ag and Au-Pt-Pd mineralisation. *Geological Quarterly*, 46(1), p.1-24.

Pages, A., Barnes, S., Schmid, S., Coveney Jr, R.M., Schwark, L., Liu, W., Grice, K., Fan, H. and Wen, H., 2018. Geochemical investigation of the lower Cambrian mineralised black shales of South China and the late Devonian Nick deposit, Canada. *Ore Geology Reviews*, 94, pp.396-413.

Parnell, J., 1988. Metal enrichments in solid bitumens: a review. *Mineralium Deposita*, 23(3), pp.191-199.

Parnell, J. and Eakin, P., 1987. The replacement of sandstones by uraniferous hydrocarbons: significance for petroleum migration. *Mineralogical Magazine*, 51(362), pp.505-515.

Peabody, C.E. and Einaudi, M.T., 1992. Origin of petroleum and mercury in the Culver-Baer cinnabar deposit, Mayacmas district, California. *Economic Geology*, 87(4), pp.1078-1103.

Pearson, G., 1963. Hard and Soft Acids and Bases: *Journal of the American Chemical Society*, 85, p. 3533–3539.

Peter, J.M., and Scott, S.D., 1988, Mineralogy, composition, and fluid-inclusion microthermometry of seafloor hydrothermal deposits in the Southern Trough of Guaymas Basin, Gulf of California: *Canadian Mineralogist*, v. 26, p. 567–587.

Peters, K.E., Walters, C.C., and Moldowan, J.M., 2004, *The Biomarker Guide: Volume 1, Biomarker and Isotopes in the Environment and Human History*: Cambridge University Press.

Price, L.C., and Wenger, L.M., 1992, The influence of pressure on petroleum generation and maturation as suggested by aqueous pyrolysis: *Organic Geochemistry*, v. 19, p. 141–159.

Potočnik, J., Nenadović, M., Jokić, B.M., Popović, M. and Rakočević, Z.L., 2016. Properties of Zig-Zag Nickel Nanostructures Obtained by GLAD Technique. *Science of Sintering*, 48(1), pp.51-56

Ragsdale, S.W., 2009. Nickel-based enzyme systems. *Journal of Biological Chemistry*, 284(28), pp.18571-18575.

Saintilan, N.J., Spangenberg, J.E., Chiaradia, M., Chelle-Michou, C., Stephens, M.B. and Fontboté, L., 2019. Petroleum as source and carrier of metals in epigenetic sediment-hosted mineralization. *Scientific reports*, 9(1), p.8283.

Sanz-Robinson, J. and Williams-Jones, A.E., 2019. Zinc solubility, speciation and deposition: A role for liquid hydrocarbons as ore fluids for Mississippi Valley Type Zn-Pb deposits. *Chemical Geology*, 520, pp.60-68.

Sanz-Robinson, J., Sugiyama, I., and Williams-Jones A.E., (Accepted for publication). The Solubility of Palladium (Pd) in Crude Oil at 150, 200 and 250 °C and its Application to Ore Genesis. *Chemical Geology*

Scott, R.J., Meffre, S., Woodhead, J., Gilbert, S.E., Berry, R.F. and Emsbo, P., 2009. Development of framboidal pyrite during diagenesis, low-grade regional metamorphism, and hydrothermal alteration. *Economic Geology*, 104(8), pp.1143-1168.

Seifert, W.K., 1975. Carboxylic acids in petroleum and sediments. In: Fortschritte der Chemie Organischer Naturstoffe/Progress in the Chemistry of Organic Natural Products. Springer, Vienna, pp. 1–49.

Speight, J.G., 2001, Handbook of Petroleum Analysis (J. G. Speight, Ed.): John Wiley & Sons, Inc.

Steiner, M., Wallis, E., Erdtmann, B.D., Zhao, Y., and Yang, R., 2001. Submarine-hydrothermal exhalative ore layers in black shales from South China and associated fossils - Insights into a Lower Cambrian facies and bio-evolution; *Palaeogeography, Palaeoclimatology, Palaeoecology*, v. 169, p. 165–191.

Strauss, H., Melezhik, V.A., Lepland, A., Fallick, A.E., Hanski, E.J., Filippov, M.M., Deines, Y.E., Illing, C.J., Črne, A.E. and Brasier, A.T., 2013. 7.6 Enhanced Accumulation of Organic Matter: The Shunga Event. In *Reading the archive of Earth's oxygenation* (pp. 1195-1273). Springer, Berlin, Heidelberg.

Sugihara, J.M. and Bean, R.M., 1962. Direct determination of metalloporphyrins in Boscan crude oil. *Journal of Chemical and Engineering Data*, 7(2), pp.269-271.

Sugiyama, I. and Williams-Jones, A.E., 2018. An approach to determining nickel, vanadium and other metal concentrations in crude oil. *Analytica chimica acta*, 1002, pp.18-25.

Summons, R.E. and Powell, T.G., 1992. Hydrocarbon composition of the Late Proterozoic oils of the Siberian Platform: Implications for the depositional environment of source rocks. In *Early Organic Evolution* (pp. 296-307). Springer, Berlin, Heidelberg.

Sun, Y.Z., 1998. Influences of secondary oxidation and sulfide formation on several maturity parameters in Kupferschiefer. *Organic Geochemistry*, 29(5-7), pp.1419-1429.

Wagner, C.D., 1972. Auger lines in x-ray photoelectron spectrometry. *Analytical Chemistry*, 44(6), pp.967-973.

Wang, G., Wang, T.G., Han, K., Wang, L. and Shi, S., 2015. Recognition of a novel Precambrian petroleum system based on isotopic and biomarker evidence in Yangtze platform, South China. *Marine and Petroleum Geology*, 68, pp.414-426.

Wei, Z., Mankiewicz, P., Walters, C., Qian, K., Phan, N.T., Madincea, M.E. and Nguyen, P.T., 2011. Natural occurrence of higher thiadiamondoids and diamondoidthiols in a deep petroleum reservoir in the Mobile Bay gas field. *Organic geochemistry*, 42(2), pp.121-133.

Wenger, L.M., Davis, C.L. and Isaksen, G.H., 2002. Multiple controls on petroleum biodegradation and impact on oil quality. *SPE Reservoir Evaluation & Engineering*, 5(05), pp.375-383.

Williams-Jones, A.E., Bowell, R.J. and Migdisov, A.A., 2009. Gold in solution. *Elements*, 5(5), pp.281-287.

Williams-Jones, A.E. and Migdisov, A.A., 2014. Experimental constraints on the transport and deposition of metals in ore-forming hydrothermal systems. *Society of Economic Geologists*, 18, pp.77-96.

Worden, R.H., Smalley, P.C. and Cross, M.M., 2000. The influence of rock fabric and mineralogy on thermochemical sulfate reduction: Khuff Formation, Abu Dhabi. *Journal of Sedimentary Research*, 70(5), pp.1210-1221.

Young, S.A., Loukola-Ruskeeniemi, K. and Pratt, L.M., 2013. Reactions of hydrothermal solutions with organic matter in Paleoproterozoic black shales at Talvivaara, Finland: Evidence from multiple sulfur isotopes. *Earth and Planetary Science Letters*, 367, pp.1-14.

Yu, C., Zhang, L., Guo, X., Xu, Z., Sun, X., Xu, C. and Zhao, S., 2015. Association model for nickel and vanadium with asphaltene during solvent deasphalting. *Energy & Fuels*, 29(3), pp.1534-1542.

Zhu, G., Wang, T., Xie, Z., Xie, B. and Liu, K., 2015. Giant gas discovery in the Precambrian deeply buried reservoirs in the Sichuan Basin, China: Implications for gas exploration in old cratonic basins. *Precambrian Research*, 262, pp.45-66.

Zou, C., Wei, G., Xu, C., Du, J., Xie, Z., Wang, Z., Hou, L., Yang, C., Li, J. and Yang, W., 2014. Geochemistry of the Sinian–Cambrian gas system in the Sichuan Basin, China. *Organic geochemistry*, 74, pp.13-21.

## Supplementary Materials for

The solubility of Nickel (Ni) in crude oil at 150, 200 and 250°C and its Application to Ore

Genesis

Sanz-Robinson and Williams-Jones

### A. Calculation of the thiol content of the Rodney Crude oil

$API = \frac{141.5}{SG} - 131.5$ , where API is a measure of the weight of petroleum liquids and SG is the specific gravity of the oil.

$$\text{Therefore, } SG = \frac{141.5}{API+131.5}$$

The API value for the Rodney Crude is 32. (Ho et al., 1974)

$$SG_{Rodney\ Crude} = \frac{141.5}{32+131.5} = 0.865$$

$$SG = \frac{\rho_{oil}}{\rho_{H_2O}} \text{ where } \rho \text{ is the density.}$$

Assuming  $\rho_{H_2O} = 1.0 \text{ g/mL}$

$$\rho_{Rodney\ Crude} = SG_{Rodney\ Crude} = 0.865 \text{ g/mL}$$

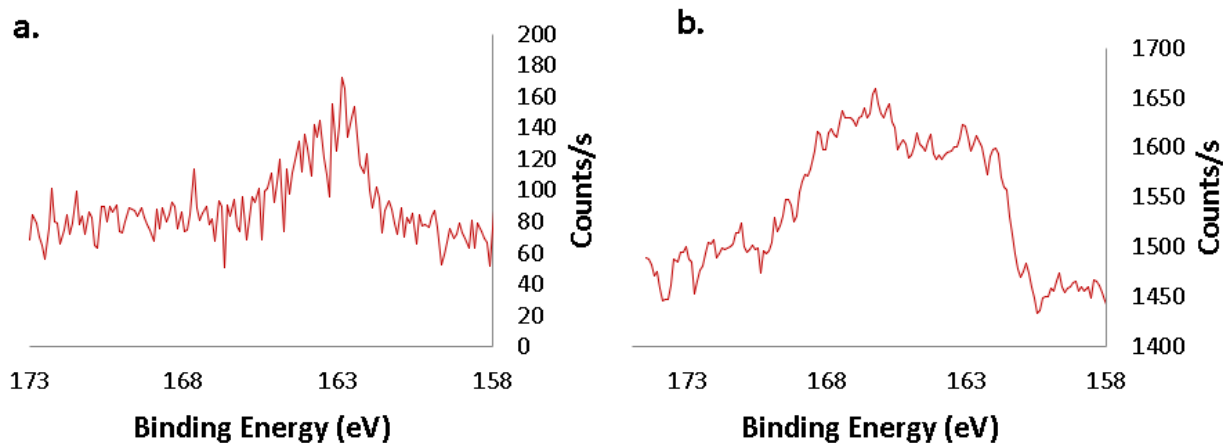
$$\text{Mercaptan Number} = \frac{\text{mg of thiol S}}{100\text{mL}} \quad (\text{Oswald, 1961})$$

The Mercaptan number for the Rodney Crude is 275 (Ho et al., 1974)

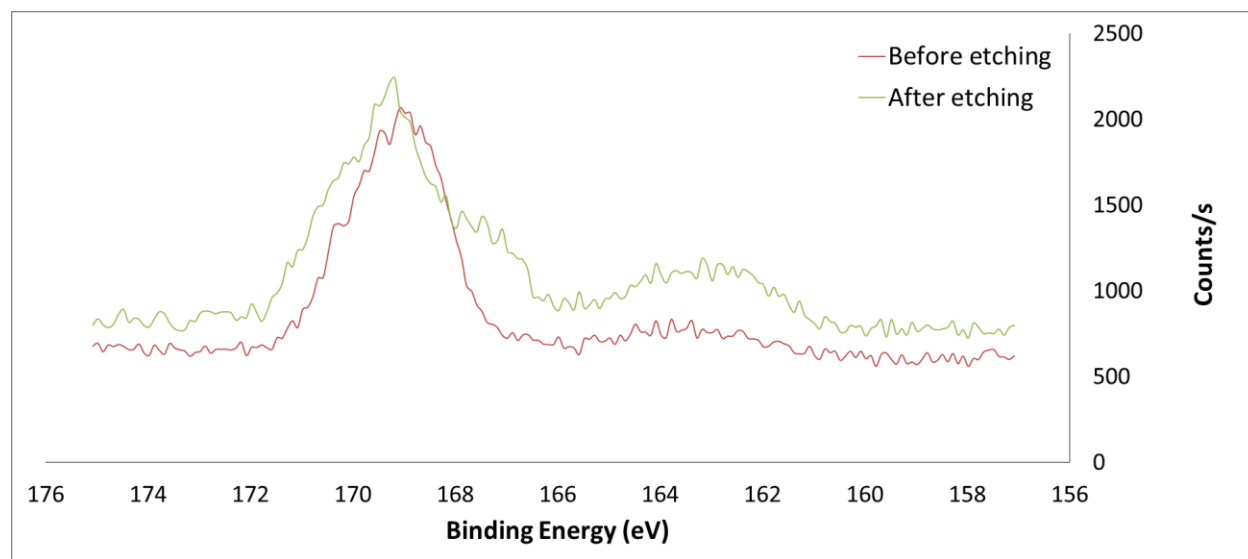
$$\text{Mercaptan Number} = \frac{275 \text{ mg of thiol S}}{100\text{mL}} = \frac{275 \text{ mg thiol S} \times \frac{1000\mu\text{g}}{\text{mg}}}{100\text{mL} \times \rho_{Rodney\ Crude}} = \frac{275000 \mu\text{g}}{100\text{mL} \times \frac{0.865\text{g}}{\text{mL}}} = 3179 \text{ ppm}$$

Thus, the Rodney Crude contains 3179 ppm of thiol S.

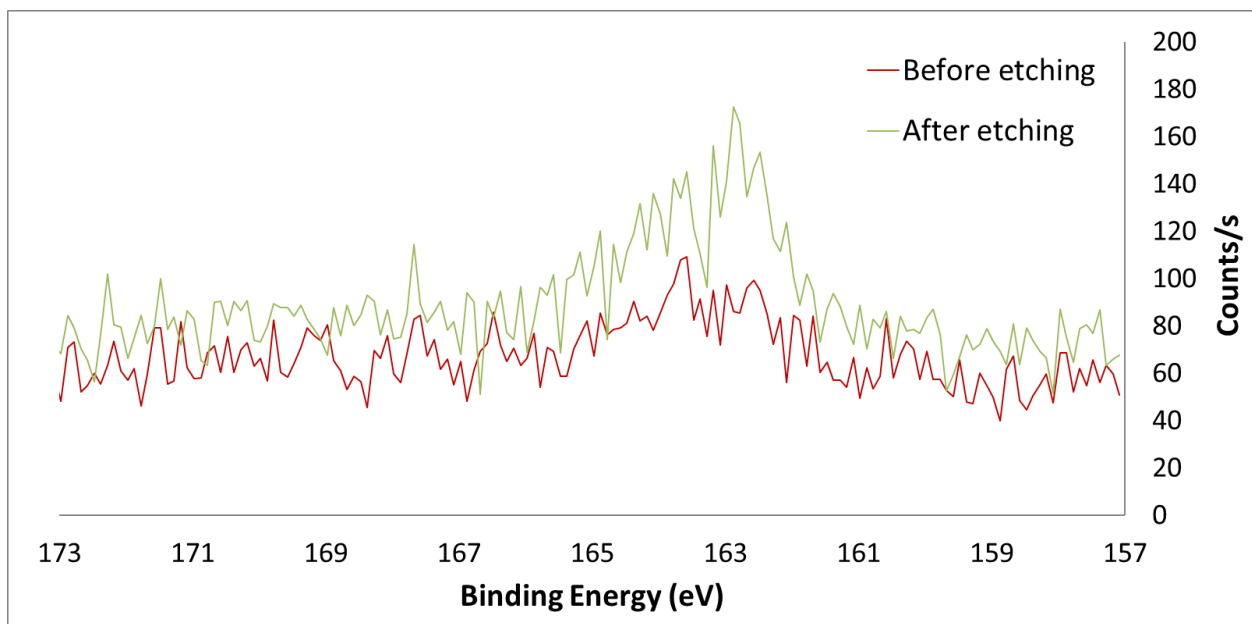
## B. Supplementary Figures



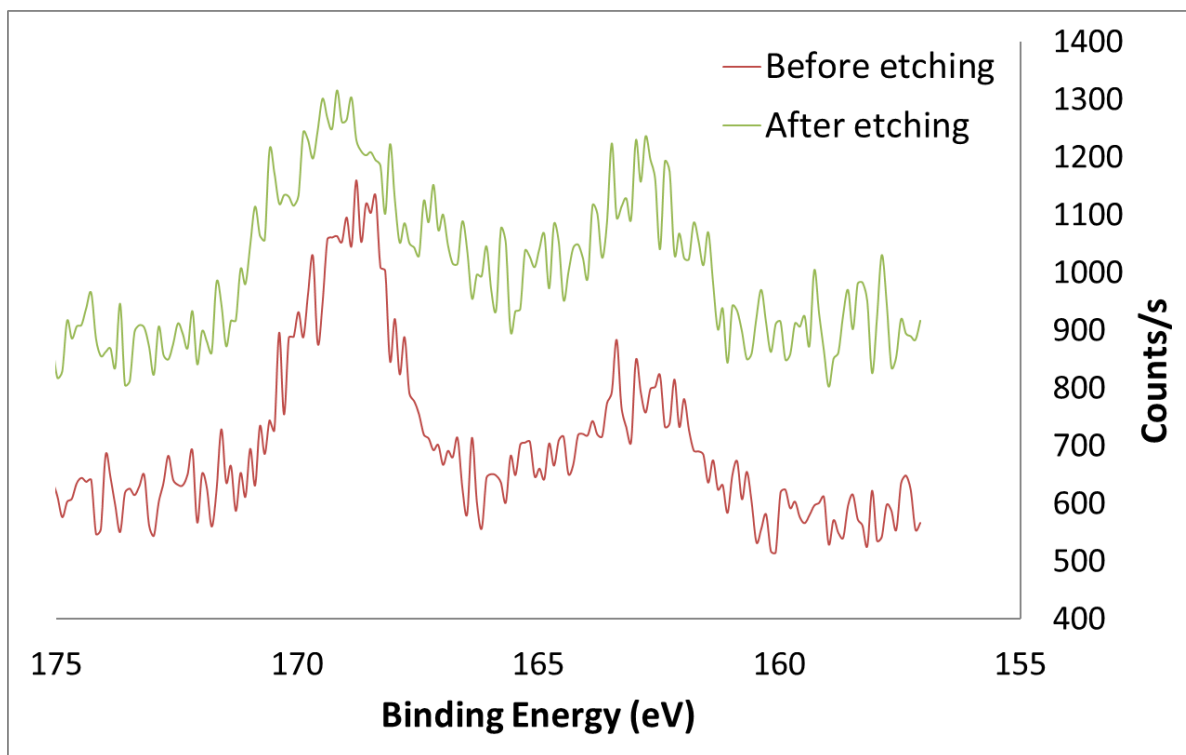
**Sup. Fig. 4.1** X-ray photoelectron spectra of the residual oil left on the Ni wire after reaction with Oil A at a) 200° and b) ambient temperature.



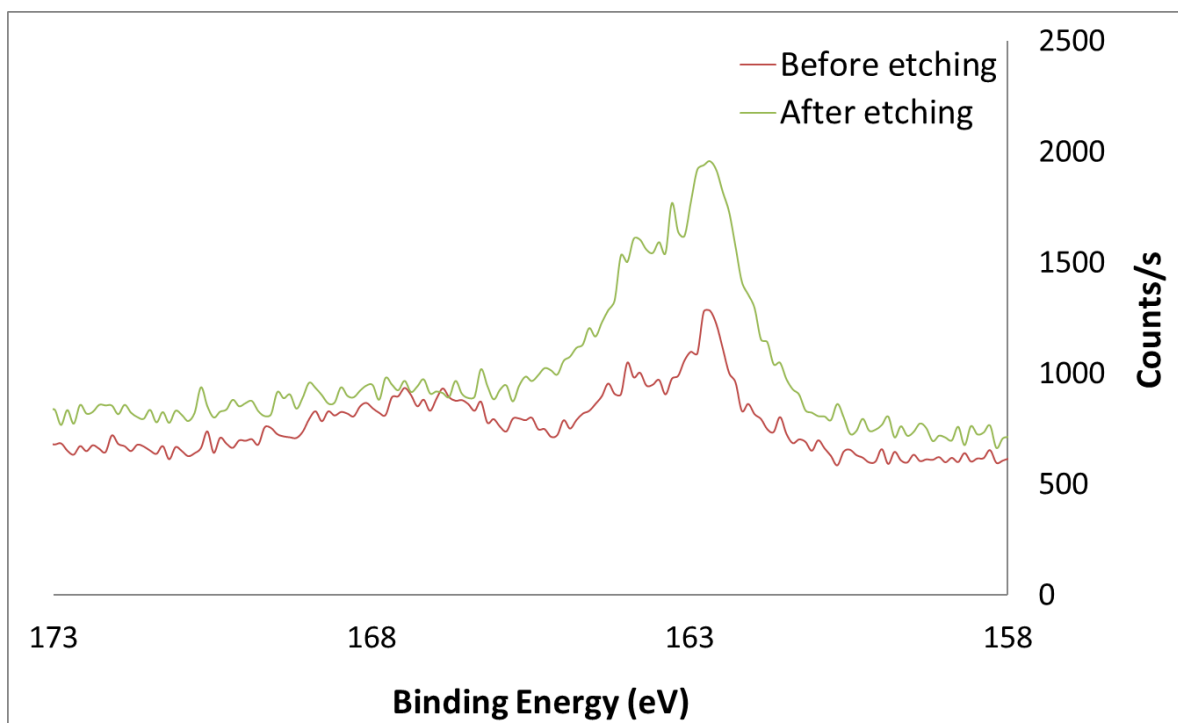
**Sup. Fig. 4.2** Sulfur (S2p) XPS of the residual oil left on the Ni wire after reaction with Oil A at 150°C before and after etching.



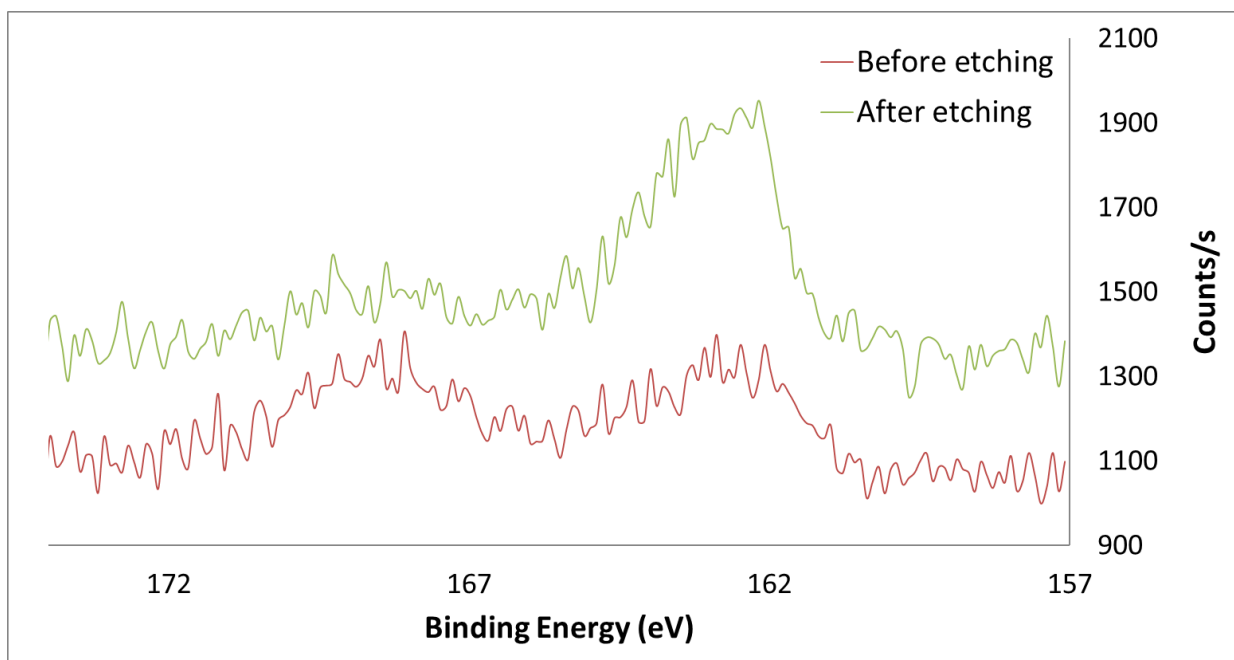
**Sup. Fig. 4.3** Sulfur (S2p) XPS of the residual oil left on the Ni wire after reaction with Oil A at 200°C before and after etching.



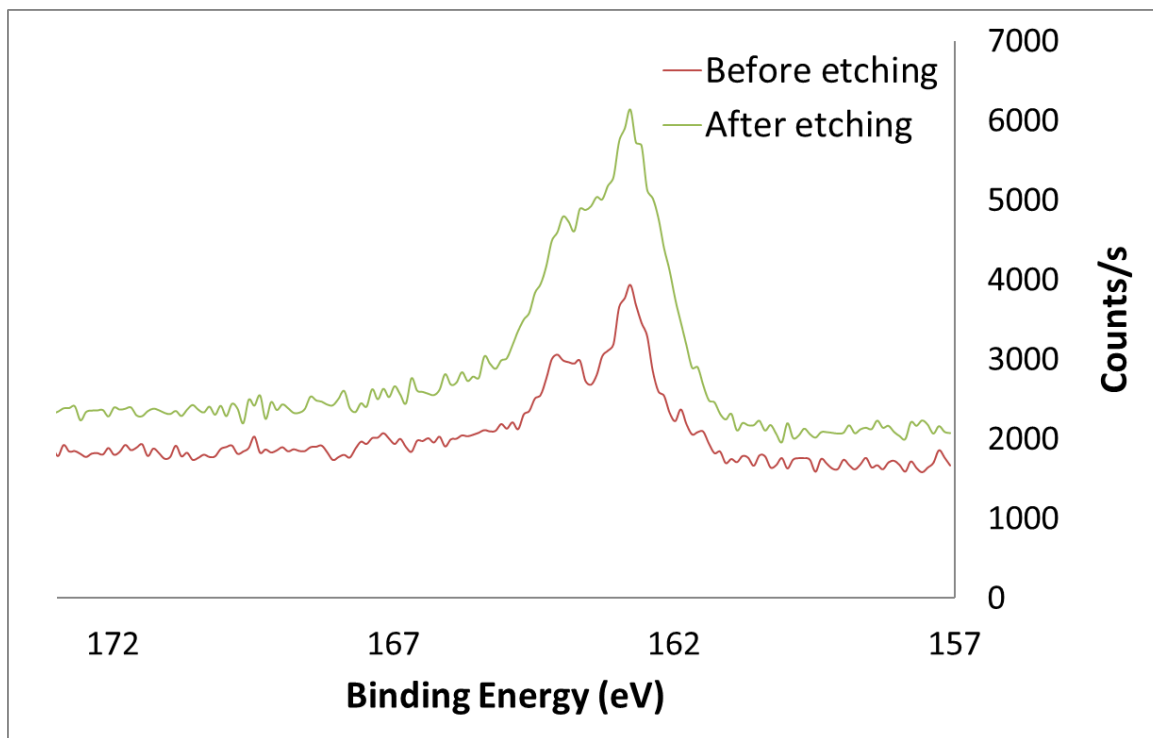
**Sup. Fig. 4.4** Sulfur (S2p) XPS of the residual oil left on the Ni wire after reaction with Oil B at 150°C before and after etching.



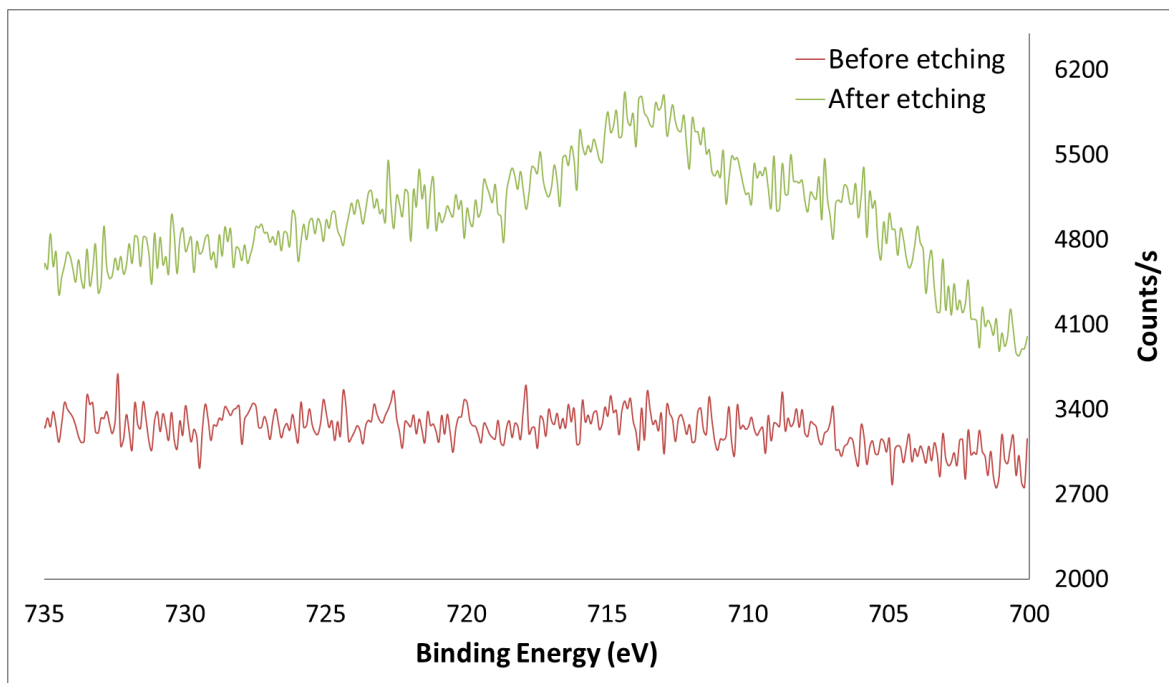
**Sup. Fig. 4.5** Sulfur (S2p) XPS of the residual oil left on the Ni wire after reaction with Oil B at 200°C before and after etching.



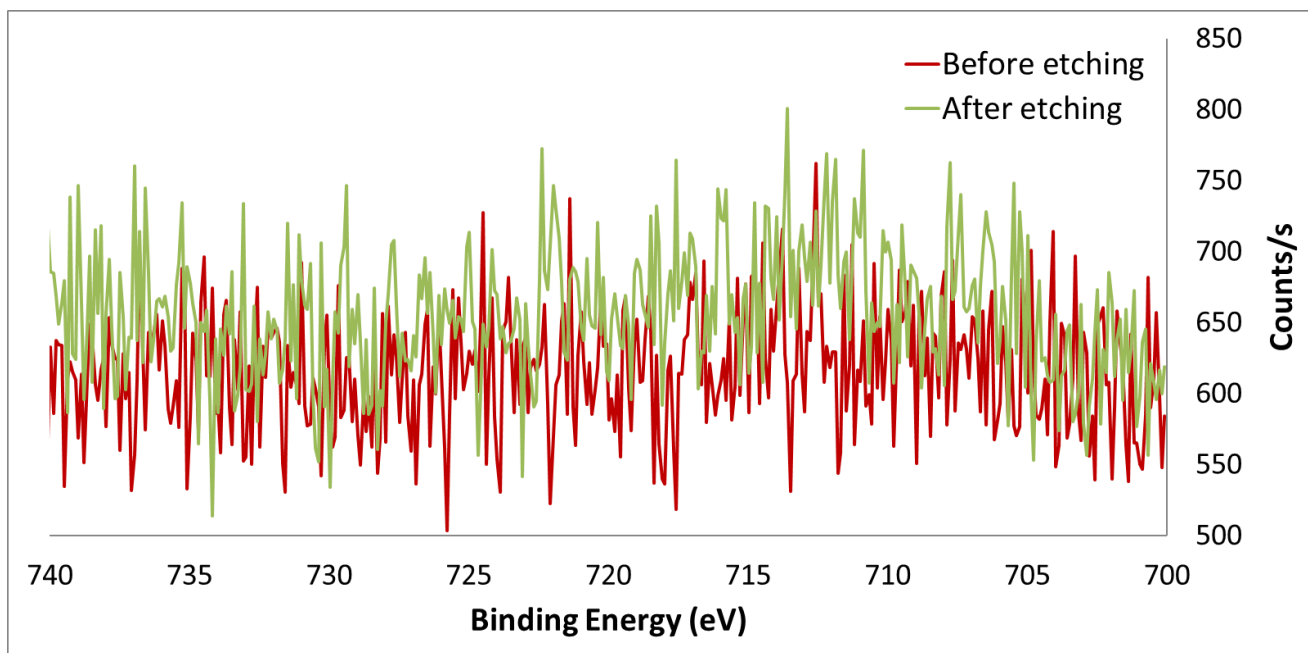
**Sup. Fig. 4.6** Sulfur (S2p) XPS of the residual oil left on the Ni wire after reaction with Oil C at 150°C before and after etching.



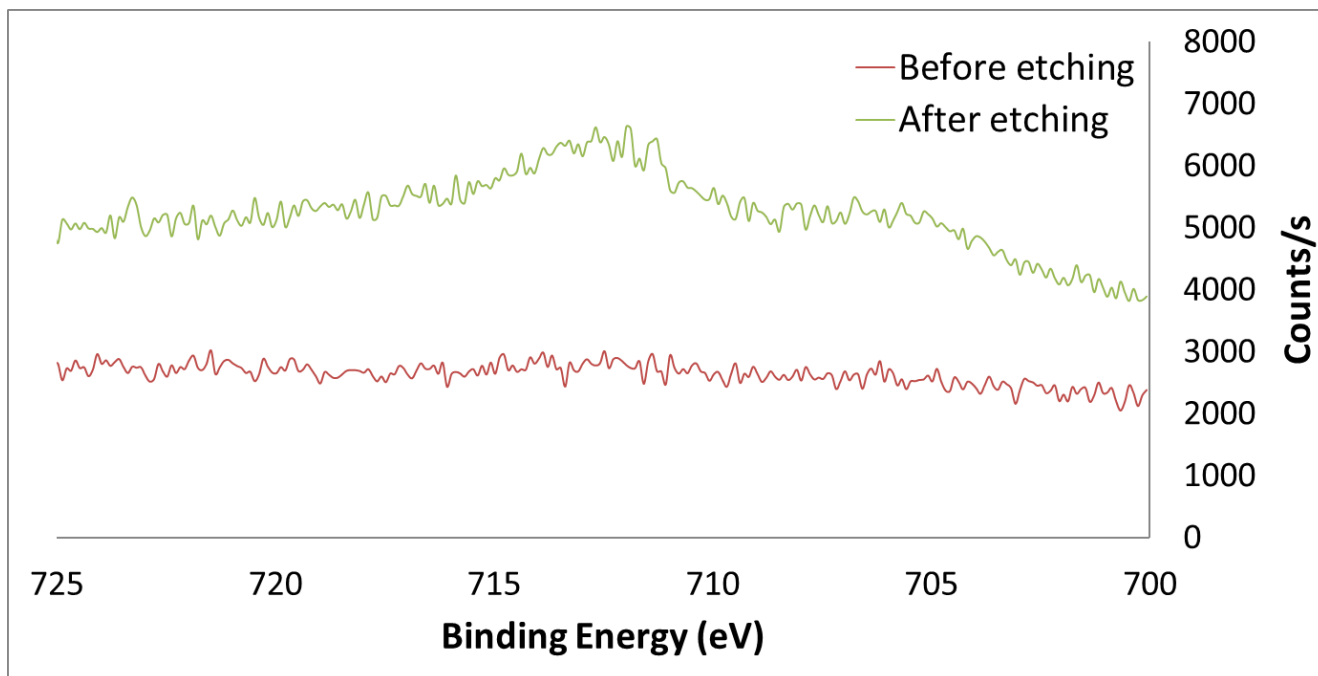
**Sup. Fig. 4.7** Sulfur (S<sub>2p</sub>) XPS of the residual oil left on the Ni wire after reaction with Oil C at 200°C before and after etching.



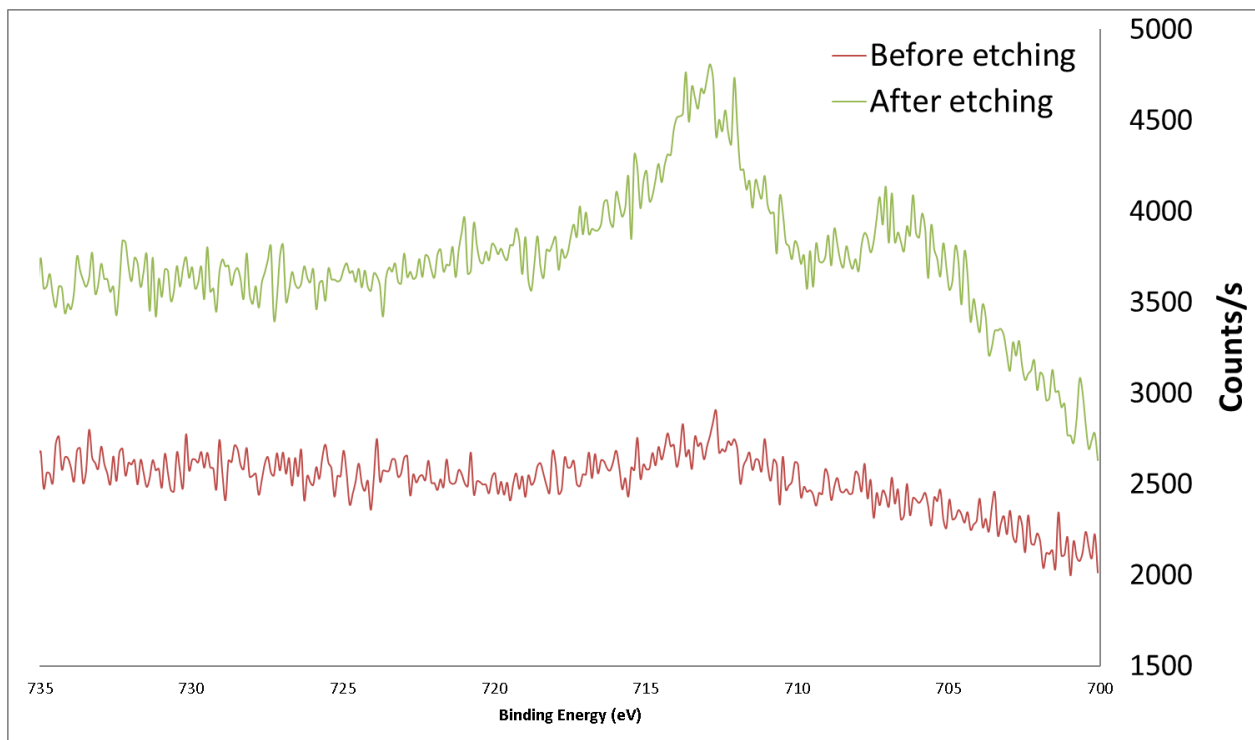
**Sup. Fig. 4.8** Iron (Fe<sub>2p</sub>) XPS of the residual oil left on the Ni wire after reaction with Oil A at 150°C before and after etching.



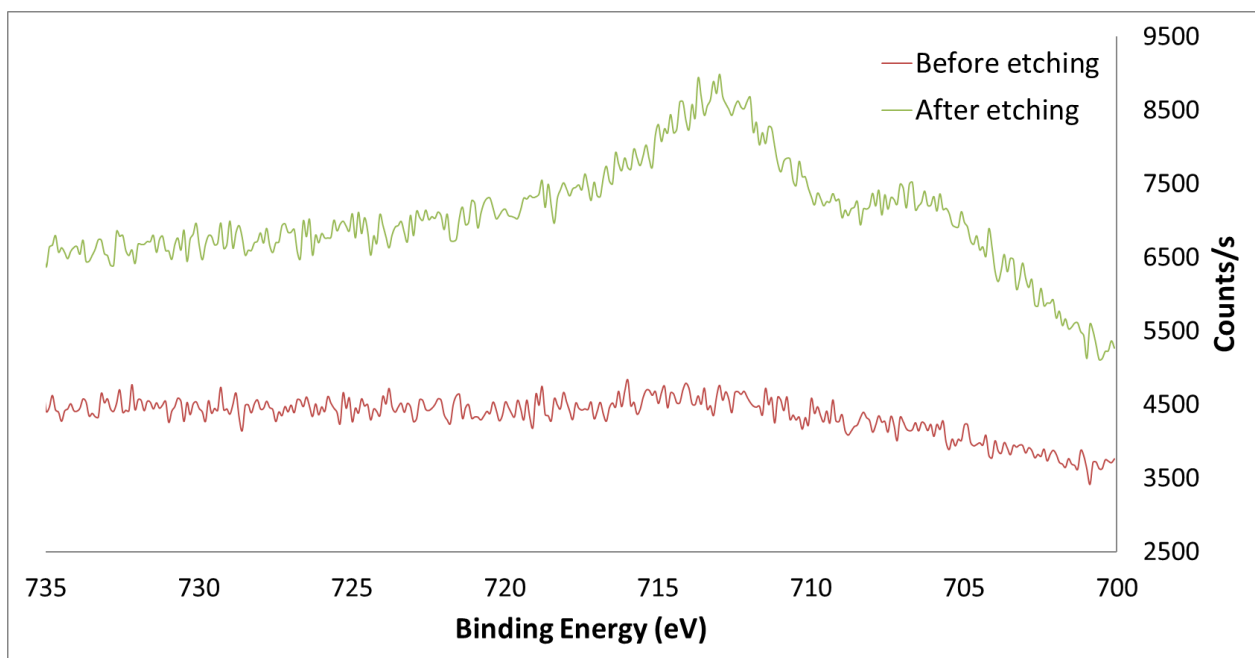
**Sup. Fig. 4.9** Iron (Fe2p) XPS of the residual oil left on the Ni wire after reaction with Oil A at 200°C before and after etching.



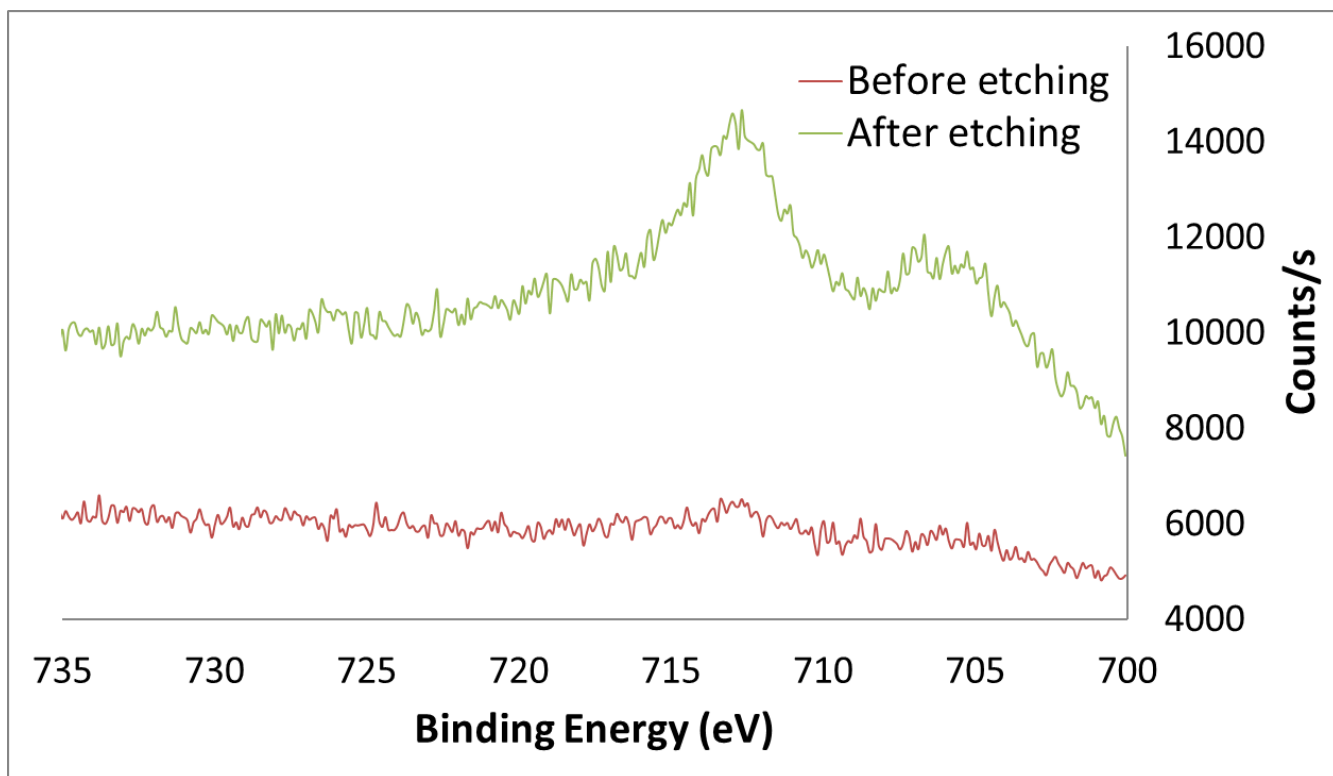
**Sup. Fig. 4.10** Iron (Fe2p) XPS of the residual oil left on the Ni wire after reaction with Oil B at 150°C before and after etching.



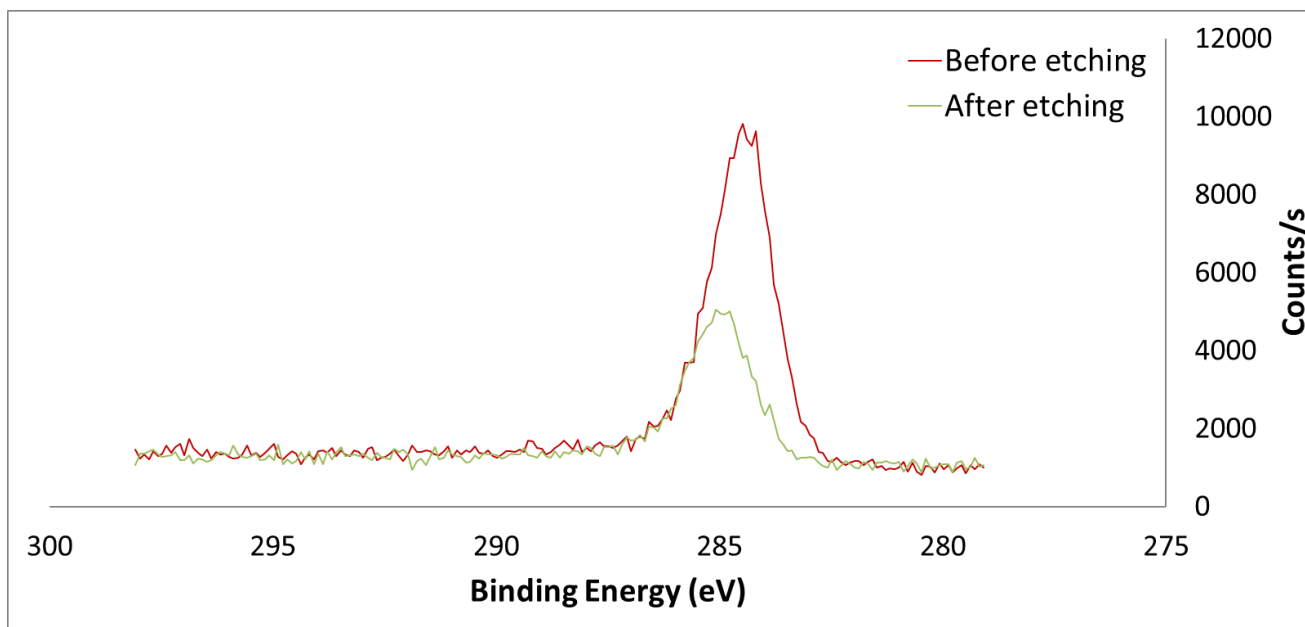
**Sup. Fig. 4.11** Iron (Fe2p) XPS of the residual oil left on the Ni wire after reaction with Oil B at 200°C before and after etching.



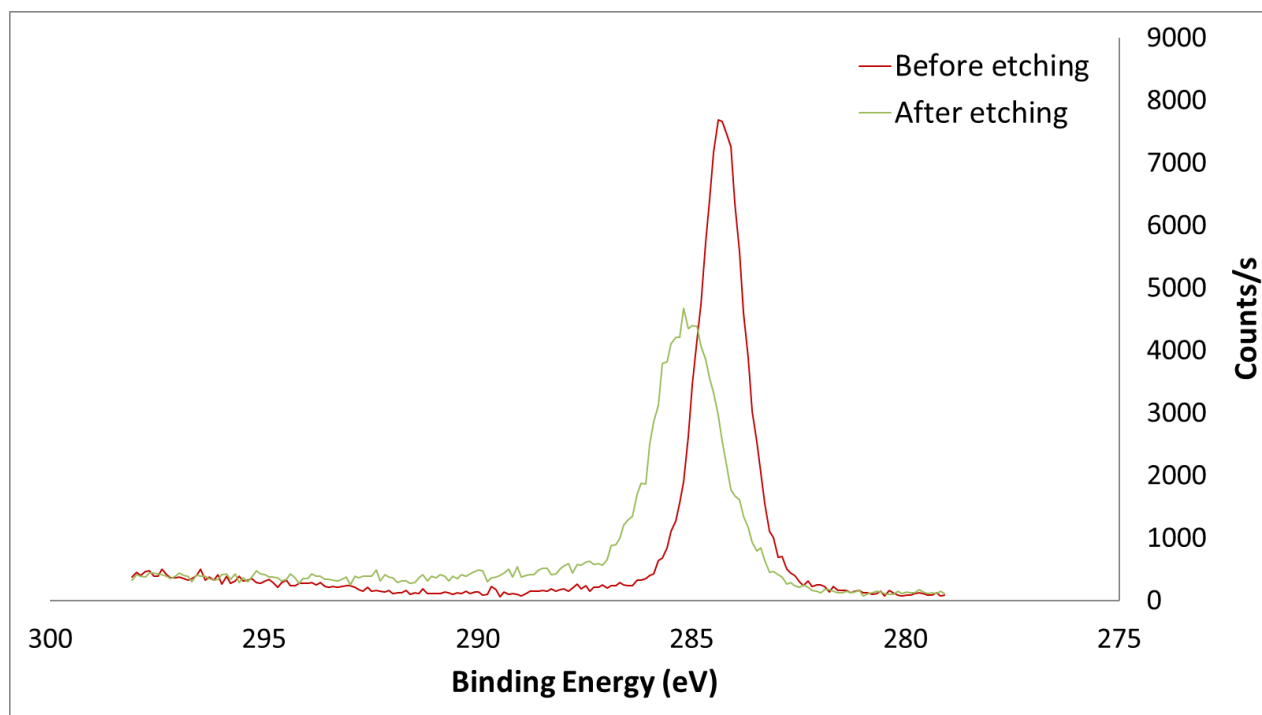
**Sup. Fig. 4.12** Iron (Fe2p) XPS of the residual oil left on the Ni wire after reaction with Oil C at 150°C before and after etching.



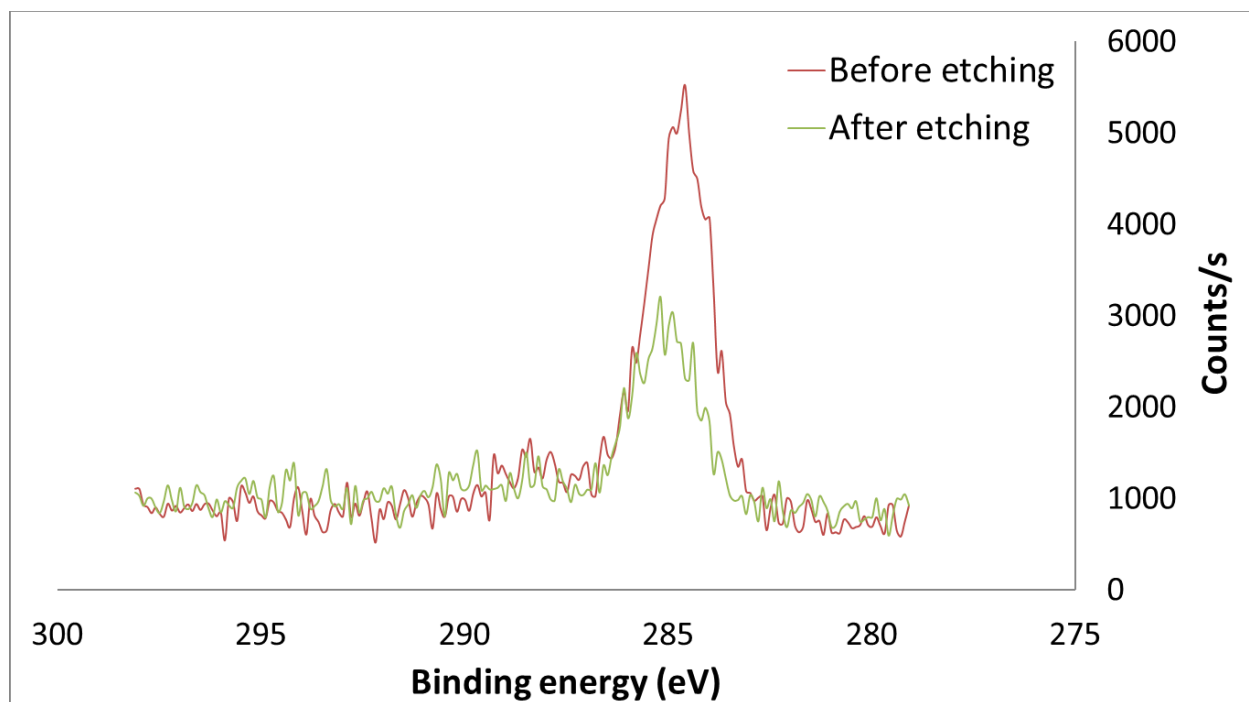
**Sup. Fig. 4.13** Iron (Fe2p) XPS of the residual oil left on the Ni wire after reaction with Oil C at 200°C before and after etching.



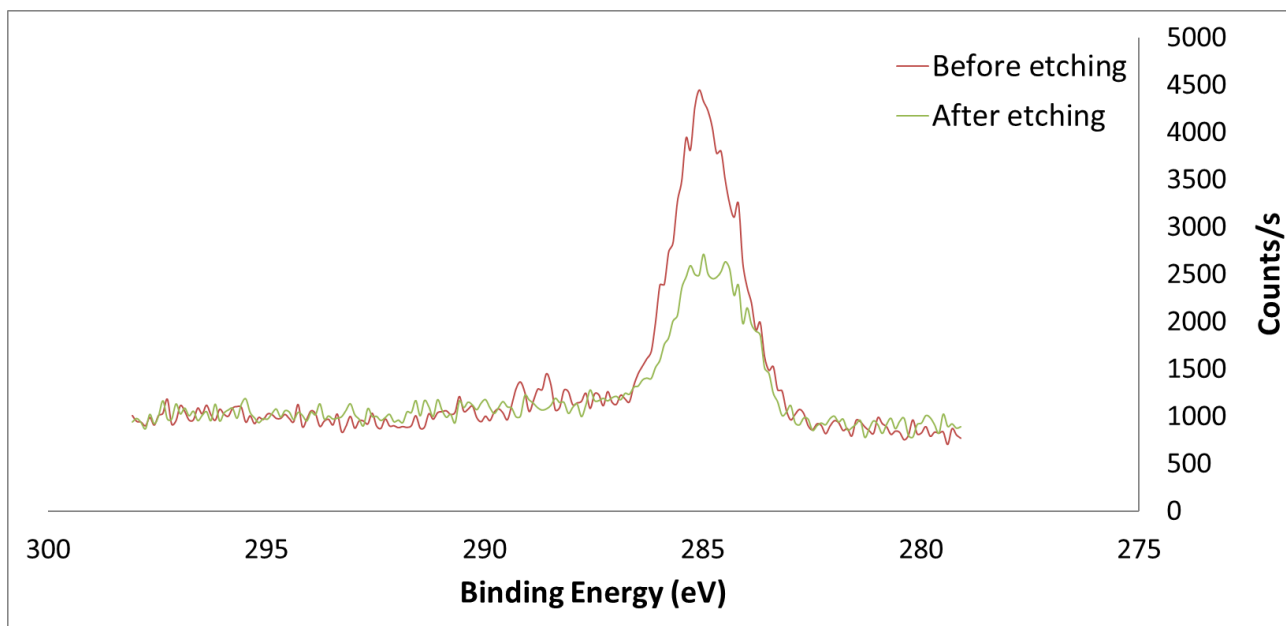
**Sup. Fig. 4.14** Carbon (C1s) XPS of the residual oil left on the Ni wire after reaction with Oil A at 150°C before and after etching.



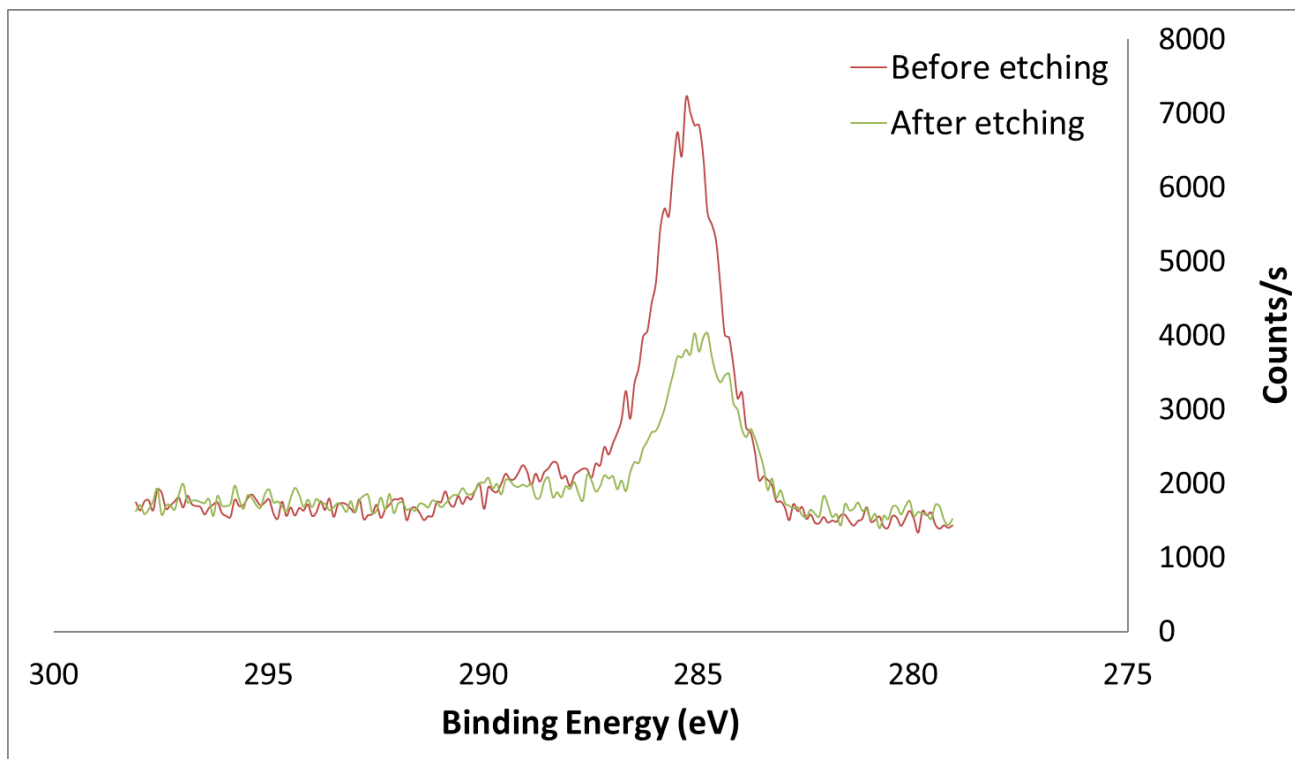
**Sup. Fig. 4.15** Carbon (C1s) XPS of the residual oil left on the Ni wire after reaction with Oil A at 200°C before and after etching.



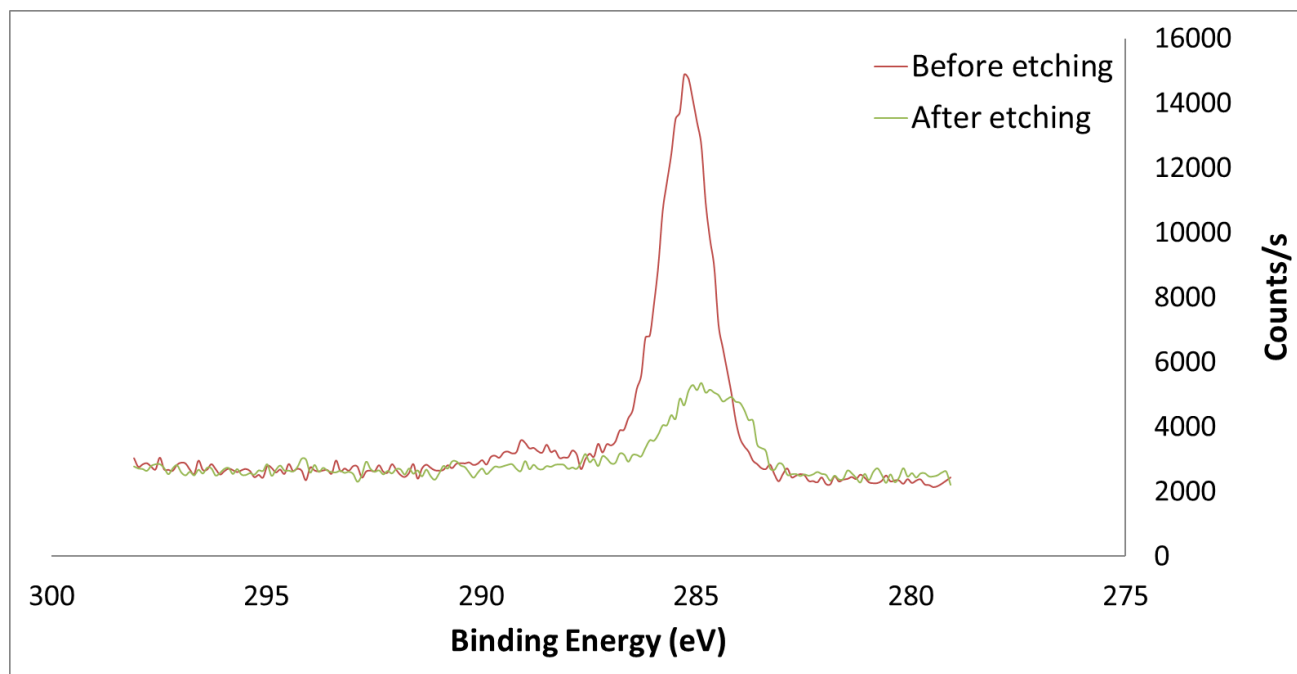
**Sup. Fig. 4.16** Carbon (C1s) XPS of the residual oil left on the Ni wire after reaction with Oil B at 150°C before and after etching.



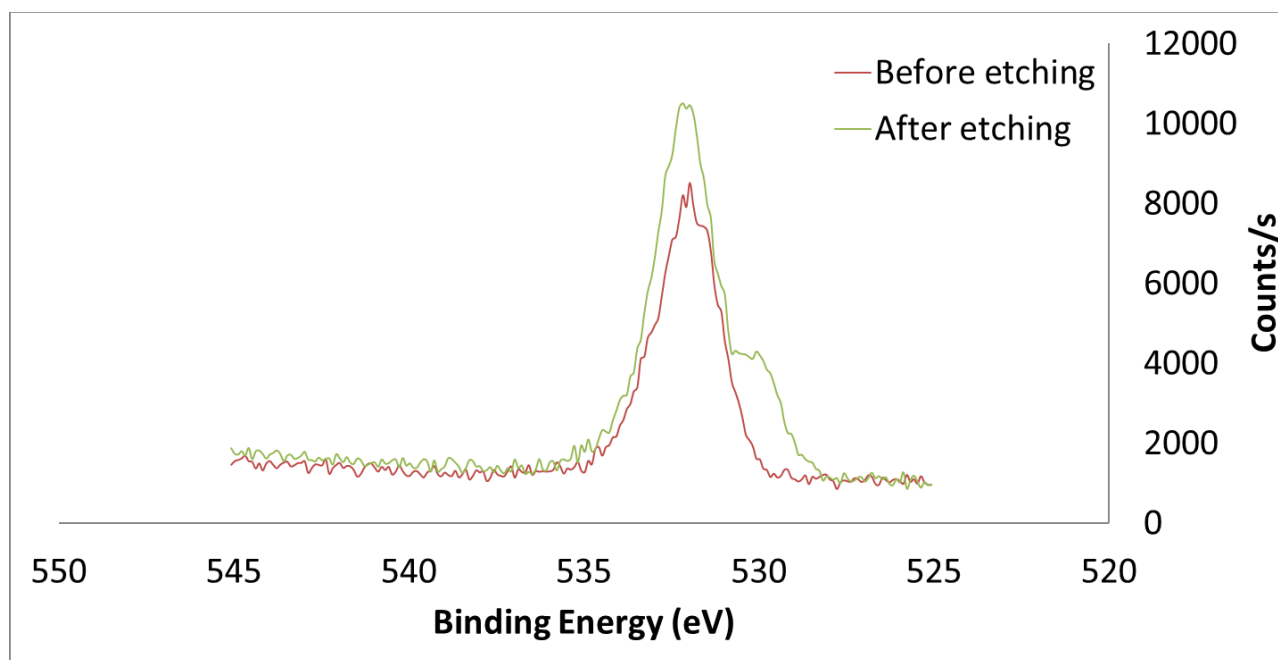
**Sup. Fig. 4.17** Carbon (C1s) XPS of the residual oil left on the Ni wire after reaction with Oil B at 200°C before and after etching.



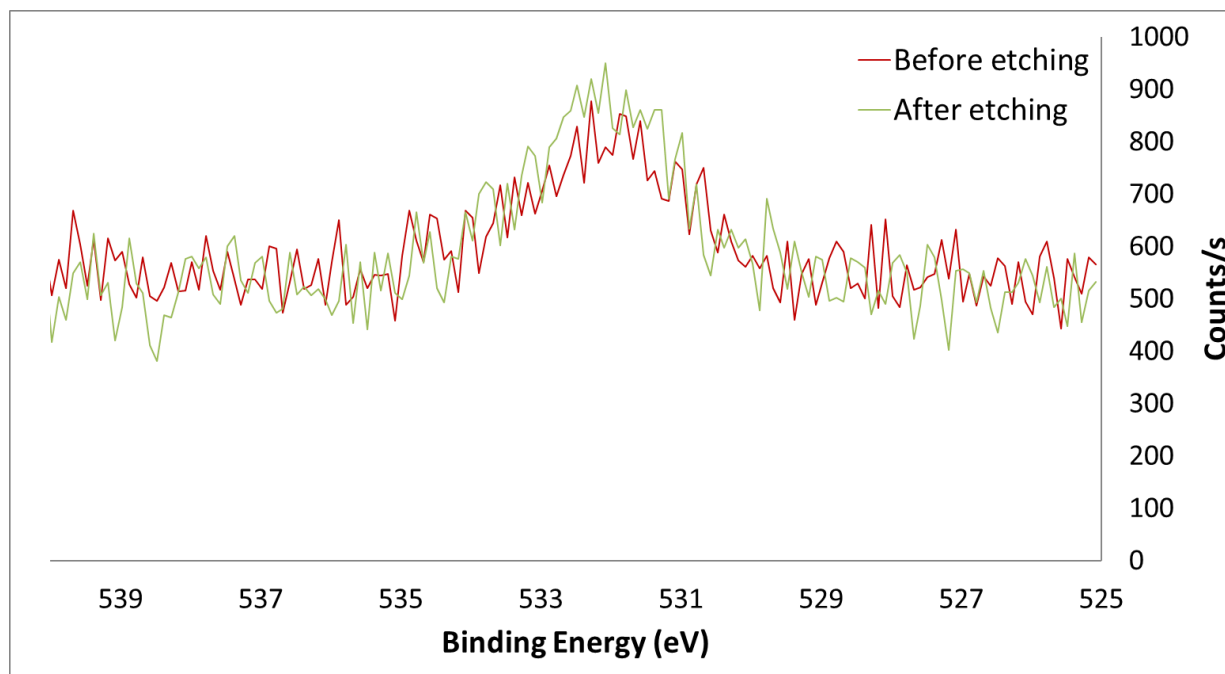
**Sup. Fig. 4.18** Carbon (C1s) XPS of the residual oil left on the Ni wire after reaction with Oil C at 150°C before and after etching.



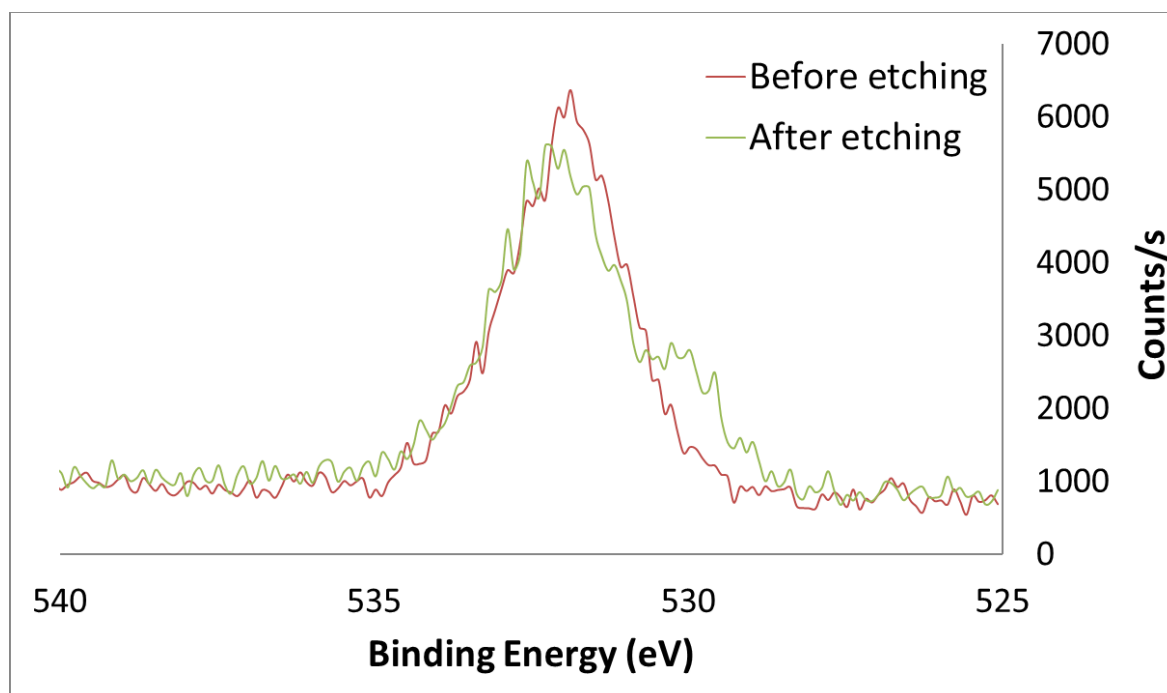
**Sup. Fig. 4.19** Carbon (C1s) XPS of the residual oil left on the Ni wire after reaction with Oil C at 200°C before and after etching.



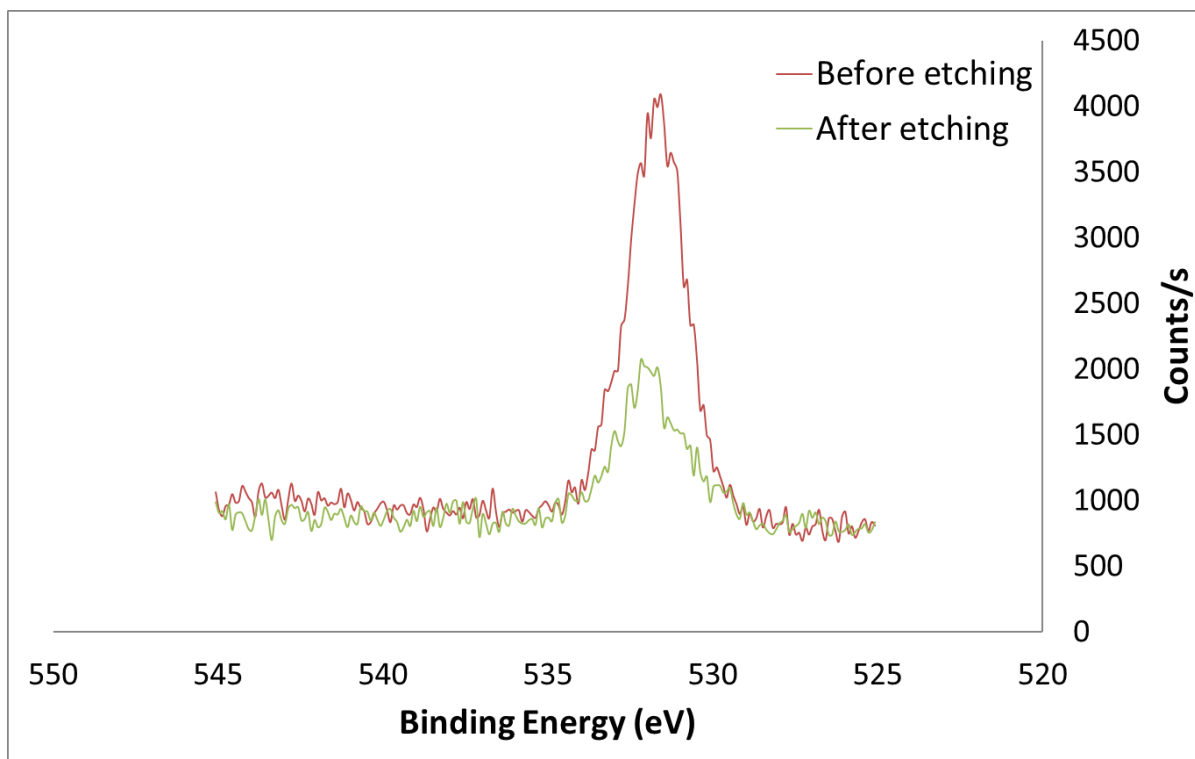
**Sup. Fig. 4.20** Oxygen (O1s) XPS of the residual oil left on the Ni wire after reaction with Oil A at 150°C before and after etching.



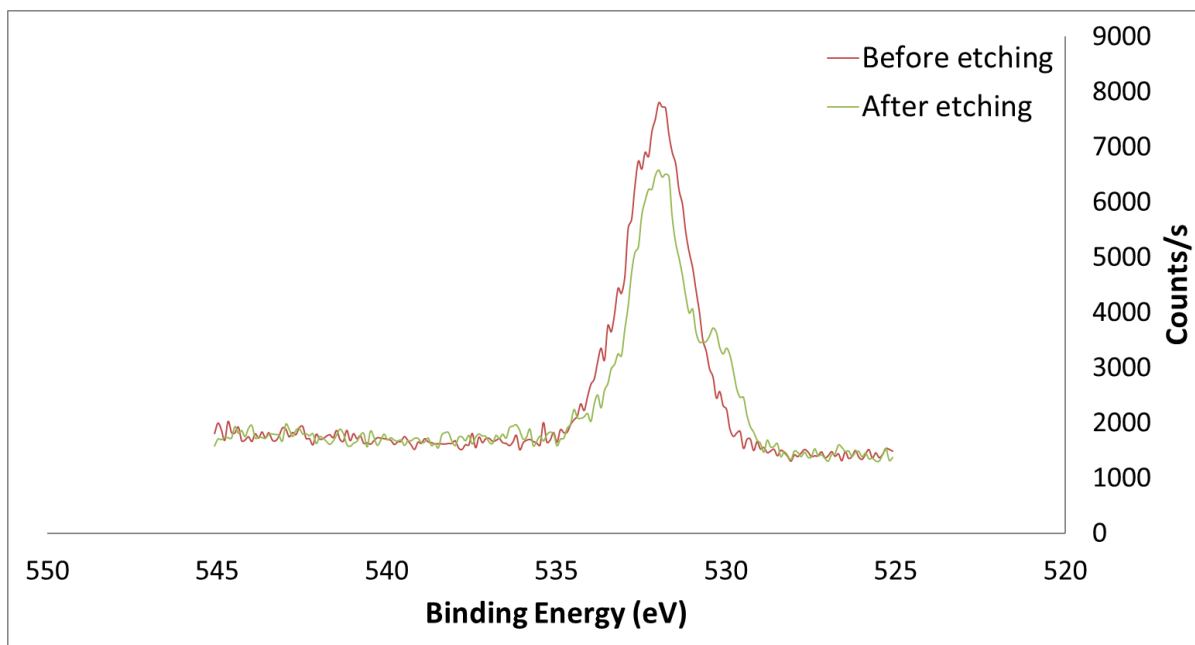
**Sup. Fig. 4.21** Oxygen (O1s) XPS of the residual oil left on the Ni wire after reaction with Oil A at 200°C before and after etching.



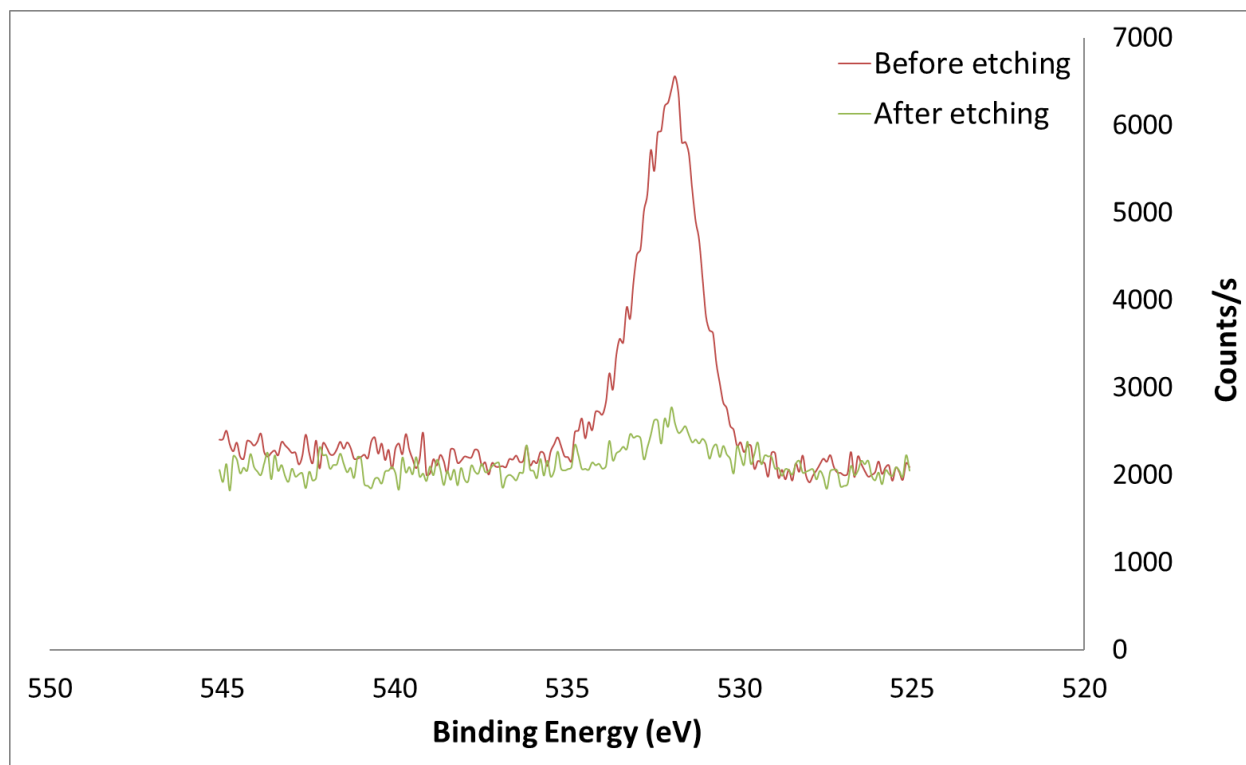
**Sup. Fig. 4.22** Oxygen (O1s) XPS of the residual oil left on the Ni wire after reaction with Oil B at 150°C before and after etching.



**Sup. Fig. 4.23** Oxygen (O1s) XPS of the residual oil left on the Ni wire after reaction with Oil B at 200°C before and after etching.



**Sup. Fig. 4.24** Oxygen (O1s) XPS of the residual oil left on the Ni wire after reaction with Oil C at 150°C before and after etching.



**Sup. Fig. 4.25** Oxygen (O1s) XPS of the residual oil left on the Ni wire after reaction with Oil C at 200°C before and after etching.

## 5. Conclusions

---

### 5.1 General Conclusions and Contributions to Knowledge

The weight of the experimental evidence indicates that Pd, Zn and Ni can be dissolved in crude oil in concentrations that would be sufficient to form an ore deposit. For example, results of the experiments show that Zn concentrations in crude oil can reach at least 1700 ppb, which greatly exceeds that measured in aqueous inclusions from ore deposits. Moreover, the solubility of Zn in crude oil is controlled by the acidity of the oil and so acidic (high TAN) oils are capable of dissolving high concentrations of Zn. The highest concentration of Zn obtained (1700 ppm) was for the most acidic oil considered in the experiments (TAN=2.7mgKOH/g). Some crude oils, however, are reported to have TAN in excess of 16 mgKOH/g indicating that Zn concentrations in crude oil can be potentially much higher than those measured in this study. Estimations utilizing the oil reserves of the Canning Basing suggest that a crude oil containing just 1000 ppm Zn would be able to produce the entire Zn reserve of the Cadjebut Deposit, which is associated with this basin. This is a Mississippi Valley Type (MVT) Deposit that received an injection of crude oil from the underlying Goldwyer Shale at approximately 350Ma (Warren and Kempton, 1997; Wallace et al., 2002). Thus, it is entirely plausible that petroleum served as an ore fluid for the Zn and Pb deposits of the Canning Basin as well as numerous other MVT Zn-Pb deposits around the world that have also experienced an epigenetic injection of crude oil. These include the Laisvall Deposit in Sweden, the Gays River deposit in Nova Scotia and the San Vincente Deposit in Peru (Gize and Barnes, 1987; Etminan and Hoffmann, 1989; Spangenberg et al., 1999; Saintilan et al., 2016). Furthermore, the experiments also show that a mixture of Zn-rich crude oil floating atop a calcite-buffered brine will spontaneously produce sphalerite crystals at room temperature when exposed to hydrogen sulfide gas (a geochemical environment that was

designed to resemble the limestone reefs where MVT mineralization occurs). Thus, it is possible that at least some of the major MVT deposits around the world formed entirely through processes involving the transport of zinc as carboxylate complexes in petroleum. It is hypothesized that, during the abiotic reaction of metalliferous petroleum with aqueous sulfate, the petroleum is gradually consumed to form carbonate minerals and hydrogen sulfide gas, at which point the Zn dissolved deposits as sphalerite. This reaction is referred to as Thermochemical Sulfate Reduction (TSR) and is commonly known to occur in petroleum reservoirs and in the ore zones of MVT ore deposits at depths of up to 7 km below the subsurface and temperatures varying between 100 and 240°C (Goldstein and Aizenshtat, 1994, Hao et al., 2008).

The experiments with Pd and Ni showed that both metals are relatively soluble in crude oil, (up to 127 ppb Pd and 240ppm Ni). As is the case with the Zn deposits of the Canning Basin, it is estimated, based on the reserves of the Carboniferous Rotliegend petroleum system, that petroleum containing 127ppb Pd could easily supply the entire Pd reserve of the adjacent Polish Kupferschiefer. Significantly, it has been reported that the shales of the Kupferschiefer contain high concentrations of Polyaromatic Sulfur Hydrocarbons, a class of compounds that is commonly present in petroleum, thereby indicating that the Kupferschiefer sediments may have been infiltrated by Carboniferous crude oil (Püttmann and Goßel, 1990). The experimental findings show that Pd and Ni have a strong affinity for thiols in crude oil and anomalously high concentrations of thiols are commonly reported in crude oils that have undergone Thermochemical Sulfate Reduction (TSR). Furthermore, it is likely that Thermochemical Sulfate Reduction contributed to the formation of the sulfide ores at the Kupferschiefer deposit and Ni deposits such as the Talvivaara deposit in Finland (Sun, 1998; Young, et al, 2013). Thus,

processes involving the thermal breakdown of petroleum are likely to be influential in the formation of many of the sediment-hosted deposits described in the literature.

It is noteworthy that Ni not only appears to have an affinity for thiols in crude oil but also helps catalyze the reduction of sulfur compounds in crude oil, as evidenced by the formation of thiols on the surface of a Ni wire that has been left to react in a crude oil that was initially devoid of thiols. Although our experiments with Pd in crude oil preclude this finding, we consider that Pd may also catalytically promote the reduction of sulfur compounds in petroleum, given its location in the same period of the Periodic Table as Ni. From this we predict that Ni (and possibly Pd) concentrations may not only increase in crude oils that have undergone TSR but may also catalytically promote this reaction. Furthermore, our experiments show that the dissolution of Ni and reduction of sulfur compounds in crude oils are enhanced in oils that contain large concentrations of Fe. Thus, it is likely that Fe, like Ni also serves as a catalyst in promoting TSR.

## **5.2 Recommendations for future studies**

Previous models for the genesis of sediment-hosted metallic mineral deposits do not account for the fact that there is spatio-temporal association between the ores and petroleum hydrocarbons in many of these deposits (such as oil inclusions in the ore minerals). One of these genetic models, the hydrothermal model, considers that the metals are transported to the site of ore deposition dissolved in hydrothermal fluids and precipitated by in-situ sulfate reduction (Jowitt and Keays, 2011). However, this model fails to explain the high concentrations of Ni (~7wt%) present in deposits such as the hyper enriched black shales (HEBS) of Southern China, considering the very

low solubility of Ni in hydrothermal fluids (Liu et al., 2012). The other model for the formation of these deposits asserts that all the ore metals in these sediment-hosted deposits were derived from seawater and precipitated as sulfide minerals by microbial processes at the sediment-water interface (Jowitt and Keays, 2011; Lehmann et al, 2016). As it stands, more research needs to be done on sediment-hosted deposits to determine the degree to which the reduced sulfur in these deposits is derived from the activity of sulfur reducing microbes living in the sediments versus the abiotic breakdown of petroleum by TSR. These processes are difficult to distinguish, microscopically or even compositionally but have been successfully differentiated using stable isotope techniques. For example, whole rock ore samples that have undergone TSR will display mass-anomalous  $\Delta^{33}\text{S}$  fractionation ( $\Delta^{33}\text{S} = > 0 \pm 0.2 \text{ ‰}$ ) and crude oils, kerogen, condensates and bitumen that have undergone TSR typically display high total sulfur content,  $\delta^{34}\text{S}$  enrichment and  $\delta^{13}\text{C}$  depletion relative to those that have undergone BSR (Machel, 2001; Young et al., 2013).

Another avenue for future research lies in determining whether the carbonaceous matter that hosts the ore in sediment-hosted deposits is of sedimentary origin, derived from locally generated liquid hydrocarbons or from petroleum that has undergone secondary migration from a shale unit deep within the basin. In many sediment-hosted deposits, where the ore is hosted in carbonaceous seams (such as the Witwatersrand deposits), it is not immediately apparent that these seams are indeed residues of petroleum migration. To this end, Rhenium-Osmium (Re-Os) geochronology could be used to determine whether the non-mineralized shales surrounding the ore zone are the same age as the ore minerals, bitumen and pyrobitumen from within the ore zone. If the sulfide minerals from the ore zone formed during (or after) the injection of petroleum

into the deposit, they will be radiogenically younger than the non-mineralized shales (the pre-existing host rock that became infiltrated by the petroleum). Furthermore, the Os isotopic ratio at the time of formation ( $^{187}\text{Os}/^{188}\text{Os}$ )<sub>0</sub> can be deduced from Re-Os isochrons and used as a proxy for the source of the ore minerals and the organic matter in the non-mineralized rocks. If ore metals are transported into the deposit from an external source in a hydrocarbon fluid, then their source proxy will be different to that of the host rocks but perhaps more akin to that of oil source rocks deeper in the stratigraphy.

Sediment-hosted deposits are an important source of many industrially useful metals and are therefore worth understanding from a purely economic point of view. The study of these deposits may also contribute to a better understanding of the abiotic reactions that simultaneously control the composition of minerals (sulfides, clays, sulfates, oxides, phosphates and carbonates), hydrocarbons and hydrothermal fluids. The TSR reaction, in particular, is worthy of further study since it links mineral deposit and petroleum systems and is also responsible for linking the carbon and the sulfur cycle in the geosphere (Goldstein and Aizenshtat, 1994). It has long been considered that the mass-anomalous fractionation of sulfur isotopes in Archean rocks is due to the photolysis of sulfur dioxide gas by UV radiation in an oxygen-free atmosphere, although this notion is now being challenged since the same mass-anomalous fractionations can also be achieved by TSR. Consequently, the sulfur isotope record of sedimentary rocks may be linked to the biological and thermal evolution of Earth in ways different than previously thought (Watanabe, 2009). In certain sediment-hosted deposits such as those of the MVT class, the Kupferschiefer deposit, the Talvivaara deposit and potentially numerous others, the breakdown of hydrocarbons by TSR is the primary mode of ore formation. Moreover, the formation of some of these sediment-hosted deposits is coeval with important events in Earth's history. For

example, the Zunyi deposit in Southern China, which outcrops discontinuously for 2000 km spanning China from one side to the other, is early Cambrian in age and has been studied to gain insight into the processes that contributed to the Cambrian Explosion (Steiner et al, 2001). Thus, the formation of carbonaceous sediment-hosted deposits demands further investigation for their potential relation to major historic perturbations in the Earth's global carbon and sulfur cycles and major life events.

### **5.3 References**

Etminan, H. and Hoffmann, C.F., 1989. Biomarkers in fluid inclusions: A new tool in constraining source regimes and its implications for the genesis of Mississippi Valley-type deposits. *Geology*, **17(1)**, pp.19-22.

Gize, A.P. and Barnes, H.L., 1987. The organic geochemistry of two Mississippi Valley-type lead-zinc deposits. *Economic Geology*, **82(2)**, pp.457-470.

Goldstein, T. and Aizenshtat, Z., 1994. Thermochemical sulfate reduction a review. *Journal of Thermal Analysis and Calorimetry*, **42(1)**, pp.241-290.

Hao, F., Guo, T., Zhu, Y., Cai, X., Zou, H. and Li, P., 2008. Evidence for multiple stages of oil cracking and thermochemical sulfate reduction in the Puguang gas field, Sichuan Basin, China. *AAPG bulletin*, **92(5)**, pp.611-637.

Jowitt, S.M. and Keays, R.R., 2011. Shale-hosted Ni–(Cu–PGE) mineralisation: a global overview. *Applied Earth Science*, 120(4), pp.187-197.

Lehmann, B., Frei, R., Xu, L. and Mao, J., 2016. Early Cambrian black shale-hosted Mo-Ni and V mineralization on the rifted margin of the Yangtze Platform, China: reconnaissance chromium isotope data and a refined metallogenic model. *Economic Geology*, 111(1), pp.89-103.

Liu, W., Migdisov, A. and Williams-Jones, A., 2012. The stability of aqueous nickel (II) chloride complexes in hydrothermal solutions: Results of UV–Visible spectroscopic experiments. *Geochimica et Cosmochimica Acta*, 94, pp.276-290.

Machel, H.G., 2001. Bacterial and thermochemical sulfate reduction in diagenetic settings—old and new insights. *Sedimentary Geology*, 140(1-2), pp.143-175.

Püttmann, W. and Goßel, W., 1990. The Permian Kupferschiefer of southwest Poland: a geochemical trap for migrating, metal-bearing solutions. *Applied Geochemistry*, 5(1-2), pp.227-235.

Saintilan, N.J., Spangenberg, J.E., Samankassou, E., Kouzmanov, K., Chiaradia, M., Stephens, M.B. and Fontboté, L., 2016. A refined genetic model for the Laisvall and Vassbo Mississippi Valley-type sandstone-hosted deposits, Sweden: constraints from paragenetic studies, organic geochemistry, and S, C, N, and Sr isotope data. *Mineralium Deposita*, 51(5), pp.639-664.

Spangenberg, J.E., Fontbote, L. and Macko, S.A., 1999. An evaluation of the inorganic and organic geochemistry of the San Vicente mississippi valley-type zinc-lead district, central Peru; implications for ore fluid composition, mixing processes, and sulfate reduction. *Economic Geology*, **94(7)**, pp.1067-1092.

Steiner, M., Wallis, E., Erdtmann, B.D., Zhao, Y. and Yang, R., 2001. Submarine-hydrothermal exhalative ore layers in black shales from South China and associated fossils—insights into a Lower Cambrian facies and bio-evolution. *Palaeogeography, palaeoclimatology, palaeoecology*, *169(3-4)*, pp.165-191.

Sun, Y.Z., 1998. Influences of secondary oxidation and sulfide formation on several maturity parameters in Kupferschiefer. *Organic Geochemistry*, *29(5-7)*, pp.1419-1429.

Wallace, M.W., Middleton, H.A., Johns, B. and Marshallsea, S., 2002, October. Hydrocarbons and Mississippi Valley-type sulfides in the Devonian reef complexes of the eastern Lennard Shelf, Canning Basin, Western Australia. In *The sedimentary basins of Western Australia 3. Proceedings of the West Australian basins Symposium: Perth, Petroleum Exploration Society of Australia* (pp. 795-815).

Warren, J.K. and Kempton, R.H., 1997. Evaporite Sedimentology and the Origin of Evaporite-Associated Mississippi Valley-Type Sulfides in the Cadjebut Mine Area Lennard Shelf, Canning Basin, Western Australia.

Watanabe, Y., Farquhar, J. and Ohmoto, H., 2009. Anomalous fractionations of sulfur isotopes during thermochemical sulfate reduction. *Science*, 324(5925), pp.370-373.

Young, S.A., Loukola-Ruskeeniemi, K. and Pratt, L.M., 2013. Reactions of hydrothermal solutions with organic matter in Paleoproterozoic black shales at Talvivaara, Finland: Evidence from multiple sulfur isotopes. *Earth and Planetary Science Letters*, 367, pp.1-14.